NASA CONTRACTOR REPORT

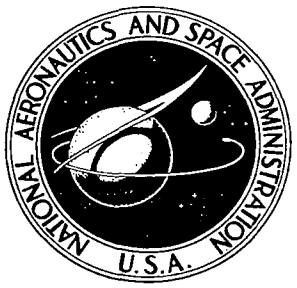

APPLICATION OF MULTIVARIABLE SEARCH TECHNIQUES TO STRUCTURAL DESIGN OPTIMIZATION

by R. T. Jones and D. S. Hague

Prepared by
AEROPHYSICS RESEARCH CORPORATION
Bellevue, Wash. 98009
for Langley Research Center

NATIONAL AERONAUTICS AND SPACE ADMINISTRATION • WASHINGTON, D. C. • JUNE 1972

1. Report No.	2. Government Accession No.	3. Recipient's Catalog No.
NASA CR-2038		

4. Title and Subtitle	5. Report Date
APPLICATION OF MULTIVARIABLE SEARCH TECHNIQUES TO STRUCTURAL DESIGN OPTIMIZATION	June 1972
	6. Performing Organization Code
7. Author(s)	8. Performing Organization Report No.
R. T. Jones and D. S. Hague	
9. Performing Organization Name and Address	10. Work Unit No.
Aerophysics Research Corporation Bellevue, Washington	126-14-16-03
	11. Contract or Grant No.
	NAS1-9936
	13. Type of Report and Period Covered
12. Sponsoring Agency Name and Address	Contractor Report
National Aeronautics and Space Administration Washington, D.C. 20546	14. Sponsoring Agency Code

15. Supplementary Notes

16. Abstract

Multivariable optimization techniques are applied to a particular class of minimum weight structural design problems: the design of an axially loaded, pressurized, stiffened cylinder. Minimum weight designs are obtained by a variety of search algorithms: first- and second-order, elemental perturbation, and randomized techniques. An exterior penalty function approach to constrained minimization is employed. Some comparisons are made with solutions obtained by an interior penalty function procedure. In general, it would appear that an interior penalty function approach may not be as well suited to the class of design problems considered as the exterior penalty function approach. It is also shown that a combination of search algorithms will tend to arrive at an extremal design in a more reliable manner than a single algorithm. The effect of incorporating realistic geometrical constraints on stiffener cross-sections is investigated. A limited comparison is made between minimum weight cylinders designed on the basis of a linear stability analysis and cylinders designed on the basis of empirical buckling data. Finally, a technique for locating more than one extremal is demonstrated.

17. Key Words (Suggested by Author(s))	18. Distribution Statement
Stiffened cylinder, mathematical programming, nonlinear programming, AESOP, optimization, minimum weight	Unclassified - Unlimited

19. Security Classif. (of this report)	20. Security Classif. (of this page)	21. No. of Pages	22. Price*
Unclassified	Unclassified	210	$ 3.00

*For sale by the National Technical Information Service, Springfield, Virginia 22151

PREFACE

This report describes a research study completed under Contract NAS 1-9936, "Application of Multivariable Search Techniques to Optimal Structural Design." The study was carried out in the period from April to December, 1970.

The study was funded by the National Aeronautics and Space Administration, Langley Research Center, Structures Division. Mr. H. G. McComb, Jr. and Dr. W. J. Stroud served as technical monitors for the study.

Study effort was accomplished by Aerophysics Research Corporation (ARC) at its Bellevue, Washington facility. Mr. D. S. Hague functioned as project manager, and Mr. R. T. Jones functioned as principal investigator of the study. This manuscript was prepared by Mrs. Jane Yonke of Aerophysics Research Corporation.

The study was based on the application of an existing multivariable optimization program developed under a previous NASA-sponsored study, Contract NAS 2-4507. Mr. Richard H. Petersen, Office of Advanced Research and Technology, Ames Research Center, was the NASA technical monitor for that study. An existing stiffened cylinder synthesis program constructed under another previous NASA-sponsored study, Grant No. NsG 110-61, was also employed in the study.

TABLE OF CONTENTS

TABLE OF CONTENTS

TABLE OF CONTENTS

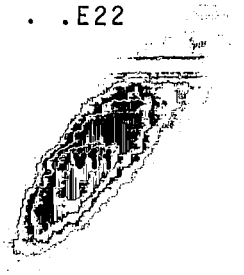

TABLE OF CONTENTS

LIST OF FIGURES

LIST OF FIGURES

LIST OF FIGURES

LIST OF FIGURES

LIST OF TABLES

LIST OF TABLES

LIST OF TABLES

LIST OF TABLES

NOMENCLATURE

Symbol	Description
A_y	X-section area of intermediate frame, inches^2
B	Intermediate frame spacing (length between "simple" supports), inches
C.B.L.	Circumferential stiffener buckling for a contraction of the cylinder, $\varepsilon_{\phi p}/\varepsilon_{\phi cr}$
C.B.U.	Circumferential stiffener buckling for an expansion of the cylinder, $\varepsilon_{\phi p}/\varepsilon_{\phi cr}$
C.Y.C.	Circumferential stiffener yield in compression, $\sigma_{\phi sp}/\sigma_{\phi 0C}$
C.Y.T.	Circumferential stiffener yield in tension, $\sigma_{\phi sp}/\sigma_{\phi 0T}$
D_1, D_2, D_3	Bending stiffnesses of skin
d	Stiffener depth
E_x, E_ϕ, E	Moduli of elasticity of skin
$E_{xs}, E_{\phi s}$	Moduli of elasticity of stiffeners
e_x, e_ϕ	Eccentricity of stiffeners (+ inside, - outside

Symbol	Description
f	Actual value of behavior variable
f_{cr}	Critical value of behavior variable
G_x, G_ϕ	Shear modulus of stiffeners
G	Shear modulus of skin
G.B.	Gross buckling, N/N_{cr}
h	Shell wall thickness, inches
H_{s1}, H_{s2}, H_ν	Extensional stiffnesses of skin
H_x, H_ϕ	Extensional stiffnesses of stiffeners
I_y	Intermediate frame x-section moment of inertia, inches^4
J_x, J_ϕ	Torsional constants of stiffeners
K	Torsional stiffness of skin
L	Axial length between "fixed" supports, inches
L.B.	Lower bound
L.C.	Load condition

Symbol	Description
L.S.B.	Longitudinal stiffener buckling, σ_{xsp}/σ_{cr}
L.Y.C.	Longitudinal stiffener yield compression, $\sigma_{xsp}/\sigma_{xOC}$
L.Y.T.	Longitudinal stiffener yield tension $\sigma_{xsp}/\sigma_{xOT}$
m	Number of half-waves in the axial direction
M	Applied bending moment, inch-lbs.
MS	Margin of safety
$M_x, M_\phi, M_{x\phi}, M_{\phi x}$	Moment resultants
n	Number of full waves in the circumferential direction
N	Applied axial force per unit length of circumference
n_ϕ, n_x	Number of stiffeners in each direction
N_x, N_ϕ	Force resultants
P	Applied axial load, lbs.
p	Radial pressure, lbs/inch^2

Symbol	Description
P.B.	Panel buckling, N/N_{cr}
Q	Applied uniform external lateral pressure, $lbs/inch^2$
R	Cylinder radius or mid-plane radius of cone, inches
R^*	$(1 + R_R - 1/R_R)\ R_1 \cos(\xi)$, inches
R_1	Radius at small end of cone, inches
R_2	Radius at large end of cone, inches
R_A	Ratio of applied axial load to allowable (P/P_{CR})
R_B	Ratio of applied bending moment to allowable (M/M_{CR})
R_P	Ratio of applied lateral pressure to allowable (Q/Q_{CR})
R_R	$\sqrt{1/2(1 + R_2/R_1)}$
S	$(h_y/h)(1-\mu^2)$
S.B.	Skin buckling, σ_{xp}/σ_{xcr}
S.Y.	Skin yield, σ_D/σ_{OD}

Symbol	Description
T	Shell wall temperature, degrees F.
t	Stiffener thickness
$\bar{t}$	Equivalent thickness of monocoque cylinder of equal weight
T_x, T	Torsional stiffnesses of stiffeners
$T_s, t_x, t_\phi, d_x, d_\phi, \ell_x, \ell_\phi$	Design variables
U	Factor of utilization
U.B.	Upper bound
V	Applied shear load, lbs.
W	Weight of cylinder
w_A	Allowable load/inch due to axial load, lbs/inch
w_B	Allowable load/inch due to bending moment (MAX), lbs/inch
w_s	Allowable maximum load/inch due to shear, lbs/inch.
w_p	Allowable load/inch due to lateral pressure, lbs/inch

Symbol	Description
Z	Curvature parameter $[B^2(1-\mu^2)^{1/2}/hR\cos(\xi)]$
$\overline{Z}$	$\pi^2/6\ C_A\sqrt{1-\mu^2}$
Z^*	$\frac{B^2(1-\mu^2)^{1/2}}{R^*h}$
β	$R_1/[h\cos(\xi)]$
β_1	$e^{-\sqrt{\beta}/16}$
$\gamma, \gamma_A, \gamma_B, \gamma_P, \gamma_S$	Interaction equation exponent
γ	Weight density, lbs/inch^3
$\gamma_x, \gamma_\phi, \gamma_x$	Weight densities of the skin, circumferential stiffeners, and longitudinal stiffeners
$\delta_{x\phi}, \delta_{xw}, \delta_{\phi w}$	Weight densities of the skin, circumferential stiffeners, and longitudinal stiffeners
$\varepsilon_x, \varepsilon_\phi, \gamma_{x\phi}$	Strains
$\varepsilon_{\phi cr}$	Buckling strain of circumferential stiffener
$\varepsilon_{xp}, \sigma_{\phi p}$	Prebuckle strains
ζ	Ratio of stiffener depth to the radius of its unsupported edge

Symbol	Description
η	Ratio of allowable to elastic buckling stress (plasticity correction factor)
θ_x, θ_ϕ	Rotation of shell per unit length
λ	$m\pi R/L$
λ, η	Wave parameters
μ, ν	Poisson's ratio
μ_x, μ_ϕ	Poisson's ratios of skin
ρ	Density of material, lbs/inch^3
ρ_x, ρ_ϕ	Radii of gyration of stiffeners about the skin midsurface
σ_A	Allowable buckling stress (axial), lbs/inch^2
σ_B	Allowable buckling stress (bending) lbs/inch^2
σ_C	Critical buckling stress in longitudinal stiffeners
σ_P	Allowable buckling stress (pressure), lbs/inch^2

Symbol	Description
σ_S	Allowable buckling stress (shear), lbs/inch^2
σ_y	Yield stress, lbs/inch^2
α_A/η	Elastic buckling stress (axial), lbs/inch^2
σ_B/η	Elastic buckling stress (bending), lbs/inch^2
$\sigma_{OD}, \sigma_{xOT}, \sigma_{xOC}, \sigma_{\phi OT}, \sigma_{\phi OC}$	Yield stresses in skin
σ_p/η	Elastic buckling stress (pressure), lbs/inch^2
$\sigma_x, \sigma_\phi, \tau_{x\phi}$	Stresses in skin
$\sigma_{xp}, \sigma_{\phi p}$	Prebuckle stresses in skin
$\sigma_{xs}, \sigma_{\phi s}$	Stresses in stiffeners
$\sigma_{xSOC}, \sigma_{xSOT}, \sigma_{\phi SOC}, \sigma_{\phi SOT}$	Yield stresses in stiffeners
$\sigma_{xsp}, \sigma_{\phi sp}$	Prebuckle stresses in stiffener
σ/η	An elastic buckling stress
τ	Applied torsion moment, inch-lbs.
ξ	Semivertex angle of cone, degrees
σ_s/η	Elastic buckling stress (shear),lbs/inch^2

APPLICATION OF MULTIVARIABLE SEARCH TECHNIQUES TO STRUCTURAL DESIGN OPTIMIZATION

By R. T. Jones and D. S. Hague

SUMMARY

Multivariable search techniques are applied to a particular structural design problem, that of determining the minimum weight design for a stiffened cylindrical shell subject to multiple load conditions. The cylinder is stiffened in both longitudinal and circumferential directions. Stability analyses are limited to linear bifurcation buckling theory. A variety of multivariable search techniques embodied in an existing non-linear optimization code, AESOP, are applied to this design problem. These techniques include elementary single parameter perturbation methods, organized search such as steepest-descent, quadratic, and Fletcher-Powell methods, randomized procedures, and a generalized search acceleration technique. Design variables are seven in number and define stiffener spacings, stiffener dimensions, and skin thickness. The relative efficiency of the techniques are compared. It is shown that a combination of search strategies may be superior to any one strategy in the solution of the structural design optimization problem considered. It is also shown that more than one local extremal design may exist in the class of problem treated; however, these multiple extremals are apparently the result of *non-convex constraint boundaries*.

In general, the multiple extremal problem may be treated by the warping transformation introduced by Hague in reference 1. This approach was applied to stiffened cylinder design in the present study. However, the solutions converged reliably to a unique solution with or without the transformation. The exterior penalty function approach itself, when properly applied, is able to effectively define the global constrained extremal design. The multiple extremal warping transformation was applied to an elementary unconstrained two-variable two-extremal optimization problem during the study. The transformation consistently obtained both extremal solutions. The optimal solutions reported here were obtained by application of a generalized multivariable search code, AESOP, originally constructed under contract to the National Aeronautics and Space Administration's Office of Advanced Research and Development. Original documentation of this code is given in references 1 to 3; an outline of the analysis underlying this code is presented below.

MULTIVARIABLE SEARCH

The general non-linear multivariable optimization problem is concerned with the maximization or minimization of a *pay-off* or *performance function* of the form

$$\phi = \phi(\alpha_i), \quad i = 1, 2, \ldots, N \tag{1}$$

Subject to an array of constraints

$$C_j = C_j(\alpha_i) = 0, \quad j = 1, 2, \ldots, p \tag{2}$$

The α_i are the *independent variables* whose values are to be determined so as to maximize or minimize the performance function $\phi(\alpha_i)$ subject to the constraints of equation (2). The α_i may be looked upon as the components of a *control vector*, $\bar{\alpha}$, in a space R^N of dimension N. Since maximization of a function is equivalent to minimization with a change of sign, it suffices to discuss the case in which the performance function is to be *minimized*.

Multivariable optimization problems involving *inequality constraints* may also be encountered. If the constraints are applied directly to the independent variables

$$\alpha_i^L < \alpha_i < \alpha_i^H \tag{3}$$

the inequality constraints define a region of the control space within which the solution must lie. Inequality constraints on *functions of the independent variables* similarly restrict the region in which the optimal solution is to be obtained. In this case

$$E_k^L(\alpha_i) \leq E_k(\alpha_i) \leq E_k^H(\alpha_i) \tag{4}$$

Inequality constraints can be used to restrict the search region directly, or, alternatively, they may be applied in an indirect fashion by a *transformation to equality constraints*. Several transformations may be used for this purpose. For example, let an equality constraint, C_k, be defined by the transformation

$$C_k = \begin{cases} (E_k^L - E_k)^2, & E_k < E_k^L \\ 0, & E_k^L \leq E_k \leq E_k^H \\ (E_k^H - E_k)^2, & E_k^H < E_k \end{cases} \tag{5}$$

Constraining C_k to zero will result in the constraint of equation (4) being satisfied.

Problems involving equality constraints can be treated as unconstrained problems by replacing the actual performance function, $\phi(\alpha_i)$, by an *augmented performance function*, ϕ^*, where

$$\phi^* = \phi + \sum_{j=1}^{P} U_j C_j^2 \qquad (6)$$

It can be shown that, provided the positive weighting constants U_j are sufficiently large in magnitude, minimization of the performance function subject to the constraints, equation (2), is equivalent to minimization of the unconstrained penalized performance function defined by equation (6). This approach permits search techniques for finding unconstrained minima to be applied in the solution of constrained minima problems *at the cost of some increased complexity* in the behavior of the performance function, the performance *response surface*. In practical application, the weighting constants U_j are determined *adaptively* on the basis of response surface behavior.

Alternatives to this approach are available, notably Bryson's approach to the steepest-descent search, reference 4. This method has been exploited in connection with the numerical solution of variational problems encountered in the optimization of aerospace vehicle flight paths, references 5, 6, and 7. However, the use of such techniques implies *smoothness* of the response surface. This smoothness may not be present in general; hence, the AESOP code is limited to the less restrictive penalty function approach of equation (6)

Numerical Solution of Non-Linear Multivariable Optimization Problems

This section is devoted to a discussion of the search algorithms for solution of non-linear multivariable optimization problems available in the AESOP code. A wide variety of search algorithms have been devised for the solution of multivariable optimization problems. Many of these algorithms are restricted to the solution of linear or quadratic problems. Algorithms of this type must be supplemented by more general search procedures if generality of solution is sought; for engineering problems tend to lead to non-linear formulation with the possibility of discontinuities in both the performance function response surface and its derivative. Most of the searches which prove effective in these problems combine a direction generating algorithm,such as steepest-descent, with with a one-dimensional search. Distance traversed through the control space in the selected direction is measured by a step-size, or perturbation parameter, DP. The object of the one-dimensional search is to determine the value of DP which minimizes the performance function along the chosen ray and to establish the corresponding control vector.

In practice, the diverse nature of non-linear multivariable optimization problems leads to the conclusion that no one search algorithm can be uniquely described as being the "best" in all the situations which may be encountered. Rather, a combination of searches, some of which may be of quite elementary nature, provides the most reliable and economical convergence to the optimal solution.

One-dimensional search. Multivariable search problems are reduced to one-dimensional problems whenever a search algorithm is used to establish a one-to-one correspondence between the control vector and a single scalar perturbation parameter, (DP). In such a situation

$$\alpha_i = \alpha_i(DP), \quad i = 1, 2, \ldots, N \tag{7}$$

so that equation (1) becomes

$$\phi = \phi(\alpha_i) = \phi(DP) \tag{8}$$

Similarly, the right hand sides of equations (2) and (6) become functions of the scalar perturbation parameter.

The relationship, equation (7), specifies a ray through the control space. As noted above, the objective of the one-dimensional search along this ray is to locate the value of DP which provides the minimum performance function value.

Numerical search for the one-dimensional minima can be carried out in a local fashion, by the Newton-Raphson method, for example, or by a global search of the ray throughout the feasible region. The localized polynomial approximation is appropriate to the *terminal convergence phase* in a problem solution when some knowledge of the extremal's position has been accumulated by the preceding portion of the search and the problem involves a smooth function. The global search can be used to advantage in the *opening moves* of a search. In the early phase of a search the object is to isolate the approximate neighborhood of the minimum performance function value as rapidly as possible, usually with little or no foreknowledge of the performance function behavior. One measure of the effectiveness of a search algorithm in such

a situation is the number of evaluations required to locate the minimum point to some prespecified accuracy. It can be shown that the most effective method of locating the minimum point of a general unimodal function is a *Fibonacci search*, reference 8. In this method, the accuracy to which the minimum is to be located along the perturbation parameter axis must be selected prior to the commencement of the search. Since the accuracy required is highly dependent on the behavior of the performance function, this quantity is difficult to prespecify.

Prespecification of the accuracy to which the extremal's position is to be located can be avoided for little loss in search efficiency by use of an alternative search based on the so-called golden section, reference 8. This is the method employed in the AESOP code one-dimensional search procedure. Search by the golden section commences with the evaluation of the performance function at each end of the search interval and at $G = 2/(1 + \sqrt{5})$ of the interval from both of these bounding points. This is illustrated in Figure 1.

The boundary point furthest from the lowest resulting performance function value is discarded. The three remaining points are retained, and the search continues in a region which is diminished in size by G. The internal point at which the performance function is known in the reduced interval will be at a distance G of the reduced interval from the remaining bounding point of the original interval for $(1 - G) = G^2$. The search can, therefore, be continued in the reduced interval with a single additional evaluation of the performance function. It follows after Q evaluations of the performance function that the position of the extremal point will be known to within R of the original search region

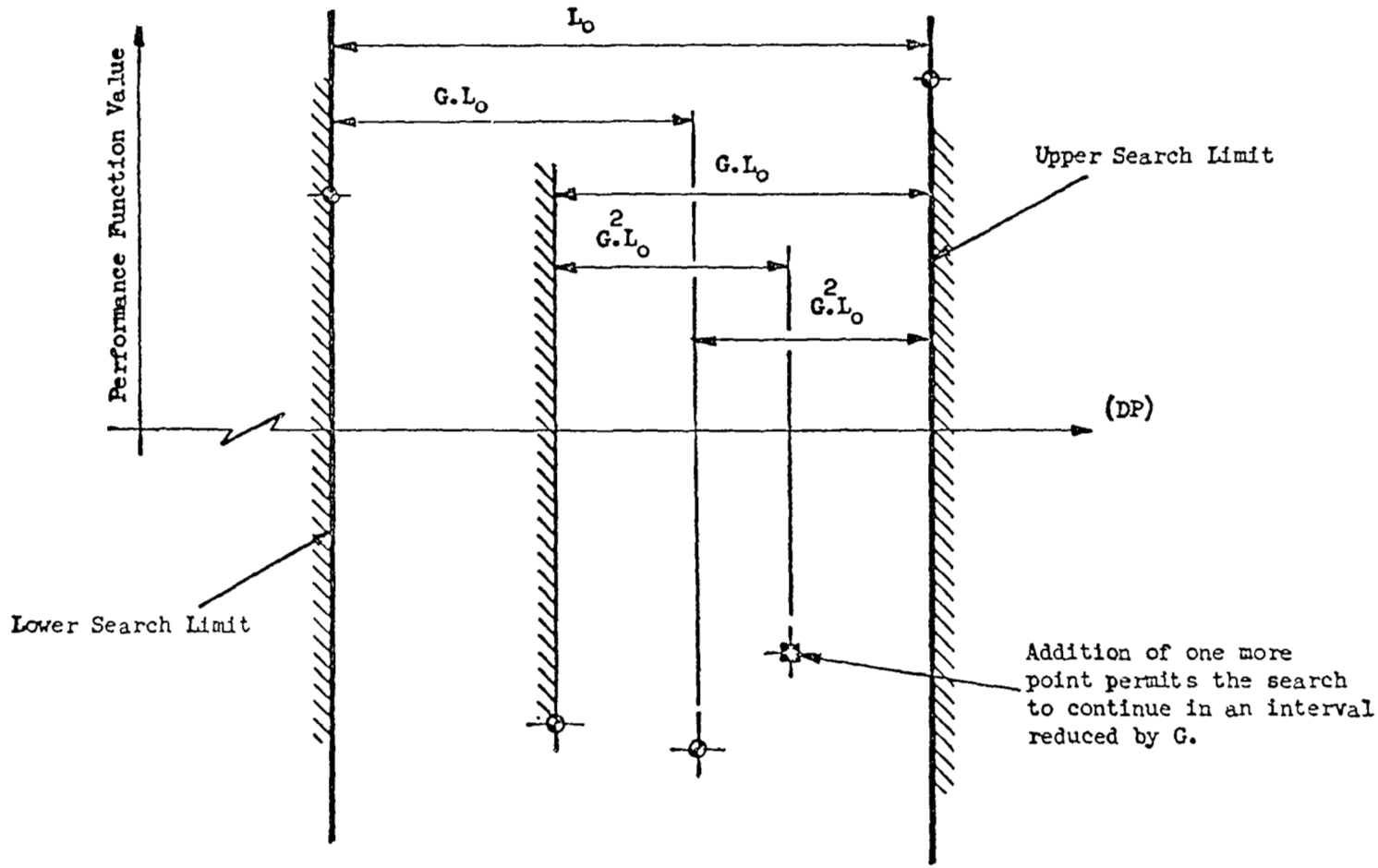

FIGURE 1. SEARCH BASED ON THE GOLDEN SECTION

where

$$R = G^{(Q-3)} \tag{9}$$

To reduce the interval of uncertainty to .00001 of the original search interval, about 27 evaluations of the performance function are required. For a reasonable number of evaluations of the performance function this type of search is almost as efficient as a Fibonacci search.

It should be noted that search by the golden section proceeds under the assumption of unimodality; hence, it will often fail to detect the presence of more than one minimum when the performance function is multimodal. If more than one minimum does exist, the one located depends on performance function behavior within the original search interval.

Multiple Extremals on One-Dimensional Ray. The one-dimensional section search described above is unable to distinguish one local extremal from another; it will merely find one local extremal. This difficulty can be largely eliminated by the addition of some logic to the search, at least for moderately well behaved performance functions; that is, for functions having a limited number of extremals in the control space region of interest. An effective method for detecting multiple extremals is to combine the one-dimensional search with a random one-dimensional search on the same ray through the control space. This is illustrated in figures 2 and 3. In figure 2 the response contours of a performance function having two minima are illustrated together with the initial points used in a global one-dimensional search by the golden section method. The behavior of the function at these points is shown in figure 3. The left hand minimum is not apparent from these points. If a single random point is added in the interval L_0, the probability of this point revealing the

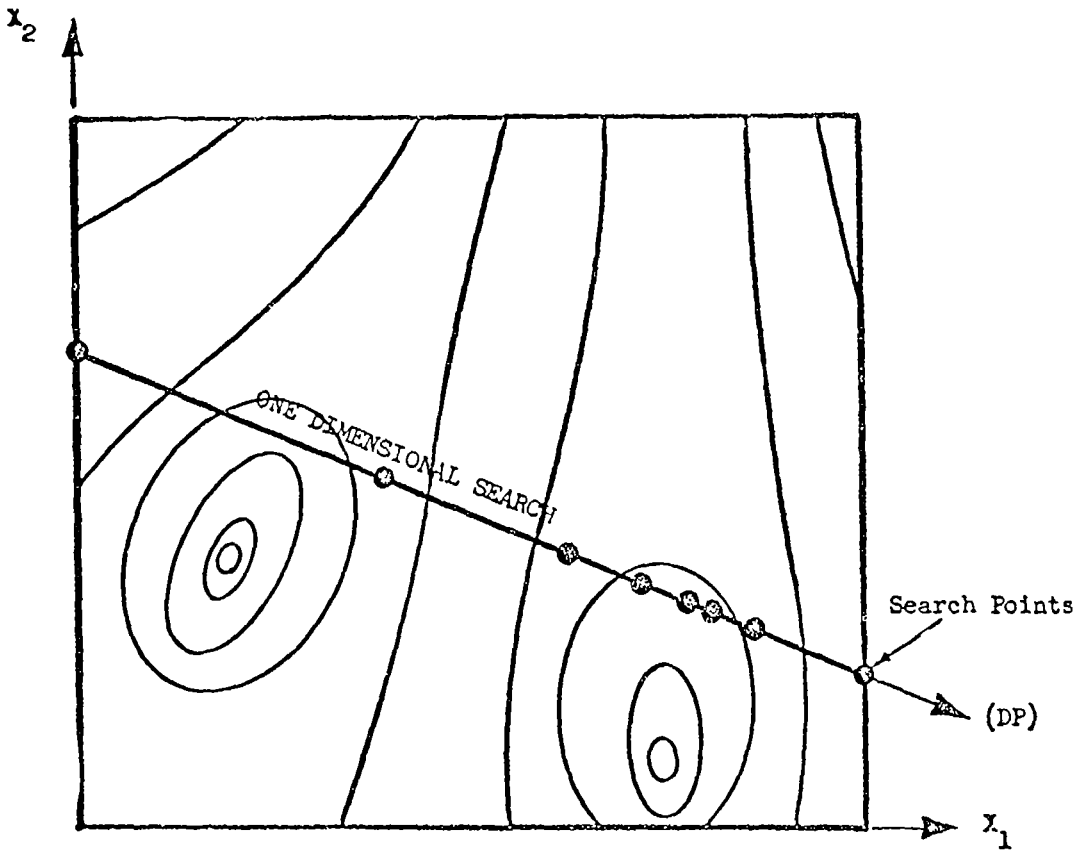

FIGURE 2. RESPONSE SURFACE WITH TWO TROUGHS

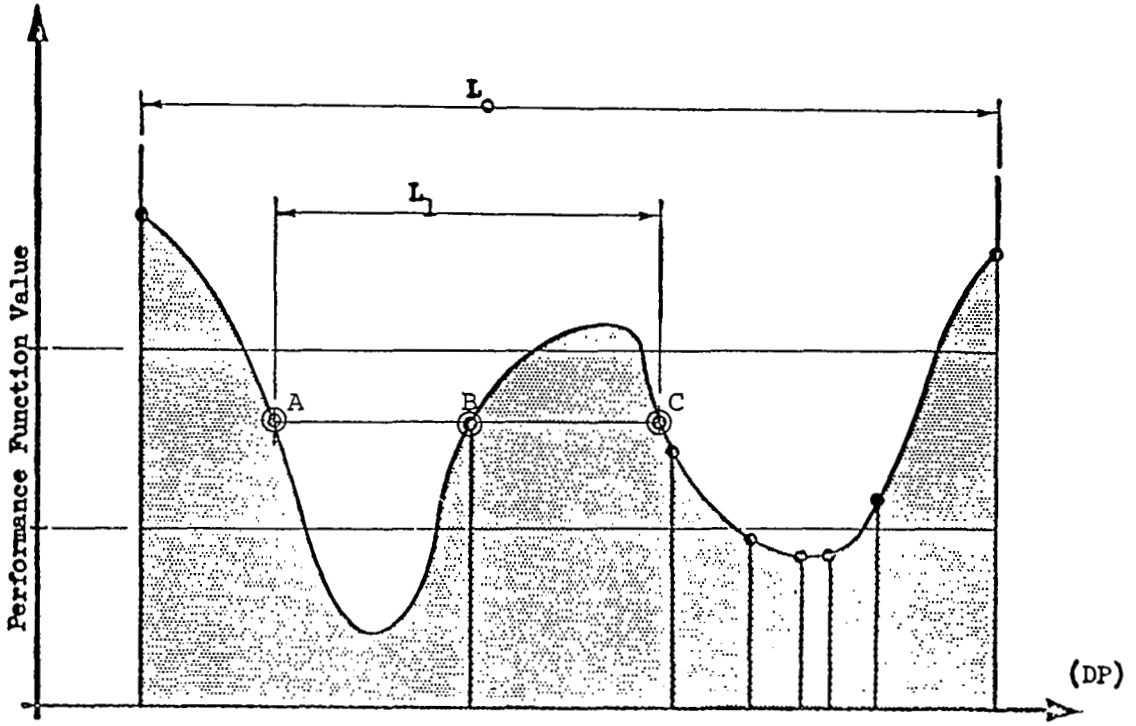

FIGURE 3. SEARCH BY GOLDEN SECTION FAILS TO DETECT MULTIPLE TROUGHS ON ONE DIMENSIONAL CUT

presence of the second minimum is

$$P_1 = L_1/L_o \tag{10}$$

for any point in the interval AB indicates the presence of a local minimum somewhere in the interval AB, and any point in the interval BC indicates the presence of a local maximum somewhere in the interval BC. In this latter case, there must be a minimum of the function both to the left and to the right of the newly introduced point.

If R random uniformly distributed points are added in the interval L_o, the probability of locating the presence of the second minimum becomes

$$P_R = 1.0 - (1.0 - L_1/L_o)^R \tag{11}$$

The function (L_1/L_o) is a measure of the performance function behavior. For a given value of this behavior function the number of random points which must be added to the one-dimensional search to provide a given probability of locating a second minimum can be determined.

The presence of multiple minima on a one-dimensional cut through an N-dimensional space does not necessarily indicate that the performance function possesses more than one minimum in a multi-dimensional sense. It may be that the performance function is merely non-convex. This is illustrated by figure 4. The performance function behavior on the one-dimensional search in figures 2 and 4 is identical. In figure 2 this indicates the presence of two local extremals; in figure 4, a non-convex performance function.

When a one-dimensional search detects the presence of multiple extremals in the local sense above, a decision must

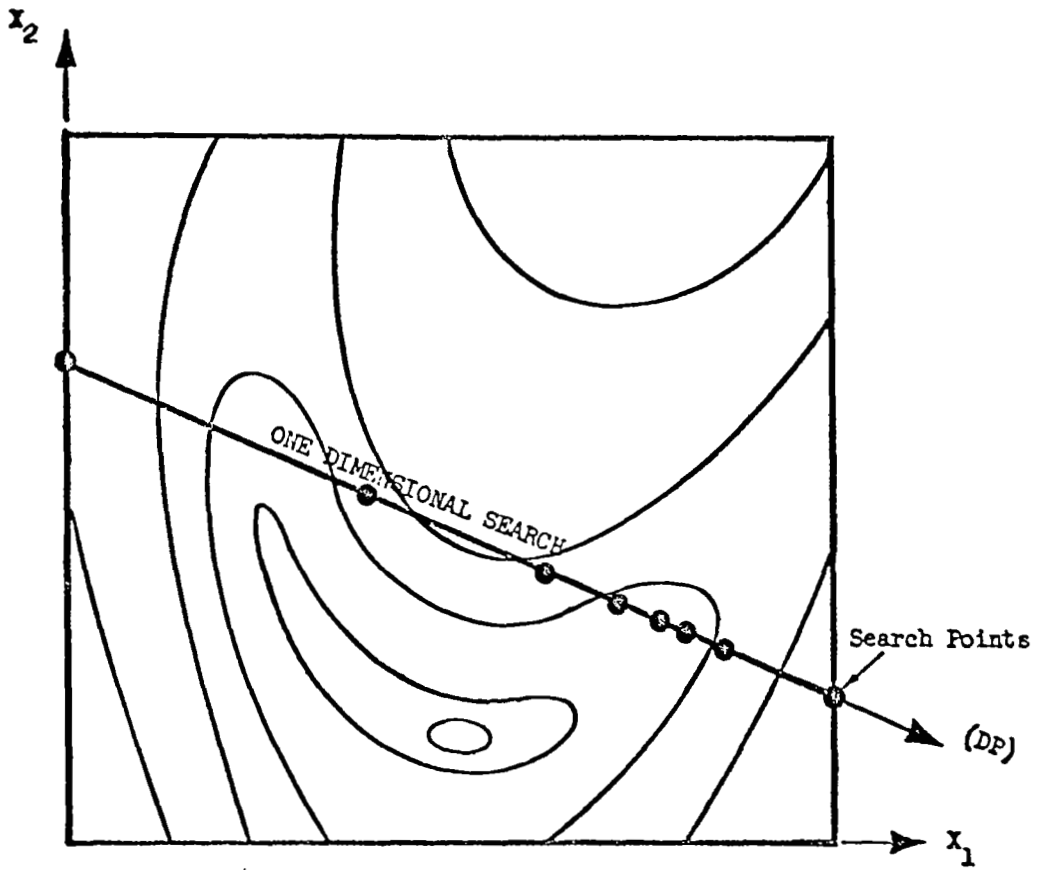

FIGURE 4.-NON-CONVEX RESPONSE SURFACE

be made as to which of the apparent extremals is to be pursued during the remainder of the search. Here, without foreknowledge of the performance function behavior, logic must suffice. Typically, the left or right hand extremal, the extremal which results in the best performance, or even a random choice may be made.

It should be noted that logic of this type is not currently available in the AESOP code. The AESOP one-dimensional search procedure has three distinctive phases. *First*, each search algorithm defines an initial perturbation using either past perturbation stepsize information or a perturbation magnitude prediction as in the quadratic search below. *Second*, a perturbation stepsize doubling procedure is employed until a point exhibiting diminishing performance is generated. *Third*, having coarsely defined the one-dimensional extremal position from steps one and/or two, a golden section search is employed to locate the extremal with reasonable precision.

Multiple extremals - general procedure. The multiple extremal search technique included in AESOP is based on *topologically invariant warping* of the performance response surface. The response surface is warped in a manner which retains all the surface extremals but alters their relative locations and *regions of influence*. The region of influence of an extremal is defined as the hull or collection of all points which lead to the extremal if a gradient path is followed. Reducing the region of influence of an extremal

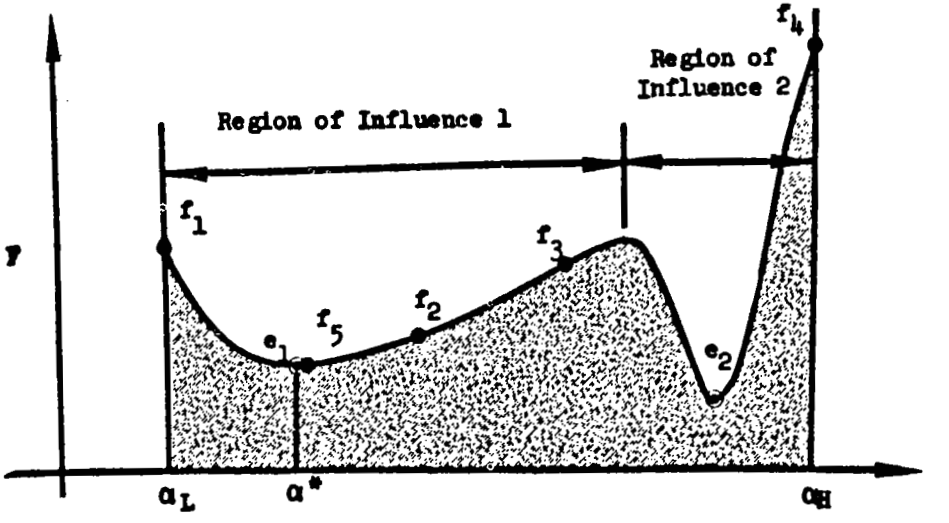

FIGURE 5. FUNCTION WITH TWO EXTREMALS

decreases the *probability* of locating a point in the neighborhood of the extremal if points are chosen at random. Again, in an organized multivariable search, the probability of locating an extremal having a small region of influence is less than that of locating an extremal having a large region of influence. For example, suppose the extremals of the one-dimensional function of figure 5 are to be determined in the range $\alpha_L < \alpha < \alpha_H$ by the sectioning approach. The four initial values employed in this technique are denoted by f_1 to f_4.

Following evaluation at these four points, f_4 is discarded, and the function is evaluated at f_5. At this point the right-hand extremal, e_2, has been eliminated from the search which now inevitably proceeds to the left hand extremal at e_1.

To find the second extremal, the Function F is warped by writing

$$F(\xi) = F(\alpha) \qquad (12)$$

$$\xi = (\alpha_H - \alpha^*)\left[\frac{\alpha-\alpha^*}{\alpha_H-\alpha^*}\right]^{2N} + \alpha^*; \quad \alpha > \alpha^*$$

$$\xi = -(\alpha^*-\alpha_L)\left[\frac{\alpha^*-\alpha}{\alpha^*-\alpha_L}\right]^{2N} + \alpha^*; \quad \alpha^* > \alpha \qquad (13)$$

where N is a positive integer, and α^* is the location of the left hand extremal.

A typical relationship between ξ and α is shown in figure 6 for the case N = 1. Differentiation of equation (13) with respect to α when N = 1 results in

$$\xi' = \frac{2[\alpha-\alpha^*]}{[\alpha_H-\alpha^*]}; \quad \alpha \geq \alpha^*$$

$$\xi' = \frac{2[\alpha^*-\alpha]}{[\alpha^*-\alpha_L]}; \quad \alpha < \alpha \qquad (14)$$

Note that as $\alpha \to \alpha^*$, $\xi' \to 0$ from both the left and right. At $\alpha = \alpha_L$ and at $\alpha = \alpha_H$, $\xi' = 2$. In the regions $\alpha_L < \alpha < \alpha^*$ and $\alpha^* < \alpha < \alpha_H$, ξ varies parabolically with α. Figure 6 illustrates these points. It can be seen that a region $\Delta\alpha_1$ centered about α^* transforms into a smaller region $\Delta\xi_1$ located in the neighborhood of $\xi = \alpha^*$. On the other hand, a region $\Delta\alpha_2$ situated in the

neighborhood of the upper search limit, α_H, maps into a wider region in the neighborhood of $\xi = \alpha_H$. In general, the slopes at $\alpha = \alpha_L$ and $\alpha = \alpha_H$ are given by 2N; the greater N, the greater the warping becomes.

The effect of introducing a moderate warping transformation on the function of figure 5 is shown in figure 7. It can be seen from figure 7 that the region of influence of e_1 is reduced, and the region of influence of e_2 is increased. On the warped surface search by sectioning commences with evaluations of performance at f_1' to f_4'. Following these initial evaluations f_1' is discarded (as opposed to the discard of f_4 on the unwarped surface), and the function is evaluated at the additional point f_5'. The points f_3' and f_5' straddle the extremal e_2 which is now inevitably located by further sectioning evaluations. Figures 8a to 8j illustrate the warping transformations for a range of N between 1 and 10 when the transformation is applied at the point $\alpha^* = .5$, the symmetric case. It can be seen that when N = 1, twenty per cent of the warped control space corresponds to approximately 45 per cent of the unwarped control space in the vicinity of the transformation origin ($\alpha = .5$). When N = 10 twenty per cent of the warped control space transforms into ninety per cent of the unwarped control space.

Sectioning Parallel to the Axes. The independent variable perturbation algorithm in the sectioning search is

$$\begin{aligned} \Delta\alpha_i &= 0, \quad i \neq r \\ &= DP, \quad i = r \quad r = 1, 2, \ldots, N \end{aligned} \tag{15}$$

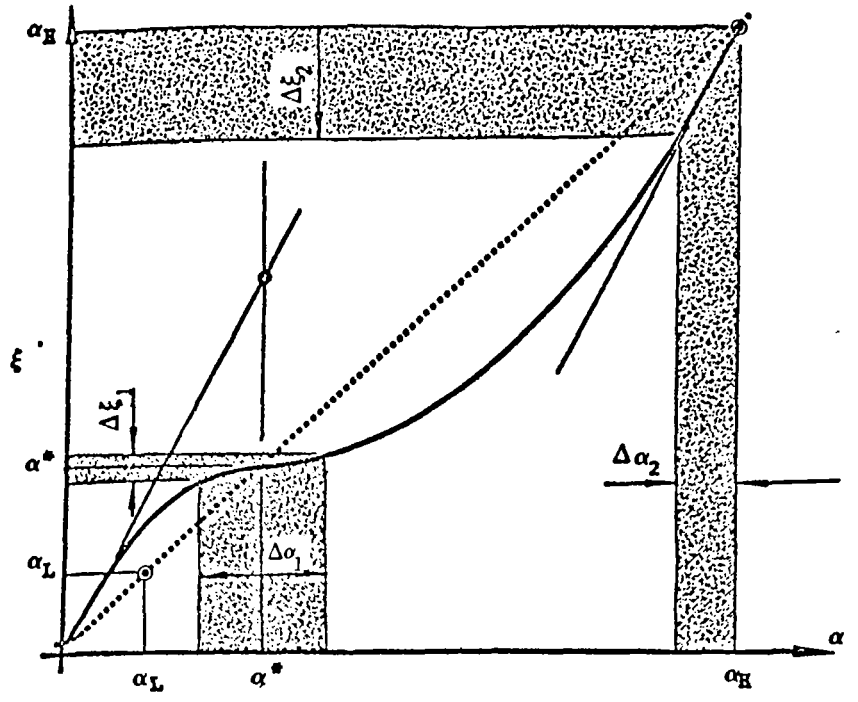

FIGURE 6. WARPING TRANSFORMATION

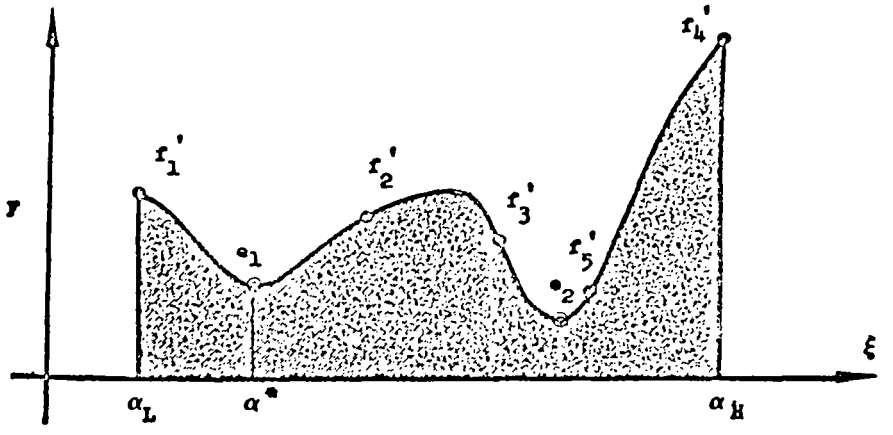

FIGURE 7. TRANSFORMED FUNCTION WITH TWO EXTREMALS

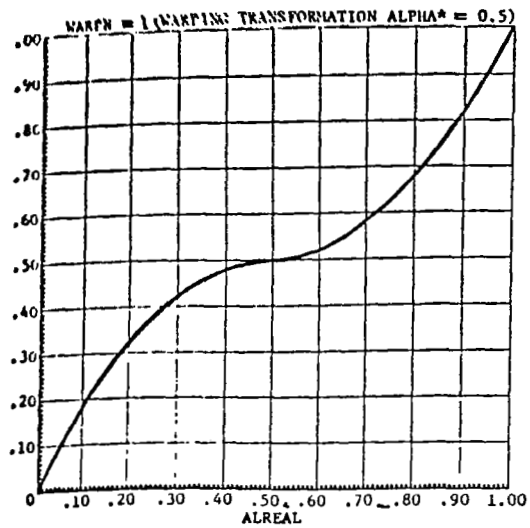

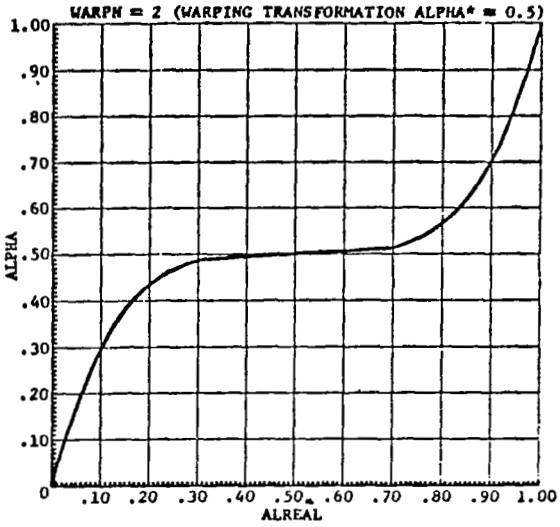

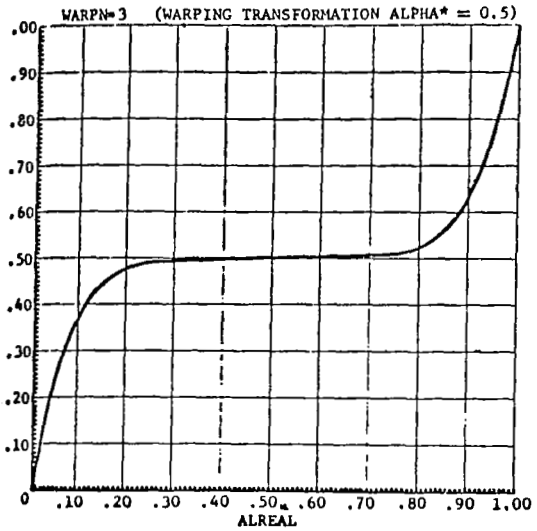

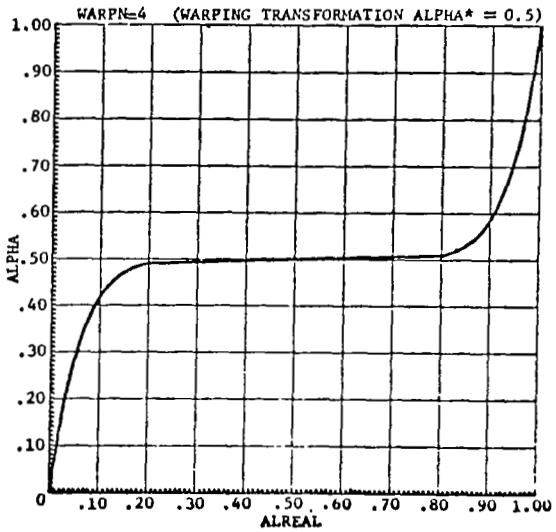

FIGURES 8(a) to 8(d). WARPING TRANSFORMATION N = 1 to 4

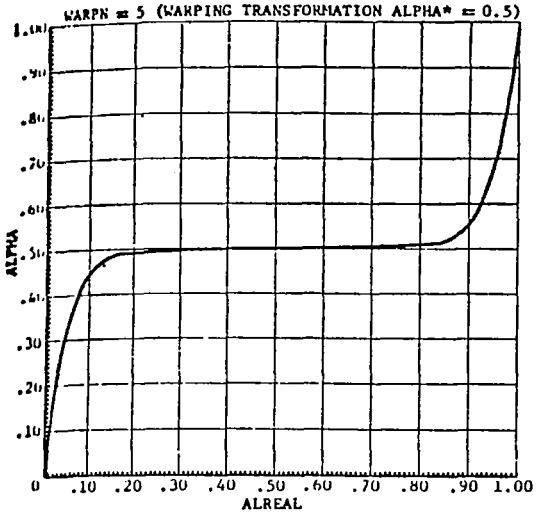

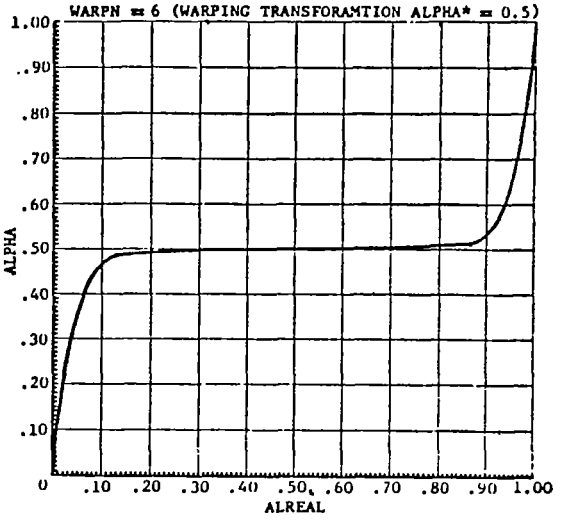

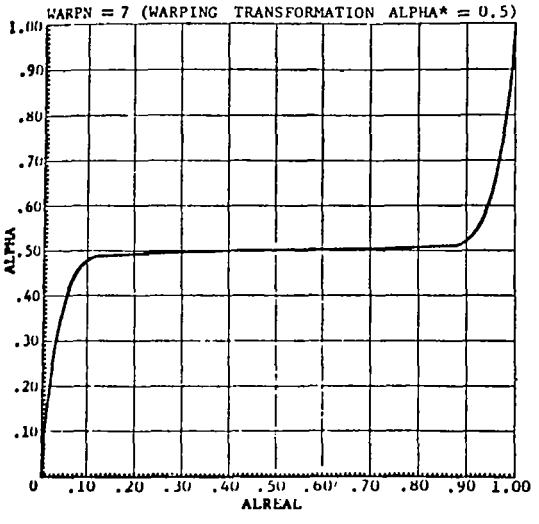

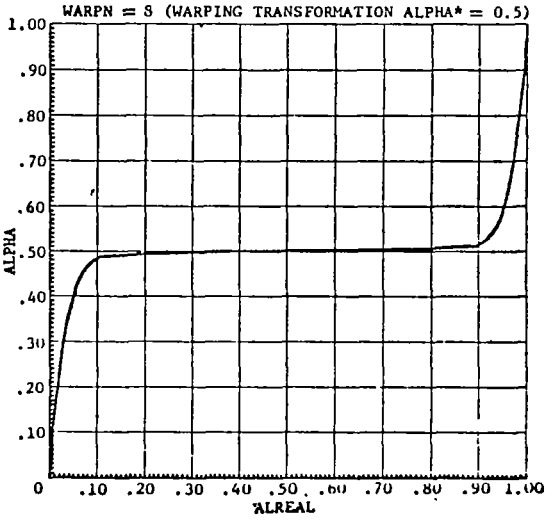

FIGURES 8(e) to 8(h). WARPING TRANSFORMATION N = 5 to 8

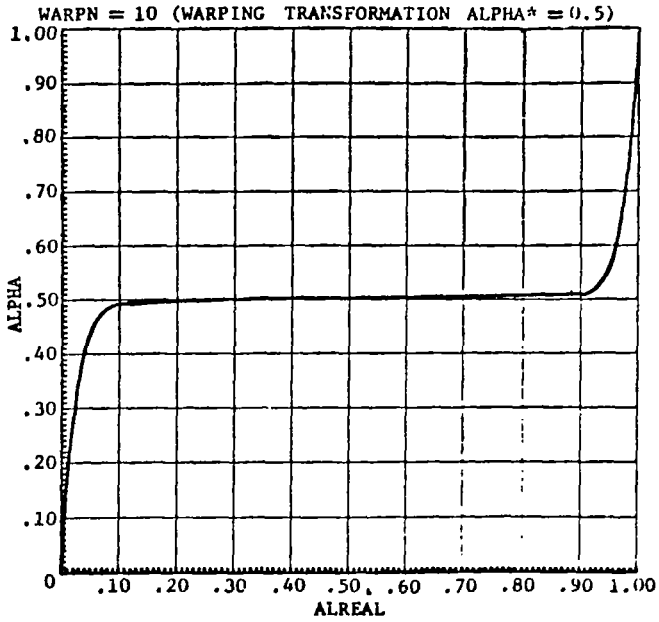

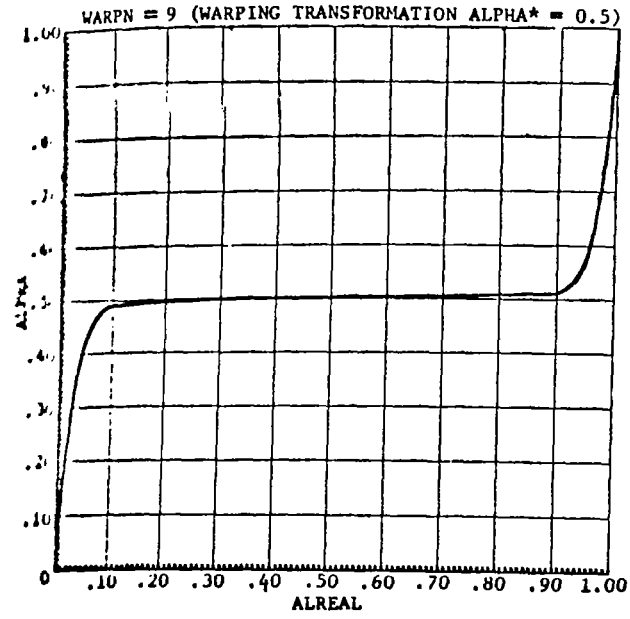

FIGURES 8(i) and 8(j). WARPING TRANSFORMATION N = 9 and 10

This is simply the parametric or univariate search approach. All but one of the independent variables are held constant while a one-dimensional search parallel to the R^{th} variable axis determines the best value of the remaining variable, α_r. The variable α_r is then *set to this value*, and the process is repeated with one of the remaining independent variables. When all N independent variables have been perturbed in this way, a sectioning search cycle has been completed.

The N-dimensional search can then be continued with another cycle of sectioning or by one of the other search techniques described below. In practice, it has been found advantageous to *perturb the independent variables in a random order* within each sectioning cycle. The method can be used in conjunction with either a local or a global search as outlined in the two preceding sections. The behavior of this search in the solution of a straightforward two-variable optimization problem is illustrated in Figure 9. It may be noted that the AESOP code searches from boundary to boundary in each variable using a golden section search procedure.

Sectioning to Define Local Sensitivities. The sectioning search can readily be applied to the problem of performance or constraint sensitivity determination. Thus, by the device of omitting the updating of each control variable α_r following the sectioning search on the r^{th} parameter, the sequence of sectioning searches is performed about a fixed nominal point. When such a search is performed in the vicinity of a known extremal point, the penalties for off-optimal design can be assessed. Away from an extremal point, the search merely provides local sensitivities in a similar manner to the manual perturbation methods employed in *conventional trial and error* design evolution.

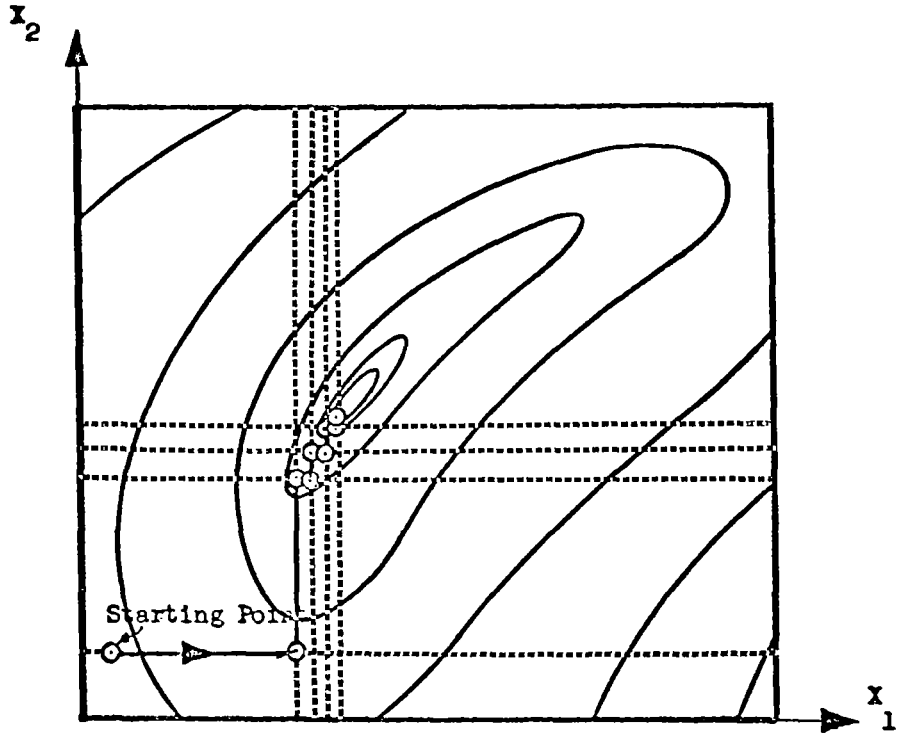

FIGURE 9. SECTIONING PARALLEL TO THE AXES

Steepest-Descent Search. The steepest-descent search algorithm is

$$\{\Delta\alpha\} = -[W]^{-1}\left\{\{\frac{\partial\phi}{\partial\alpha}\} - [\frac{\partial C}{\partial\alpha}]^T[K_3]^{-1}\{K_2\}\right\}$$

$$\times \frac{\sqrt{(DP)^2 - DC\ [K_3]^{-1}\{DC\}}}{K_1 - K_2\ [K_3]^{-1}\{K_2\}}$$

$$- [W]^{-1}\ [\frac{\partial C}{\partial\alpha}]^T\ [K_3]^{-1}\ \{DC\} \qquad (16)$$

Here, the *matrix W is the metric tensor* of the control space and serves to define a generalized measure for the *magnitude* of a control vector perturbation. The vectors $\{\partial\phi/\partial\alpha\}$ and $\{\partial C/\partial\alpha\}$ are defined as

$$\left\{\frac{\partial\phi}{\partial\alpha_1}, \frac{\partial\phi}{\partial\alpha_2}, \ldots \frac{\partial\phi}{\partial\alpha_n}\right\}$$

and

$$\left\{\frac{\partial C}{\partial\alpha_1}, \frac{\partial C}{\partial\alpha_2}, \ldots \frac{\partial C}{\partial\alpha_n}\right\}$$

respectively. The K matrices are defined as

$$K_1 = \left[\frac{\partial\phi}{\partial\alpha}\right][W]^{-1}\ \{\frac{\partial\phi}{\partial\alpha}\} \qquad (17)$$

$$\{K_2\} = [\frac{\partial C}{\partial\alpha}][W]^{-1}\{\frac{\partial\phi}{\partial\alpha}\} \qquad (18)$$

$$[K_3] = [\frac{\partial C}{\partial\alpha}][W]^{-1}\ [\frac{\partial C}{\partial\alpha}]^T \qquad (19)$$

The perturbation parameter, (DP), is defined by

$$(DP) = \lfloor \Delta\alpha \rfloor [W] \{\Delta\alpha\} \tag{20}$$

The vector $\overline{DC}$ is the *desired change in the constraint functions*. For an unconstrained problem,(16) reduces to

$$\{\Delta\alpha\} = -[W]^{-1}\{\frac{\partial\phi}{\partial\alpha}\} \sqrt{\frac{(DP)^2}{K_1}} \tag{21}$$

The performance function change associated with the perturbation of equation (16) is

$$D\phi = -\left(K_1 - \lfloor K_2 \rfloor [K_3]^{-1} \{K_2\}\right)^{.5} \left((DP)^2 - \lfloor DC \rfloor [K_3]^{-1} \{DC\}\right)^{.5} + \lfloor K_2 \rfloor [K_3]^{-1} \{DC\} \tag{22}$$

Equation (16) does not specify a one-dimensional search directly since the perturbation parameter (DP) and each component of the constraint vector change $\overline{DC}$ can be independently specified. This difficulty is conveniently eliminated if the components of $\overline{DC}$ are expressed in terms of the perturbation parameter. Let (DP) and $\overline{DC}$ be arbitrarily assigned, say (DP_0) and $\overline{DC}_0$, respectively. Now consider the one parameter set of values for $\overline{DC}$ defined by

$$\overline{DC} = \left(\frac{DP}{DP_0}\right) \cdot \overline{DC}_0 \tag{23}$$

It follows from equations (16) and (22) that (23) specifies a one parameter family of perturbations in which the non-linear performance and constraint functions *vary linearly with (DP)*, to the first order.

Equations (16) to (22) are valid for small perturbations in the independent variables provided the derivatives involved are *continuous in the region of the control space* defined by equation (20). In practice, when this condition is not satisfied, the steepest-descent algorithm can be used to locate a promising direction for a one-dimensional search provided the derivatives are computed numerically. In this case, however, equation (22) ceases to provide an accurate indication of performance function behavior along the specified ray.

When dealing with performance and constraint functions having continuous first derivatives, the perturbation parameter value to be used in equation (16) can be determined from a second order Taylor's expansion of the performance function behavior in terms of DP. The coefficients in this series expansion can be readily obtained from the conditions of zero change for DP = 0, linear slope for DP = 0, and from the actual value of the performance function at a point in the neighborhood of the point at DP = 0. This method for determining the best perturbation parameter value is discussed in some detail in references 5 and 6. When dealing with less regular functions, the one-dimensional search by sectioning can be used to determine the perturbation parameter value. This is the technique employed in the optimization program, AESOP, references 1 and 2; for the AESOP code converts all

constrained optimization problems to unconstrained problems by the penalty function device, equation (6). The resulting response surface combines both performance function and weighted constraint functions. Inevitably, this surface has a more complex topology than that of the unconstrained performance function. Program AESOP is also limited to the penalty function approach to constrained optimization, and, hence, it utilizes the reduced algorithm of equation (21) rather than the explicit constraint algorithm of equation 16.

Steepest-Descent Weighting Matrices. The weighting matrix introduced in equations (16) and (20) must be *positive definite* to assure a positive distance between any two non-coincident points in the control space. Apart from this restriction, the choice of weighting matrix is arbitrary. Inspection of equation (16) reveals that any descending direction is a steepest-descent path for some choice of the weighting matrix W. This can be simply illustrated when only two independent variables are involved. Figure 10 depicts a small region of the control space R^2. The performance function response contours appear as a series of parallel lines on this microscopic region of the control space. The perturbation zones corresponding to three weighting matrix choices are shown. The first zone corresponds to the choice of a unit matrix for W. It follows from equation (20) that for a given value of $(DP)^2$ the search zone is a circle of radius (DP). The steepest-descent direction is that in which the performance improvement is greatest. This is the direction of a line from the origin

of the circular search zone to that point on its circumference which provides the smallest value of the performance function $\phi(\bar{\alpha})$. With this choice of weighting matrix, the steepest-descent direction is perpendicular to the response contours. Paths of this type are illustrated in figure 11 by the solid lines emanating from points A and B. From the nominal point A, search perpendicular to the performance response contours is very efficient. From point B, however, this type of search results in the meandering path illustrated. It is assumed here that once a steepest-descent direction is located, an exhaustive search for the minimum in that direction will be undertaken in view of the high cost of recomputing the derivatives in many problems. Even if this were not the case, search normal to the response contours can often be improved upon. For example, it is obvious that even in the straightforward two-dimensional problem of figure 11 the dashed search direction is superior. This direction requires *a priori* knowledge of the extremal's position, information not normally available.

Returning to figure 10, the second search zone depicted corresponds to the choice of a diagonal matrix for W. The positive-definite constraint on W requires that all diagonal elements of the weighting matrix be positive. In this case the search zone becomes elliptical with the major and minor axes of the ellipse being parallel to the coordinate axes. It may be noted that as either of the diagonal elements of W becomes large in relation to the remaining element, the corresponding element in W inverse together with the predicted change in the associated independent variable becomes small. In the limit this reduces the search to a one-dimensional search in the remaining coordinate. The perturbation zone then becomes a slit

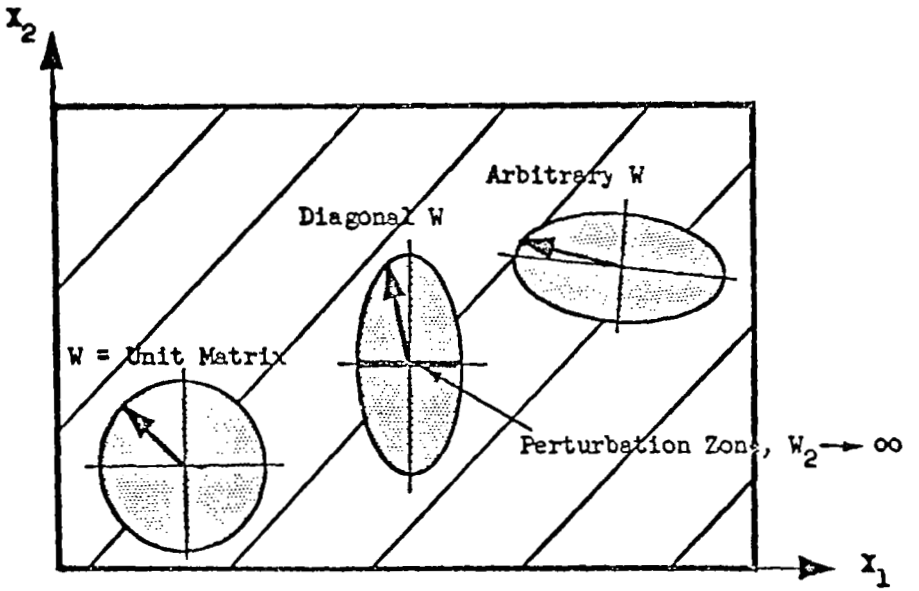

FIGURE 10.-PERTURBATION ZONES CORRESPONDING TO THREE WEIGHTING MATRICES

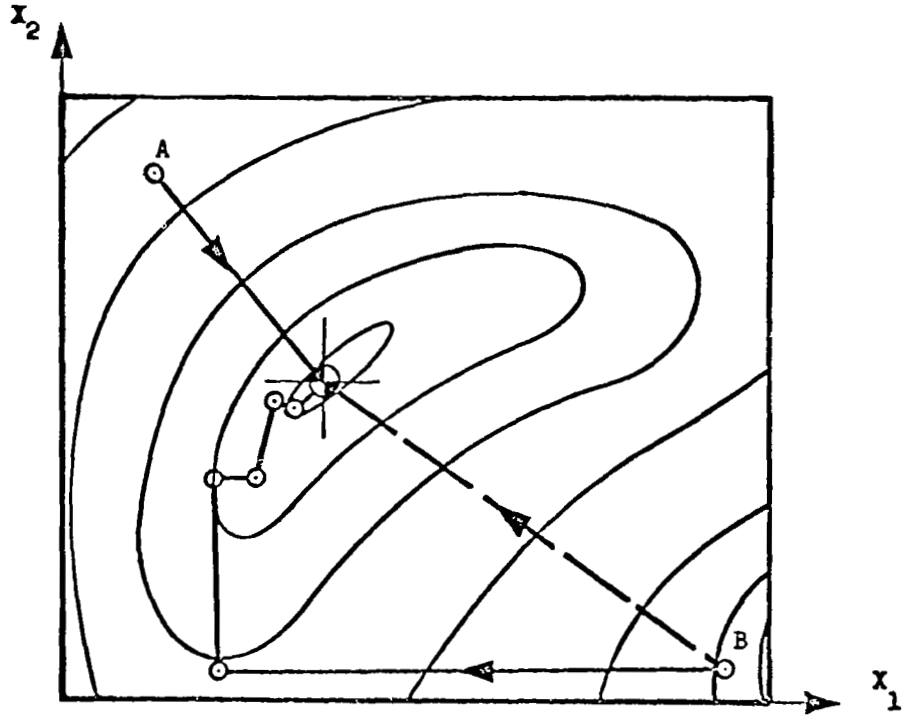

FIGURE 11.-STEEPEST-DESCENT SEARCH

parallel to that coordinate axis of length 2 · (DP), as illustrated in figure 10. In the case illustrated, the steepest-descent path is in the descending α_1 direction.

Finally, the search zone corresponding to the choice of an arbitrary positive-definite weighting matrix is shown. From equation (20) and the positive-definite constraint on W, the search zone remains elliptical, but the principle axes may now have an arbitrary orientation to the axes of α_1 and α_2. It follows that since the elliptic search zone can have any orientation and eccentricity, *any direction in the control space is a possible steepest-descent path;* for in all cases, the path of steepest-descent lies in the direction of a line joining the search zone origin to the lower point of tangency between the boundary of the search zone and the performance function response contours. The discussion above may readily be extended to control spaces of higher dimensionality.

When attempting the solution of optimization problems by the steepest-descent method, the analyst is constantly faced with the problem of choosing a satisfactory weighting matrix for the search continuation. The problem is compounded by the fact that the slopes of the performance function with respect to the independent variables can, and frequently do, vary by many orders of magnitude. The arbitrary choice of a unit matrix in such situations can lead to distressingly slow convergence of the numerical search; for it is in the nature of many problems that in those directions in which *the slopes are greatest the response surface is highly non-linear.* Only small perturbations will be successful in the direction of these strong control variables. In those directions in which the slopes are small, the contours are often relatively linear, and *large perturbations may be required in these weak control variables.*

In such situations the local steepest-descent direction for [W] = [I] is quite misleading; for contrary to the resulting steepest-descent direction which, by equation (21) results in independent variable perturbations which are in proportion to the response surface partial derivatives, the best direction in which to proceed may well involve large perturbations in the weak control variables of small slope. This behavior is illustrated for a two-dimensional case in figure 11 by the dashed line emanating from B.

The problem of choosing a satisfactory weighting matrix also arises when the steepest-descent search is applied in its variational form, reference 5, and when a combination of continuous control variables and parameters are encountered as in the optimization of multiple-arc problems in flight path optimization problems, reference 6. In these references it is suggested that the weighting matrices be based on the *first derivatives* of the unconstrained performance function with respect to the control. This approach can be used in the solution of multivariable optimization problems also, by writing

$$W_{ij}^{-1} = A_i + B_i \left|\frac{\partial \phi}{\partial \alpha_j}\right| , \quad i = j$$

$$= 0, \quad i \neq j$$

In practice, alternate use of the resulting combined weighting matrix and the unit matrix tends to provide a reasonable convergence rate at points well removed from the extremal. The AESOP code employs such a matrix in combination with a search range non-dimensionalization term and a learning factor. This factor emphasizes perturbation of control parameters which change in a monotonic direction and de-emphasizes those perturbations whose perturbations fluctuate in sign.

Random Ray Search. The difficulty, in some cases, of defining a suitable control variable metric tensor together with

the fact that any descending path is a steepest-descent direction for some choice of metric tensor suggests the possibility of searching along a random ray through the control space. The algorithm for random ray search is

$$\Delta\alpha_i = R_i(\pm DP), \quad i = 1, 2, \ldots, N \qquad (25)$$

where the R_i, proportional to the direction cosines of the ray, are uniformly distributed random numbers satisfying

$$-1.0 < R_i < +1.0, \quad i = 1, 2, \ldots, N$$

The positive sign in equation (25) is taken if $\frac{d\phi}{d(DP)}$ is negative; the negative sign is taken when this derivative is positive.

The utility of this type of search tends to be in proportion to the complexity of the performance function response contours. On a well-behaved problem there is little to recommend this type of search; on a problem involving unexpected behavior on the part of the performance function, a random ray search can be quite efficient, particularly when used with the pattern search acceleration procedure below. The method is, of course, equivalent to a steepest-descent search *using a randomly generated metric tensor*.

Quadratic search*. An alternative systematic approach to the definition of an arbitrary or empirical weighting matrix is provided by second order or quadratic method. It can be shown, for example, in reference 1, that on an elliptic second order response surface the weighting matrix

$$W_{ij} = \left(\frac{\partial^2\phi}{\partial\alpha_i\partial\alpha_j}\right) \qquad (26)$$

will immediately define the point

* Also known as the Newton-Raphson method

$$\{\alpha^*\} = \{\alpha_0\} + \{\delta\alpha\} \qquad (27)$$

where $\{\delta\alpha\}$ is computed from equation (21) with $(DP)^2 = .5K_1$. On a more general non-linear response surface, equation (27) merely defines a direction for subsequent search in the manner of the steepest-descent technique. This is illustrated in figure 12. Here, the approximating elliptical contours computed at point 0 define an approximate extremal location at P through equations (26) and (27). Subsequent search along the ray OP results in the definition of a one-dimensional extremal. This point is then used to fit another approximating elliptic contour, and the process is repeated until the extremal point at Q is located.

The quadratic search procedure can be quite rapid in control spaces of low dimensionality. In high order spaces the approach is usually impractical as a result of the requirement to establish the second order weighting matrix of equation (26). In many practical engineering problems these derivatives cannot be obtained in closed form; in such cases the derivatives must be obtained numerically, for example, reference 1. Computation of these derivatives requires at least $(N+1)(N+2)/2$ evaluations of ϕ at each point where an approximating quadratic is employed. Clearly, for large N this computation may become impractical.

Davidon or Fletcher-Powell Method. Davidon's method is a hybrid first order/second order technique. The objective of Davidon's method is to arrive at a reasonable approximation to the second order weighting matrix of equation (26) without the use of $(N+1)(N+2)/2$ evaluations of ϕ. It can be shown that on a quadratic (second order) response surface N steepest-descent searches performed in

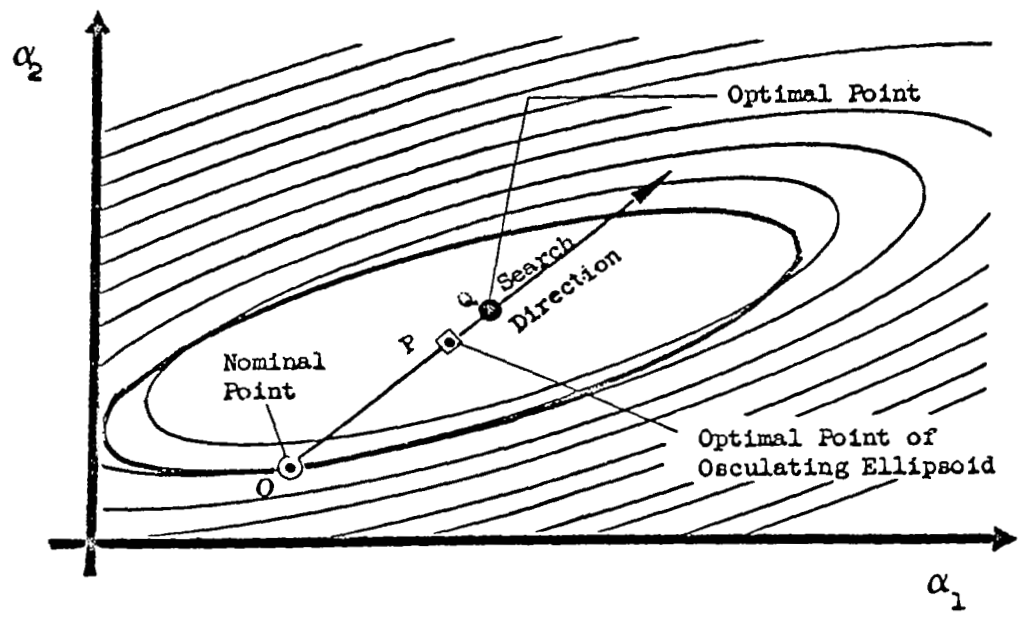

FIG. 12a. - QUADRATIC SEARCH BEHAVIOR ON A NEAR SECOND-ORDER SURFACE

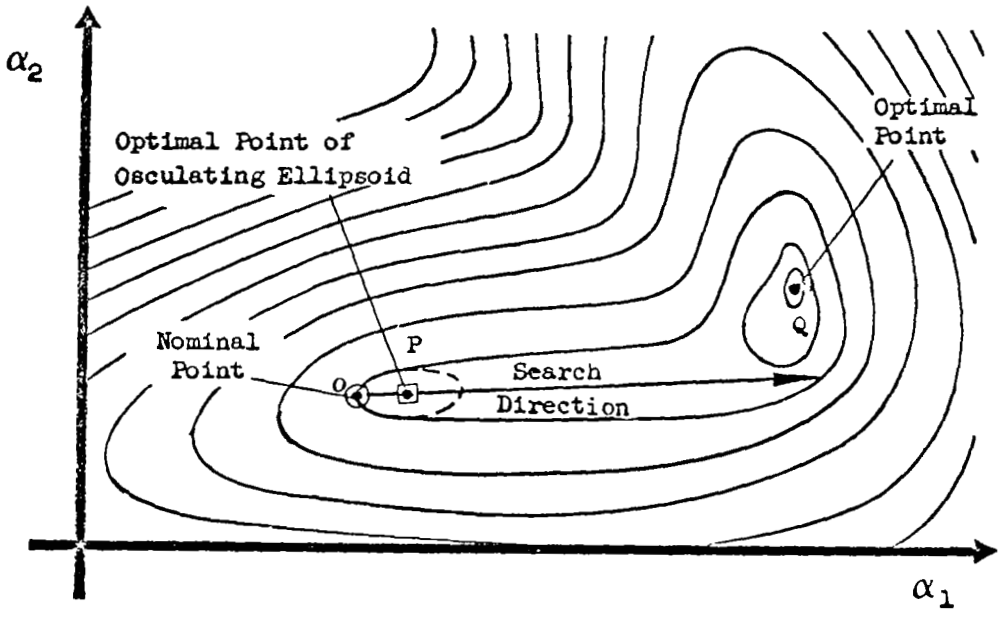

FIG. 12b.- QUADRATIC SEARCH ON A HIGHER ORDER SURFACE

the manner described previously will lead to definition of the weighting matrix of equation (26), if the following formula is employed:

$$[W]_{i+1}^{-1} = [W]_i^{-1} + [A]_i + [B]_i \tag{28}$$

where

$$[A]_i = \frac{\{\Delta\alpha\}_i \lfloor\Delta\alpha\rfloor_i}{\lfloor\Delta\alpha\rfloor_i \{\Delta \cdot \frac{\partial\phi}{\partial\alpha}\}_i} \tag{29}$$

$$[B]_i = - \frac{[W]_i^{-1}\{\Delta \cdot \frac{\partial\phi}{\partial\alpha}\}_i \lfloor\Delta \cdot \frac{\partial\phi}{\partial\alpha}\rfloor_i [W]_i^{-1}}{\lfloor\Delta \cdot \frac{\partial\phi}{\partial\alpha}\rfloor_i [W]_i^{-1}\{\Delta \cdot \frac{\partial\phi}{\partial\alpha}\}_i} \tag{30}$$

$$[W]_1^{-1} = [I] \tag{31}$$

Here, $\lfloor\Delta\alpha\rfloor_i$ is the change in position during the i^{th} one-dimensional search and

$$\left\lfloor \Delta \cdot \frac{\partial\phi}{\partial\alpha} \right\rfloor_i$$

is the change in gradient vector between the beginning and end of the i^{th} one-dimensional search. On a numerically well-behaved function this technique may work well. When appreciable numerical noise is present in the calculation, the method may produce erratic convergence to the extremal point, or convergence failure. Again, $\{\frac{\partial\phi}{\partial\alpha}\}$ is the gradient of ϕ defined as $\{\frac{\partial\phi}{\partial\alpha 1}, \frac{\partial\phi}{\partial\alpha 2} \ldots \frac{\partial\phi}{\partial\alpha n}\}$.

Pattern Search. In the present report, pattern search refers to a search which exploits a gross direction revealed by one of the other searches. The search algorithm is

$$\Delta\alpha_i = (\alpha_i^2 - \alpha_i^1) \cdot (DP), \qquad i = 1, 2, \ldots, N \tag{32}$$

where α_i^2 and α_i^1 are the components of the control vector before and after the use of a preceding search technique. This type of search is illustrated in figure 13 following a section search. The combination of a section search and a pattern search in the problem illustrated leads directly to the neighborhood of the extremal. Repeated sectioning, on the other hand, would be a very slowly converging process due to the orientation of the contours with respect to the axes of the independent variables. It may be noted that a simple rotation of the independent variable axes by 45° results in sectioning alone becoming a rapidly converging process in this example. The pattern search can also be used to accelerate the steepest-descent process provided it follows two successive descents as in figure 14.

Adaptive Search. Adaptive search is a form of small scale sectioning; however, instead of locating the position of the one-dimensional extremal on each section parallel to a coordinate axis, the coordinate is merely perturbed by a small amount, $\Delta\alpha_r$, in the descending direction.

The search commences with a small perturbation in one of the independent variables, α_r; a positive perturbation is first made; if this fails to produce a performance improvement, then a negative perturbation is tried. If neither of the perturbations produces an improved performance value, the variable retains its nominal value, and $\Delta\alpha_r$ is halved. If a favorable perturbation is found, the variable α_r is set to this value, and $\Delta\alpha_r$ is doubled. The process is repeated for each independent variable in turn, the order in which the variables are perturbed being *chosen randomly*. At this point an adaptive search cycle is complete, and the cycle is then repeated. A two-

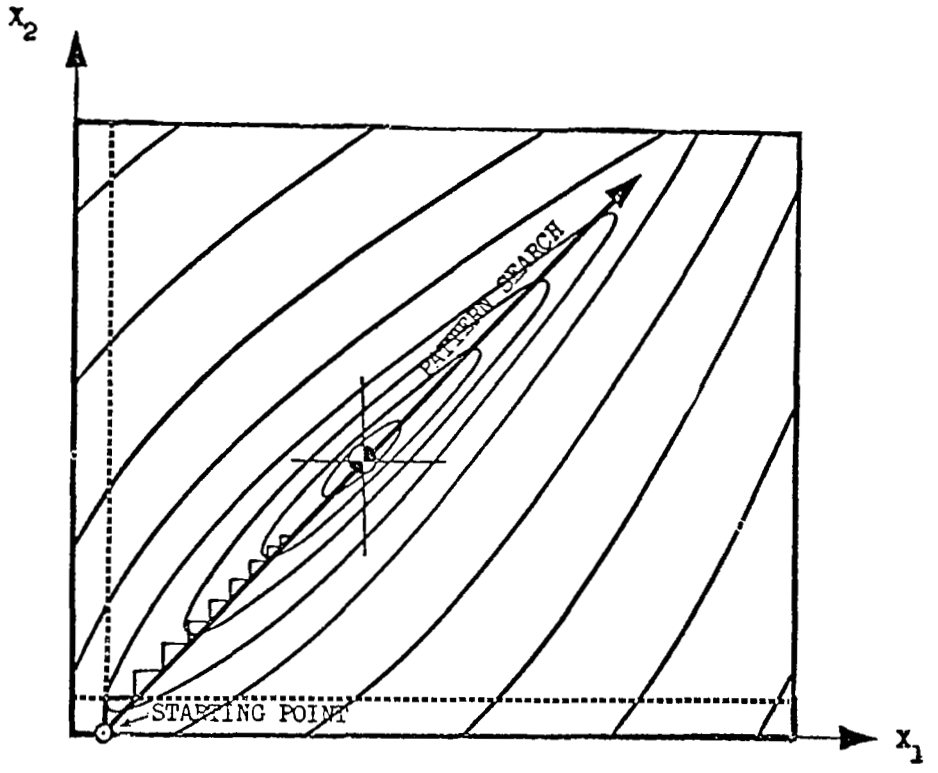

FIGURE 13. PATTERN SEARCH FOLLOWING SECTIONING PARALLEL TO THE AXES

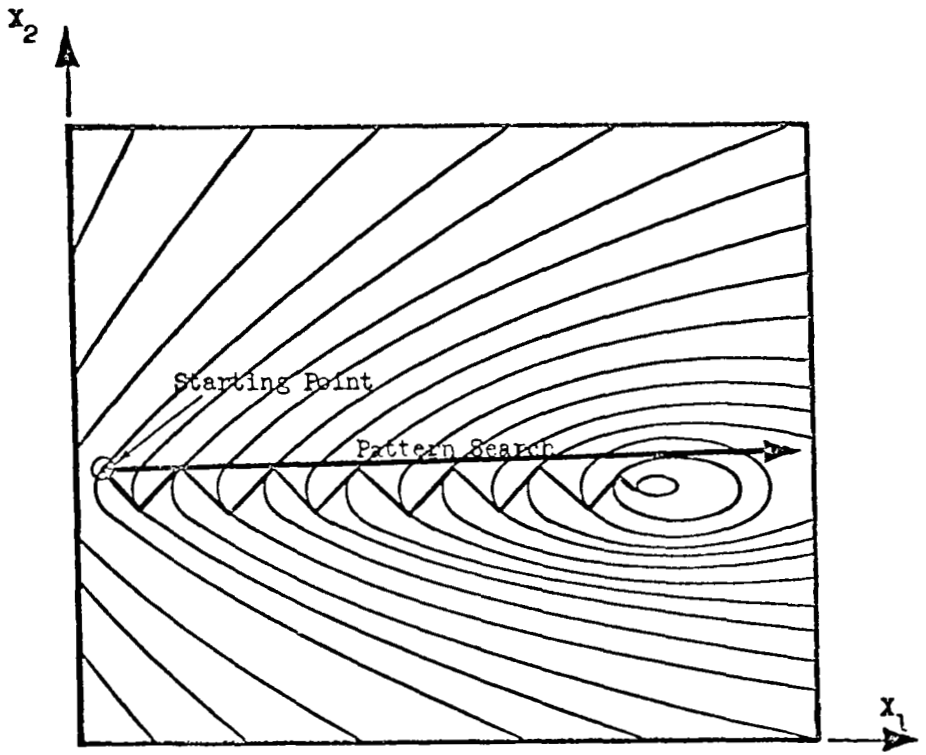

FIGURE 14.-PATTERN SEARCH FOLLOWING TWO STEEPEST-DESCENT SEARCHES

dimensional illustration of this search is presented in figure 15. In the particular problem illustrated, the method converges rapidly reaching the neighborhood of the extremal within six evaluations.

The search algorithm can be written in the form

$$\Delta\alpha_r = 2.0^{(S_r - T_r)} \cdot (DP) \qquad (33)$$

where S_r is the number of cycles in which the search has successfully perturbed the r^{th} independent variable, and T_r is the number of cycles in which a perturbation of the r^{th} variable has proved unsuccessful. While this search can be looked upon as a one-dimensional approach, this viewpoint is somewhat artificial. Here, the scalar quantity (DP) merely defines an initial perturbation for each independent variable. Once started the search proceeds inevitably to its conclusion, the perturbation in each independent variable being adaptively determined according to equation (33) on the basis of the performance function response contour behavior encountered during the particular problem solution. This search can be quite efficient when used in combination with the pattern search acceleration procedure.

Magnification. When studying discrete models of continuous systems of the type encountered in certain engineering problems such as aerodynamic shaping or structural design problems, there is a tendency on the part of some search algorithms to achieve a favorable shape before satisfying the desired constraint levels. In such cases, when it is known that the unconstrained extremal is the null vector, a simple magnification search can lead to rapid convergence to the desired solution. The magnification algorithm is

$$\Delta\alpha_i = \alpha_i \cdot (DP), \qquad i = 1, 2, \ldots, N \qquad (34)$$

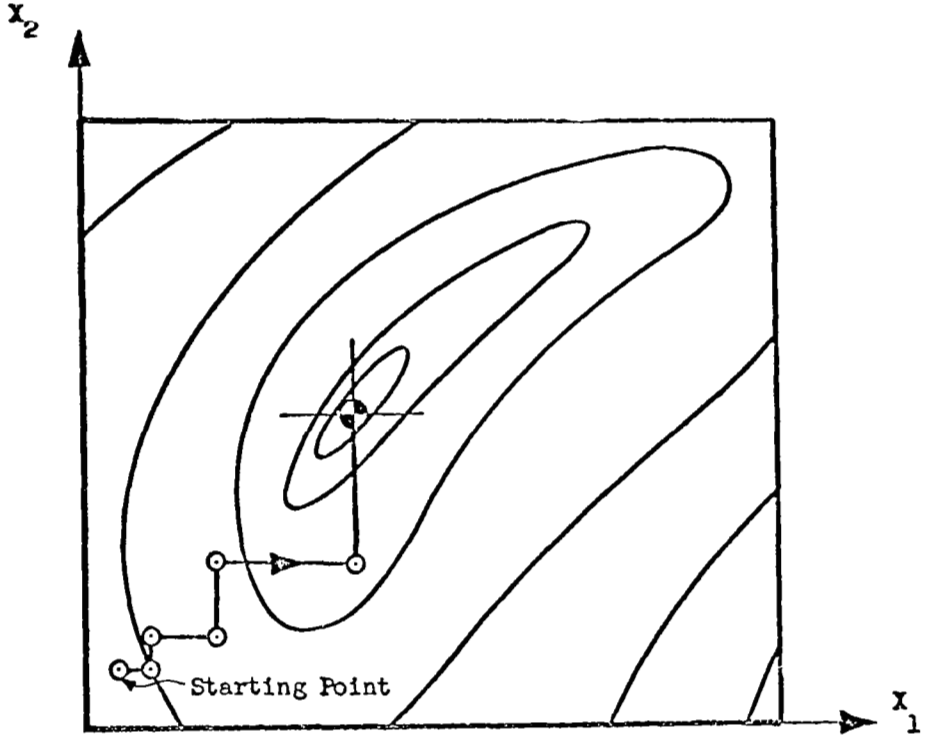

FIGURE 15. –ADAPTIVE SEARCH

Here (DP) is positive and all components of the control vector are to be simultaneously perturbed. Generally, the unconstrained extremal point corresponds to the null vector; this method may prove efficient.

Arbitrary Ray Search. In practical design optimization a search along an arbitrary multidimensional ray can be of utility. For example, when two *minimal extremal* solutions appear to be possible, a search on the ray connecting the two points should reveal the presence of a *maximal extremal* somewhere on the ray between the two minimal extremals. The algorithm for this search is

$$\Delta\alpha_i = (\alpha_i^2 - \alpha_i^1)\ (DP), \quad i = 1, 2, \ldots, N \qquad (35)$$

where α_i^1 and α_i^2 are the two minimal extremal points. In general, α_i^1 and α_i^2 may be any two points in the control space.

Random Point Search. A straightforward Monte-Carlo search which examines point designs distributed in a uniform random manner within the feasible region is often of utility when the response surface is of a complex nature. Such a search is included in the AESOP code primarily for use as a nominal point design generation procedure.

STRUCTURAL ANALYSIS OF A STIFFENED CYLINDER

The structural analysis employed in this study is *identical* to that employed in a previous National Aeronautics and Space Administration-sponsored study reported by Morrow and Schmit in reference 9. Morrow and Schmit's analysis of a stiffened cylinder is reproduced for completeness in Appendices A and B. The computer *code for the failure mode analysis* employed in the present study is that developed in reference 9 without change. However, the Fletcher-Powell/Fiacco-McCormick procedure of reference 9 was replaced by the references 1 through 3 optimization program AESOP during this study.

Figure 16 illustrates the class of structures considered. The structure is a cylinder stiffened in both longitudinal and circumferential directions. A typical shell element is presented in figure 17. The shell element is defined by seven parameters:

d_x = Depth of longitudinal stiffeners *

d_ϕ = Depth of circumferential stiffeners*

ℓ_x = Spacing of circumferential stiffeners

ℓ_ϕ = Spacing of longitudinal stiffeners

t_s = Skin thickness

t_x = Thickness of longitudinal stiffeners

t_ϕ = Thickness of circumferential stiffeners

These parameters are the *design vector components* in the stiffened cylinder design optimization problem considered.

$$\lfloor \alpha \rfloor = \lfloor t_s,\ t_x,\ t_\phi,\ d_x,\ d_\phi,\ \ell_x,\ \ell_\phi \rfloor \qquad (36)$$

The optimization problem considered is that of weight minimization subject to yield and buckling failure mode constraints. Cylinder weight, *the payoff function*, is taken from Appendix C of reference 9.

---

* Positive number means inside stiffeners; negative number means outside stiffeners.

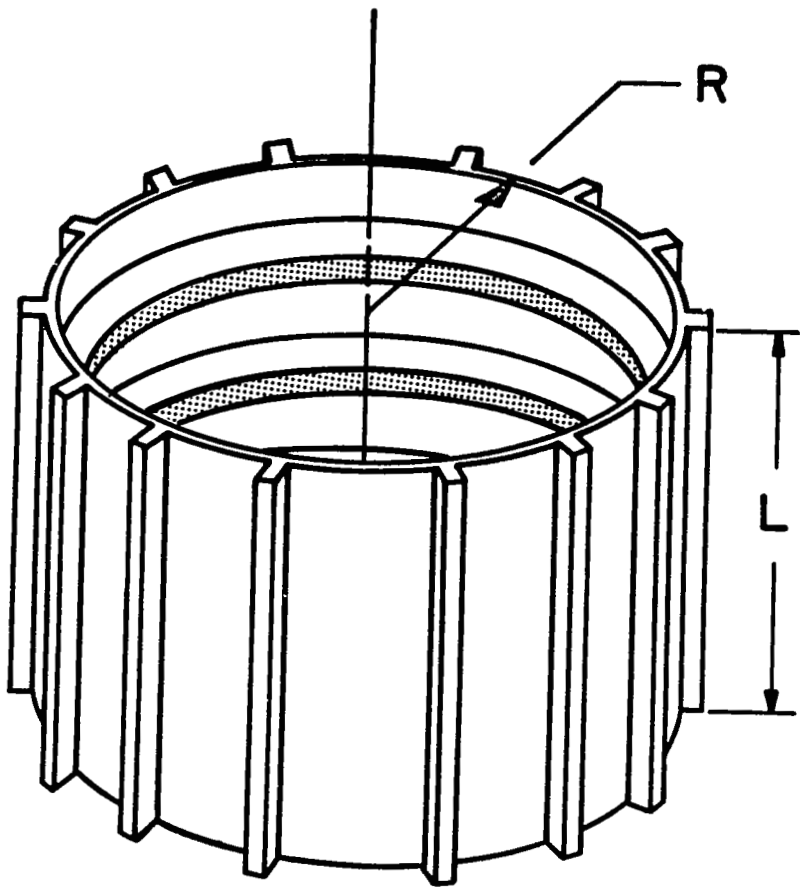

FIGURE 16. AN INTEGRALLY STIFFENED CYLINDER

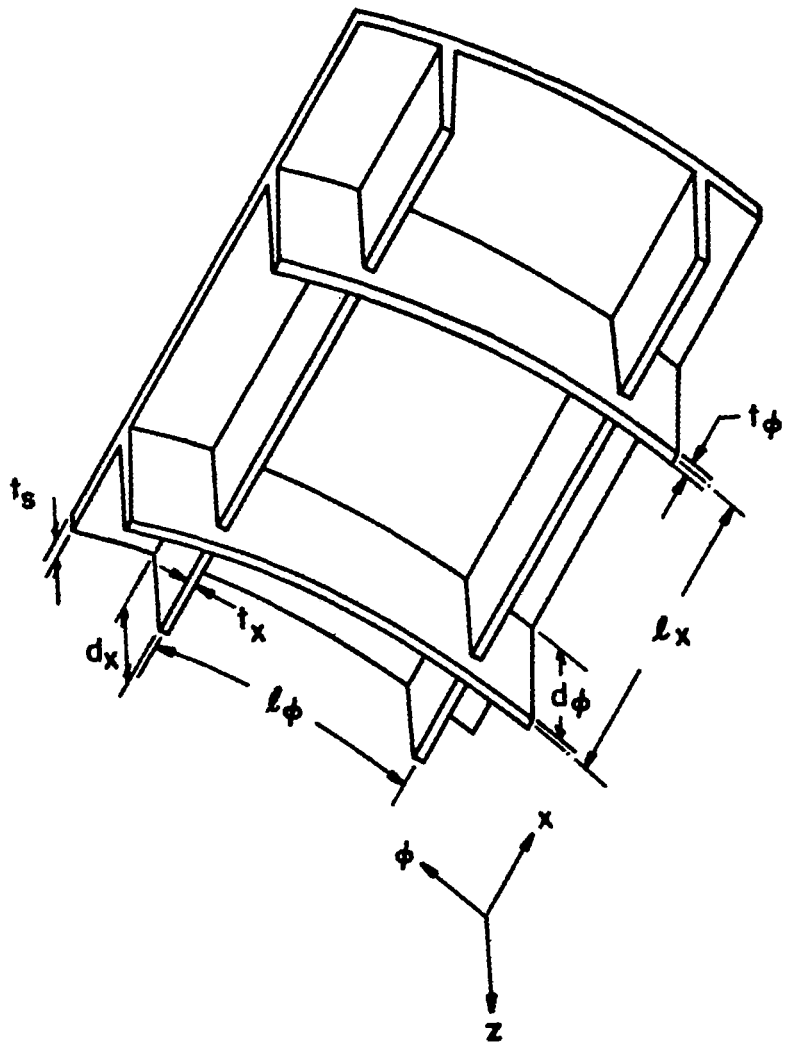

FIGURE 17. AN ELEMENT OF A STIFFENED CYLINDER

$$\phi = W = 2\pi\, RL\, t_s\, \gamma_s + |2R\, d_\phi - d_\phi^2 - t_s|d_\phi||\pi\, t_\phi\, \gamma_\phi\, n_\phi +$$

$$L\, |d_x|\, t_x\, \gamma_x\, n_x - \min(|d_x|,|d_\phi|)\delta_{x\phi}\, t_x\, t_\phi\, (\gamma_x\, \delta_{xw} + \gamma_\phi \delta_{\phi w}) n_\phi n_x \qquad (37)$$

Multiple load cases are considered. For each load case, *inequality constraints* are placed on five yield failure modes, Equations A27 and A29.

1. Skin yield
2. Longitudinal stiffener yield in tension
3. Longitudinal stiffener yield in compression
4. Circumferential stiffener yield in tension
5. Circumferential stiffener yield in compression

A distortion energy type criterion is used in the skin for the biaxial state of stress. In the stiffeners, the uniaxial state of stress must have a value between the compression yield value and the tension yield value.

Three buckling failure modes of the cylindrical shell are considered:

1. Gross buckling of the entire cylinder (gross buckling)
2. Buckling of the cylinder between circumferential stiffeners (panel buckling)
3. Buckling of the cylindrical skin (skin buckling)

In the gross buckling mode, the effect of the *stiffeners are averaged over* the stiffener spacing. For the panel buckling mode, only the longitudinal stiffeners are

averaged in. Bending stiffnesses of the stiffeners, the torsional stiffnesses, and the effects of eccentricity are taken into account. The cylinder buckling analysis is a linear classical small displacement analysis, assuming simply supported boundaries and a uniform prebuckled membrane force and displacement distribution. The same analysis is used to determine the critical loads for gross, panel, and skin buckling, by substituting the appropriate stiffness properties and displacement patterns. An expression for the buckling load in terms of the mode shape is given by equation A20 or A22. The critical buckling load is found by determining the buckling loads for a large number of mode shapes and selecting the lowest of these loads as the critical value.

Stresses and strains in the skin and stiffeners prior to buckling are determined from the membrane force distribusion, equations A12, A13, and A14. The strains in the stiffeners where they join the skin are assumed to be the same as the corresponding strains in the skin.

Three failure modes are considered for the stiffeners:

1. The longitudinal buckling stress is calculated from equation A23

2. Outside circumferential stiffeners can buckle either when the cylinder expands or contracts under load

3. Inside circumferential stiffeners can buckle only when the cylinder contracts.

The expression for the circumferential stiffener critical strain, equation A24, derived in Appendix A, Section A.9, is verified for two limiting cases in Appendix B. In the stiffener buckling analysis, simply supported boundaries are assumed at all edges where the stiffener connects with the shell or the other stiffeners.

In the optimization procedure employed herein, all buckling and yield constraints are expressed in the form

$$P_k \leq \bar{P}_k \tag{38}$$

where P_k is the load which the cylinder is to support, and $\bar{P}_k$ is the critical load for the k^{th} failure criteria. These inequality constraints are converted to equality constraints by a one-sided transformation in an analogous manner to that of equation (5).

$$\psi_k = 0; \qquad P_k \leq \bar{P}_k \tag{39}$$

$$= (P_k - \bar{P}_k)^2; \quad P_k > \bar{P}_k \tag{40}$$

Equations (30) and (31) may define a large number of constraints as k varies over all failure criteria and load conditions. For example, with fifty longitudinal and fifty circumferential buckling modes considered for gross, panel and skin buckling and ten load conditions, the number of constraints to be considered is

$$N_k = N_{FC} \times N_{ij} \times N_L \tag{41}$$

where

N_k = Number of constraints

N_{FL} = Number of failure criteria considered equals three

N_{ij} = Number of buckling mode combinations equals 50 × 50 = 2,500

N_L = Number of load conditions equals ten

In this particular example, there would be 75000 buckling constraints. Each constraint corresponds to a particular mode shape and load condition. In applications to-date, the maximum number of load conditions considered is three which, in the example, would result in the maximum of 22500 constraints.

In practice, computation of the violations for this number of constraints becomes a time consuming process when each constraint violation is checked at a number of points in the control space. In reference 9 Morrow and Schmit reduced the computational time by introducing partial or approximate analyses. At the beginning of a synthesis a complete cylinder analysis is performed. The word "complete" means that a large number of buckling mode shapes are examined. (Each mode shape is a constraint). The subset of mode shapes that is most active in the complete analysis is saved, and these mode shapes are examined in several subsequent approximate analyses. These approximate analyses are carried out during a succession of moves through design variable space. Periodically, a complete analysis is performed, and the subset of mode shapes used in the approximate analyses is redefined. An approximate analysis is approximate only in that the number of buckling mode shapes examined is small compared with the number of buckling mode shapes examined on a complete analysis.

This same procedure was employed in the present study. Following Morrow and Schmit, when a large number of constraints are checked, the analysis is defined to be *complete;* otherwise the analysis is *approximate*. In a typical load case problem a complete cylinder analysis required three seconds on a CDC 6600 computer while an approximate analysis in which 70 active constraints were retained required .03 seconds. Clearly, computer time requirements can be significantly reduced by a good mix of complete and approximate analyses. However, it must be noted that when successive complete analyses are too widely separated in the control space, convergence rates may diminish to the point where computational time gains are negated.

MINIMUM WEIGHT DESIGN OF STIFFENED CYLINDERS

In this section a variety of minimum weight stiffened cylinder designs are considered. Cylinder designs are optimized by a coupled version of the multivariable optimization program AESOP of references 1 through 3 and the Morrow and Schmit structural analysis program of reference 9. The technique employed is that of design evolution by repetitive perturbation and analysis as illustrated in figure 18. Here, a nominal design characterized by the control vector α_0 is supplied to the optimization program. The design parameters corresponding to this control vector are, in turn, passed to the system model which is, in this case, a stiffened cylinder analysis program, by the optimizer. The system model operates in a *black box* fashion and evaluates the system performance characteristics consisting of the weight and failure

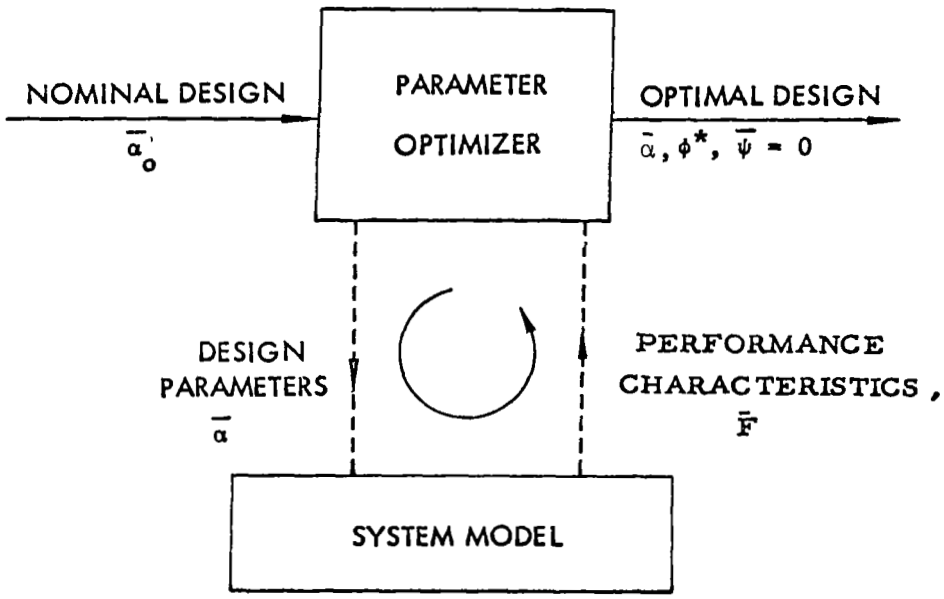

FIGURE 18. OPTIMIZER SCHEMATIC

criteria constraints. No explicit derivative computations are required by the optimizer. The performance characteristics are then transferred from the system model back to the optimization program.

At this point a succession of perturbed designs are defined within the optimization program, and the computation loop is repeated with improving designs being retained and inferior designs being rejected—an evolutionary process. The optimization program contains a variety of perturbation algorithms as illustrated in figure 19. These algorithms may be employed separately or in combination at the analyst's option. The repetitive design process outlined defines a sequence of gradually improving designs which lead from an *arbitrarily selected initial design which may or may not satisfy the constraints* to a locally minimal weight design which satisfies the constraints. The initial design need not satisfy the constraints because an exterior penalty function is used in AESOP.

Search Sequence

In general, a combination of search algorithms will tend to produce more reliable convergence in the solution of a non-linear parameter optimization problem than the repetitive applications of any single algorithm. Throughout the remainder of this report the search algorithm combination employed will be designated by an array, $\overline{M}$. The algorithm corresponding to an element of $\overline{M}$, say M_i, is obtained from the following set of values:

M_i = 1, Sectioning Search
= 2, Pattern Search
= 3, Magnification Search

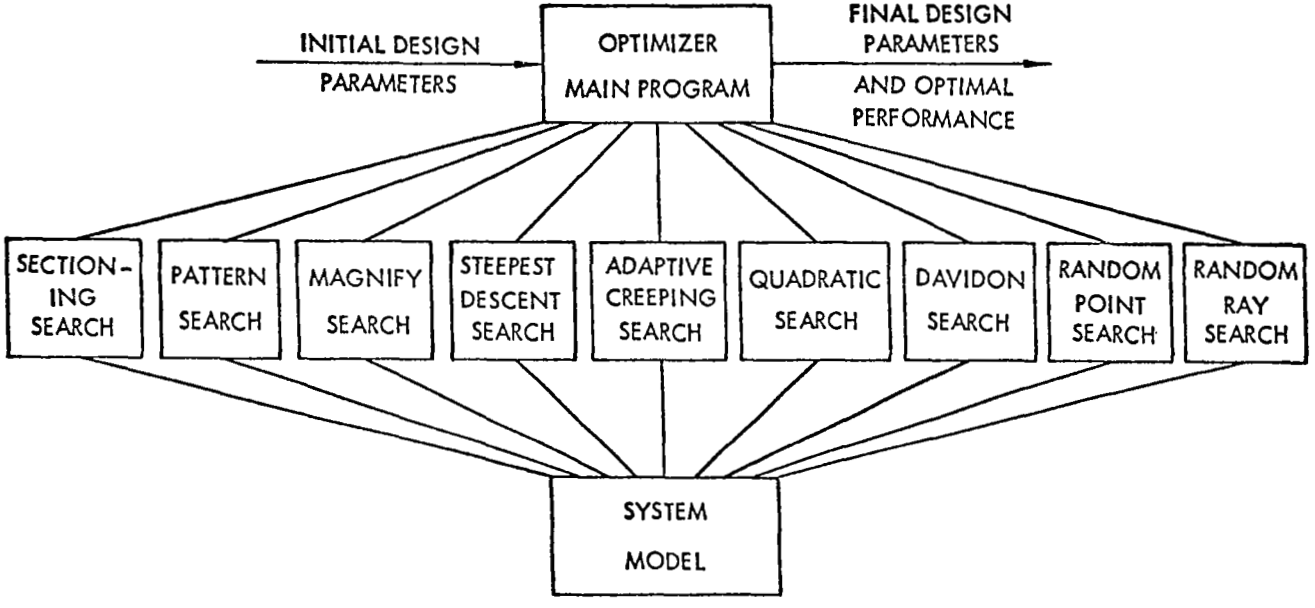

FIGURE 19. ALGORITHMS FOR OPTIMIZATION

= 4, Steepest-Descent Search
= 5, Adaptive Creeping Search
= 6, Quadratic (Newton-Raphson) Search
= 7, Davidon (Fletcher-Powell) Search
= 8, Random Point (Monte Carlo) Search
= 9, Random Ray Search

Typical Optimization Algorithm Behavior in Stiffened Cylinder Design

The relative efficiencies of a variety of optimization algorithms was studied by repeated solution of one stiffened cylinder design problem. An aluminum design was used in the study. Cylinder *physical characteristics* were:

L = 291, Cylinder length, inches
R = 95.5, Cylinder radius, inches
E = 10.5×10^6, Young's modulus of elasticity lbs/in^2
γ = .101, Weight density, lbs/in^3
ν = .33, Poisson's ratio
σ_y = 50,000., Yield stress, lbs/in^2

A single *load condition* was considered. This was:

N = 800., Applied axial force per unit length of circumference, lbs/in.
P = 0.0, Radial pressure

The problem is solved both with and without constraints on the stiffener depth/thickness (d/t) ratios. *When the (d/t) limits are omitted,* the problem considered is identical to that of problem 7-I in reference 9.

Solutions Without (d/t) Limits

Table I (figure 20) presents the results obtained when (d/t) limits are omitted. In the lower portion of the table, solutions obtained by Morrow and Schmit in reference 9 are included for comparison purposes. The table presents both final design vector and the corresponding weight obtained. The solutions obtained by program AESOP all utilize the starting vector used in Case 7-I of reference 9, that is:

$$\lfloor \bar{\alpha}_0 \rfloor = \lfloor .05,\ .1,\ .05,\ 1.,\ 2.,\ 8.,\ 3. \rfloor \qquad (42)$$

Starting vector elements are defined in equation (27). Cylinder weight corresponding to the starting vector is 1681.7 lbs.

It can be seen from figure 20 that a variety of minimal cylinder weight designs are obtained from both the AESOP search algorithms and the method of reference 9. Two search combinations achieve weights well under the solutions reported in reference 9. These combinations are

$$\lfloor M_i \rfloor = \lfloor 9,\ 2,\ 9,\ 2,\ 5,\ 2,\ 3 \rfloor$$

and

$$\lfloor M_i \rfloor = \lfloor 7,\ 2,\ 7,\ 2 \rfloor$$

The first combination is the recommended procedure for the solution of stiffened cylinder problems. These two search algorithms produce minimum weight designs of 682 and 684 lbs., respectively, *approximately 30% lighter* than

the best corresponding solution in reference 9. Depth/thickness ratios utilized in the two best AESOP designs are

$$(d/t)_\phi = 10^6 \text{ and } 320$$

$$(d/t)_x = 14.1 \text{ and } 13.9$$

It can be seen that in both cases completely unrealistic circumferential stiffener (d/t) values are being employed. The designs attained appear to be quite different from the heavier cylinder of reference 9. Detailed results of solutions without d/t limits are presented in Tables D1-D7 of Appendix D.

Solution With (d/t) Limits Imposed

Unrealistic stiffener depth-to-thickness ratios can be eliminated by the introduction of inequality constraints on stiffener section geometries. In the present report inequalities of this type are transformed into equality constraints by constraining F_x and F_ϕ to zero, where

$$F_x = 0; \quad (d/t)_x \leq 20$$

$$= [(d/t)_x - 20]^2 ; \quad (d/t)_x > 20 \qquad (43)$$

$$F_\phi = 0; \quad (d/t)_\phi \leq 20$$

$$= [(d/t)_\phi - 20]^2; \quad (d/t)_\phi > 20 \qquad (44)$$

Figure 21, Table II, presents solutions obtained with these constraints imposed. The constraints are imposed as "soft" boundaries by the device of limiting the growth of the adaptively determined constraint weighting factors, (U_j of equation 6), within the optimizing program AESOP. Detailed results of solutions with d/t limits imposed are presented in Tables D8-D13 of Appendix D.

Introduction of (d/t) limits *reduces the spread of minimal designs*, figure 21, which now exhibit a range of weights ranging from 807 to 894 pounds. It should be noted that all designs in figure 21 produce lower weight than the reference 9 designs of figure 20 which are not subject to the additional (d/t) constraints. The weight improvement over these designs varies from *eight per cent to seventeen per cent when compared to the best reference 9 design*, (979 pounds).

For all AESOP solutions shown in figures 20 and 21, except for the quadratic search in figure 20, two successive runs of approximately ninety system seconds each were made. Therefore, the results obtained indicate how well the various combinations of search procedures did for a given amount of computer time.

The spread of weights shown do *not* indicate that AESOP has obtained multiple solutions but *instead* indicate

the design vector obtained after a *given amount of computer time*. It is obvious that the AESOP solutions shown in figure 20 have not all converged. The quadratic search without d/t limits terminated during the first run due to a singular matrix.

It can be seen from figure 21 that after imposing constraints on the stiffener depth to thickness ratio, the selection of search procedure used is less critical.

Nature of the Multiple Extremal Minimum Weight Designs

Physically, the existence of multiple minimal weight designs in the design space is unlikely unless *the multiple extremals are constraint-induced;* for the cylinder weight diminishes monotonically with stiffener thickness, stiffener depth, and stiffener spacing. Now the constraint boundaries to the stiffened cylinder problem are probably highly non-convex since they include multiple buckling criteria. (One can observe a simple boundary of this type for *conical* shells on page 511 of reference 15).

TABLE I. (FIGURE 20)
SOLUTIONS FOR CASE 7 WITHOUT (d/t) LIMITS IMPOSED

AESOP Search Combination	t_s	t_x	t_ϕ	d_x	d_ϕ	ℓ_x	ℓ_ϕ	W	TABLE
9, 2, 9, 2, 5, 2, 3	.0304	.0276	.00002	.3879	20.0	3.229	1.316	682.5	D1
5, 2, 5, 2	.1090	.00959	.00020	.000008	2.007	2.469	20.0	1926	D2
6, 2	.05785	10^{-7}	10^{-7}	10^{-7}	10^{-7}	10^{-7}	12.47	1020	D3
7, 2, 7, 2	.0226	.0302	.00794	.4187	2.542	7.451	.9304	684.4	D4
4, 2, 4, 2	.1032	10^{-7}	.00001	10^{-7}	7.320	4.355	2.900	1820	D5
5, 2, 3	.07795	.1322	.03189	.01691	.6738	2.711	.8651	1558	D6
CR 1217 (Ref. 9)	.111	.725	.940	0	0	8.57	3.84	1960	
CR 1217 (Ref. 9)	.0292	.0441	.0943	.718	.810	18.2	1.42	979	
CR 1217 (Ref. 9)	.114	3.56	.400	0	1.64	42.0	11.6	2240	

TABLE II. (FIGURE 21)
SOLUTIONS FOR CASE 7 WITH (d/t) LIMITS IMPOSED

AESOP Search Combination	t_s	t_x	t_ϕ	d_x	d_ϕ	ℓ_x	ℓ_ϕ	W	TABLE
9, 2, 9, 2, 5, 2, 3	.0300	.0335	.0501	.5017	1.048	10.94	1.311	831.2	D8
5, 2, 5, 2	.0245	.0321	.0617	.4618	1.277	10.28	1.013	819.0	D9
6, 2, 6, 2	.0254	.0289	.0562	.4493	1.371	9.507	1.038	806.9	D10
7, 2	.0372	.0322	.0395	.5031	.9080	8.323	1.733	894.0	D11
4, 2	.0297	.0316	.0409	.4663	1.174	8.336	1.282	824.5	D12
1, 2	.0256	.0307	.0568	.4339	1.180	9.398	.9767	813.5	D13

Figure 22 illustrates one possible form of a non-convex constraint boundary problem in the case of a hypothetical two-dimensional problem. Here, the performance contours vary smoothly, but the constraint boundaries involve a sequence of non-convex arcs. The *forbidden region* is determined by the shaded region. In the problem illustrated, the constraints introduce five possible minimal solutions. The global extremal is the extreme left minimal solution. Two typical exterior penalty function convergence paths are shown in figure 22. In both paths, the constraint boundaries are pierced early in the search. At this stage in the optimization process, the exterior penalty function procedure is concentrating on payoff function improvement, and the constraint violation is of secondary importance. In the lower path, pursuit of improving performance leads to Point A before increasing weight on constraint violations results in a gradual loss of performance to satisfy the active constraints. This path leads to the global optimal at Point B. A significant point regarding constraint violation is that the constraint initially violated at C,and two other intermediately active constraints along arc CA, are no longer active at Point A. A second typical exterior penalty function path is illustrated by arc CD. Here, the constraint weights have been increased more rapidly than on arc CA, and an inferior extremal is located at Point D. Relaxation of the constraint weights at D will result in further payoff function improvement along a path such as DB.

On a complex response surface or in a search from a badly chosen nominal, convergence to the global extremal may require several constraint weight relaxations. As a matter of practice during this study the constraint weights were reduced at least once on each problem.

It should be noted that when high constraint weights are employed, the exterior penalty function method will usually fail to find the global extremal of a constrained optimization problem such as that illustrated in figure 22. With high constraint weights, the search turns to follow a constraint boundary as it is encountered. In consequence, the nearest constrained extremal point is found; this may or may not be the global extremal. Similar results may be encountered when an interior penalty function technique is employed with low constraint weights. This may well be the reason for some of the very high weight optimal cylinder designs obtained in reference 9.

When the unconstrained payoff function response surface itself possesses more than one extremal, successive constraint weight reductions may or may not lead to the global extremal. In such cases, the multiple extremal procedure of reference 2 may be combined with the constraint relaxation procedure in a search for successive minima.

It is apparent that the multiple "extremal" solutions of figure 20 could be attributed to non-convex buckling constraint boundaries. It will be shown in a later section that these constraint boundaries do have the general characteristics exhibited in figure 22 and that the variation in unconstrained performance along a line such as DB in figure 22 is essentially a smooth monotonic improvement to the minimal weight design point.

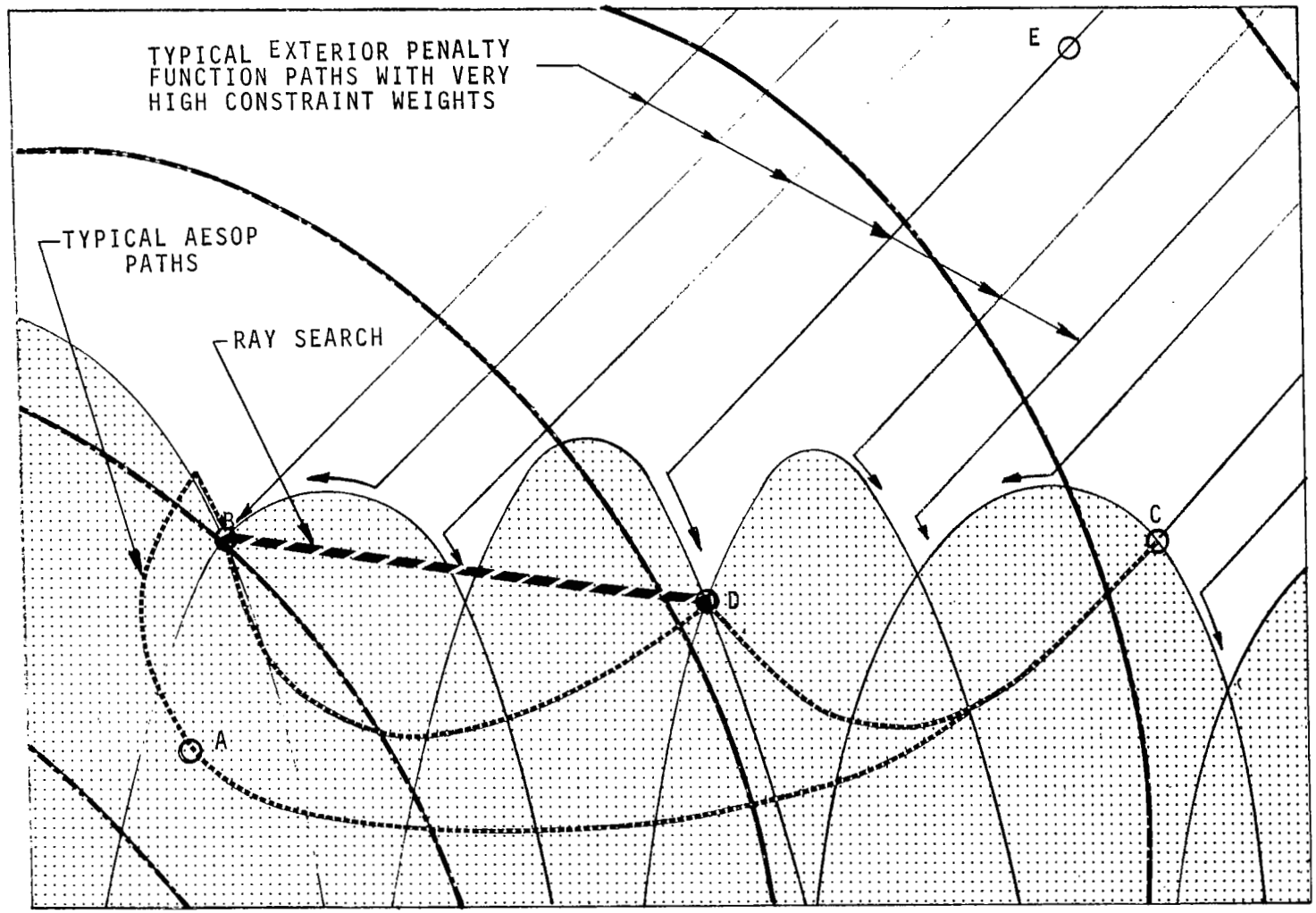

FIGURE 22. CONSTRAINT INDUCED EXTREMALS

Comparison Between Interior and Exterior Penalty Function Approach to Stiffened Cylinder Design

In this section a *series* of direct comparisons between minimum weight cylinder designs obtained by an interior and an exterior penalty function optimization approach are presented. The interior penalty function method is that of Fiacco and McCormick applied through the Fletcher-Powell unconstrained minimization algorithm as reported in reference 9. The exterior penalty function method employed is that of program AESOP, references 1 through 3, which may be utilized with any of the search algorithms of figure 19. When using the exterior penalty function approach, the constraint weights were *routinely relaxed once in each solution* as discussed in the previous section. In one particularly difficult problem, the constraint weights were relaxed four times. This problem is discussed in some detail below. All exterior penalty function solutions obtained in this section used a combination of searches.

$$\lfloor M_i \rfloor = \lfloor 9,\ 2,\ 9,\ 2,\ 5,\ 2,\ 3 \rfloor$$

Case identification conforms to that of reference 9. Each of the interior penalty function cylinder designs in reference 9 is considered; however, not all of the starting solutions of reference 9 are employed in the exterior penalty function solutions. Details of the results presented in this section are given in Appendix C.

Case 1-I, Three Load Cases, Cylinder Length = 165", Cylinder Radius = 60". Load conditions for this problem are:

1. Axial load 700 lbs/in., External pressure 0.0
2. Axial load 940 lbs/in., External pressure -2. lbs/in^2
3. Axial load 212 lbs/in., External pressure 0.4 lbs/in^2

A summary of the results obtained for Case 1-I is presented in Appendix C, Table C1. As noted, two searches were made on the computer to obtain convergence with a constraint weight reduction between the two searches. The first search consisted of 15 optimization cycles. (A cycle consists of one application of the search algorithms specified). The second search consisted of ten optimization cycles. The search techniques used in each optimization cycle were Random Ray, Pattern, Adaptive Creeping, and Magnification in the combination defined above. Values of 10.0 were arbitrarily selected as initial constraint weights for both searches.

The final values of the design variables obtained by the AESOP exterior penalty function, figure 23, and the corresponding cylinder weight 226 lbs. indicates that the AESOP solution has converged to essentially the same configuration as shown on page 71 of reference 9 , (cylinder weight of 231 lbs.). Table C2, Appendix C, presents the detailed results obtained by AESOP for Case 1-I when the final values of the design variables shown on page 71 of reference 9 are used as the nominal values for AESOP. It can be seen that a small performance gain is possible.

Table C3 presents the results obtained by AESOP for Case 1-I when the absolute values of *all behavior variables were constrained to be less than or equal to 1.0* This procedure was followed in an arbitrary attempt to force realistic circumferential stiffener geometries. The major effect of the additional constraint was to alter the dimensions of the circumferential stiffeners giving them more realistic values of depth and thickness. This procedure is less direct than introducing a constraint on (d/t). It should be noted that the critical mode shapes obtained for this solution do not differ significantly from the critical modes shown in Table C1. This would indicate that the 0.0063 thick by 2.0 deep ring (d/t≈318) is expected to force certain critical mode shapes. This probably is an optimistic assumption in practice. Imposition of the additional constraints results in a weight penalty of 24.9 pounds.

To illustrate the presence of a local extremal induced by constraints, Case 1-I was rerun using large initial constraint error weights, (4.0×10^6). The initial control vector was taken as the final vector from the sample problem on page 162 of reference 9. The results obtained are presented in table C4. It can be seen that the solution is constrained by the skin buckling for load case 2 with a minimum weight of *410 pounds*. This problem was solved above with constraint weights of 10.0 and, as noted, a lower minimum weight cylinder of *226 pounds* was achieved. It should be noted that solution was *simultaneously constrained by four constraint functions;* gross buckling, skin buckling, panel buckling and longitudinal stiffener buckling.

The inferior solution obtained when high nominal constraint weights are utilized is constrained by only *one constraint function*, skin buckling, and appears to be a clear case of an inferior, constraint induced minima.

Case 2-I', Three Load Cases, Cylinder Length = 165", Cylinder Radius = 60". Load conditions for this problem are:

1. Axial load 1400 lb/in., External pressure 0.

2. Axial load 1880 lb/in., External pressure -4. lb/in^2

3. Axial load 424 lb/in., External pressure .8 lb/in.

Problem solution details are given in Table C5, Appendix C. Cylinder minimum weight is *387 lbs.*, figure 23. This compares directly to the minimum weight of *389 lbs.* reported on page 78 of reference 9.

Case 3-I, Three Load Case, Cylinder Length = 165", Cylinder Radius = 60." Load conditions for this problem are:

1. Axial load 2100 lb/in., External pressure 0.

2. Axial load 2820 lb/in., External pressure -6. lb/in^2

3. Axial load 636 lb/in., External pressure 1.2 lb/in^2

Problem solution details are given in Table C-6, Appendix C. Cylinder minimum weight is *437 lbs.*, figure 23. This compares directly to the minimum weight of *445 lbs.* reported on page 81 of reference 9.

Case 4-0., Three Load Case, Cylinder Length = 500", Cylinder Radius = 200". Load conditions for this problem are:

1. Axial load = 2100 lb/in., External pressure = 1. lb/in^2

2. Axial Load = 8000 lb/in., External pressure = -20 lb/in^2

3. Axial load = 5000 lb/in., External pressure = 0.

This problem was solved from two nominal starting points, *starting point 1* of reference 9 and the *final solution obtained from starting point 1* of reference 9. Minimum

weights of *14252 pounds* and *14332 pounds* (Figure 23), respectively, were obtained. Final cylinder details are given in Tables C7 and C8 of Appendix C.

These results compare directly to a final weight of *21300 pounds* reported on page 86 of reference 9. More significantly, the *final weight of 21300 pounds* obtained in reference 9 is higher than the *starting weight of 16200 pounds*, yet, of necessity with the Fiacco and McCormick procedure, both the final "minimal" weight and the lighter starting weight must be feasible designs.

It should also be noted that this problem was solved from a second starting in reference 9. With an initial constraint multiplyer value of r_0 = 1500 a minimal weight of *26900 pounds* was reported;with an initial multiplyer value of r_0 = 375, a minimal weight of *14700 pounds* was reported. This last solution compares favorably with the minimum weights of 14252 and 14332 pounds obtained by the AESOP exterior penalty function solution.

Case 5-I, Three Load Case, Cylinder Length = 2000", Cylinder Radius = 200". Load conditions for this problem are:

1. Axial load = 2100 lb/in., External pressure = 1.0 lb/in^2

2. Axial load = 8000 lb/in., External pressure = -20 lb/in^2

3. Axial load = 5000 lb/in., External pressure = 0

This problem was solved from a single nominal starting point and a minimal weight of *48097 pounds* was achieved. It should be noted that considerable difficulty was experienced in obtaining this solution; the exterior penalty function constraint weights were relaxed four times. It is postulated that the prime reason underlying these convergence difficulties was the use of relatively low constraint factors. In all exterior penalty function solutions of this report starting factors of 10. were used. The range of final cylinder weights covered is from 3.8 pounds to 48000 pounds. Clearly, the constraint penalty factors should be related to the payoff function values. It is suggested that studies using the exterior penalty function procedure should employ starting constraint factors approximating 1 per cent of the anticipated performance value. The effectiveness of alternate constraint penalty factor starting values was not investigated in the present study.

The one solution to Case 5 in reference 9 produced a minimum weight of *50000 pounds*. This compares closely to the value of *48097 pounds* above. However, in view of the difficulties encountered with the exterior penalty function solution, it is felt that a second solution to this problem is required to verify the optimality, or lack of optimality, of the result.

Case 6-I, Single Load Case, Cylinder Length = 38", Cylinder Radius = 9.55". The single load case is:

Axial Load = 800 lb/in., Exterior Pressure = 0

Two solutions were obtained corresponding to Cases 6-I and 6-I', pages 90 and 91 of reference 9. Minimum weights attained by the solutions are *3.81 and 3.70 pounds*, respectively, Figure 23. This compares with *8.35 and 4.20 pounds* in reference 9.

Case 7-I, Single Load Case, Cylinder Length = 291", Cylinder Radius = 95.5". The single load condition was

Axial Load = 800 lb/in., Extremal Pressure = 0.

This case has been discussed in detail in the section "Typical Optimization Algorithm Behavior in Stiffened Cylinder Design" where the recommended search combination produced a minimum cylinder weight of *682 pounds*, figure 23. Solutions in reference 9 achieved minimum weights of *1960 pounds, 979 pounds, and 2240 pounds*, depending on the interior penalty function constraint factor, *design variable bounds* employed, and, in the case of the 2240 pound cylinder, the absence of longitudinal stiffeners. It should again be noted that the nominal feasible design employed (1680 pounds) was lighter than two of the final "minimum"weights reported in reference 9.

Case 8-I, 0, Single Load Case, Cylinder Length = 361", Cylinder Radius = 433". The single load condition was

Axial Load = 12150 lb/in., External Pressure = 0

Starting from a nominal cylinder weighing 46840 pounds, a minimum weight design of *38824 pounds* was attained, figure 23. This compares to a minimum weight of *39400 pounds* reported in reference 9.

Cylinder Design Summary

It is evident from the table of results in figure 23 that the present designs obtained by the optimization procedure embodied in program AESOP converge with a relatively high degree of reliability. The optimal designs obtained are all superior to thsse obtained previously, in some cases by a significant margin. This is thought to be due to three factors:

(a) The use of multiple search algorithms
(b) The use of an exterior penalty function constraint procedure
(c) The practice of using two runs with a relaxation of the constraint weights after each run

The solutions obtained confirm the applicability of the optimization techniques contained in program AESOP to at least one class of structural optimization problem. These same optimization techniques have now been applied successfully to problems in the fields of single vehicle and two-vehicle combat performance optimization, reference 31; minimum sonic boom overpressure body shapes, reference 32; phased array antenna design, reference 33; aerodynamic shaping, reference 34; liquid rocket engine combustor design, reference 35; and overall vehicle synthesis, reference 3.

Ray Search

The ability to perform a one-dimensional search through the multidimensional design space between two points $P_1 \equiv \bar{\alpha}_1$ and $P_2 \equiv \bar{\alpha}_2$ is an integral part of current versions of the program of references 1 through 3. Figures 24 to 26 reveal the constraint and performance function behavior along such rays. Figure 24 illustrates function behavior between the

CASE	STIFFENERS	WEIGHT (Pounds)				Improvement over best CR 1217 Result**
		Results Obtained in CR-1217		Results Obtained in AESOP		
		Nominal	Final	Nominal	Final	
1-I(1)	Inside	715	231	715	226	2%
1-I(2)	Inside	1000	230			
1-I'	Inside	715	293			
1-O	Outside	715	240			
1-I,O	Inside/Outside	715	235			
1-It	Inside*	715	303			
2-I	Inside	370	340			
2-I'	Inside	418	389	418	387	$\frac{1}{2}$%
2-O	Outside	836	363			
2-I,O	Inside/Outside	746	358			
3-I	Inside	835	445	835	437	2%
3-I'	Inside	835	490			
3-O	Outside	836	468			
3-I,O	Inside/Outside	835	457			
4-I	Inside	15900	14600			
4-O(1)	Outside	16184	21300	16184	14252	2%
4-O(2)	Outside	44900	26900			
4-O'	Outside	44900	14700			
4-O(A)	-	-	-	21300	14332	2%
5-I	Inside	124500	50000	124500	48097	4%
6-I	Inside	13.7	8.35	13.7	3.8	9.5%
6-I'	Inside	11.8	4.20	11.8	3.7	12%
6-O'	Outside	11.8	4.30			
6-I,O'	Inside/Outside	11.8	3.76			
6-Os	Longitudinal	12.7	8.54			
6-Is	Longitudinal	12.7	8.40			
7-I	Inside	1680	1960	1680	683	30%
7-I'	Inside	1680	979			
7-I"	Circumferential	1680	2240			
8-I,O	Inside/Outside	46840	39400	46840	38824	2%

* Reduced modulus in second load case

** CR-1217 considers the problem to be converged if the value of the function is estimated to exceed its minimum by two per cent or less. Note the two per cent in half the cases.

FIGURE 23. COMPARISON BETWEEN MINIMUM WEIGHT CYLINDER DESIGNS

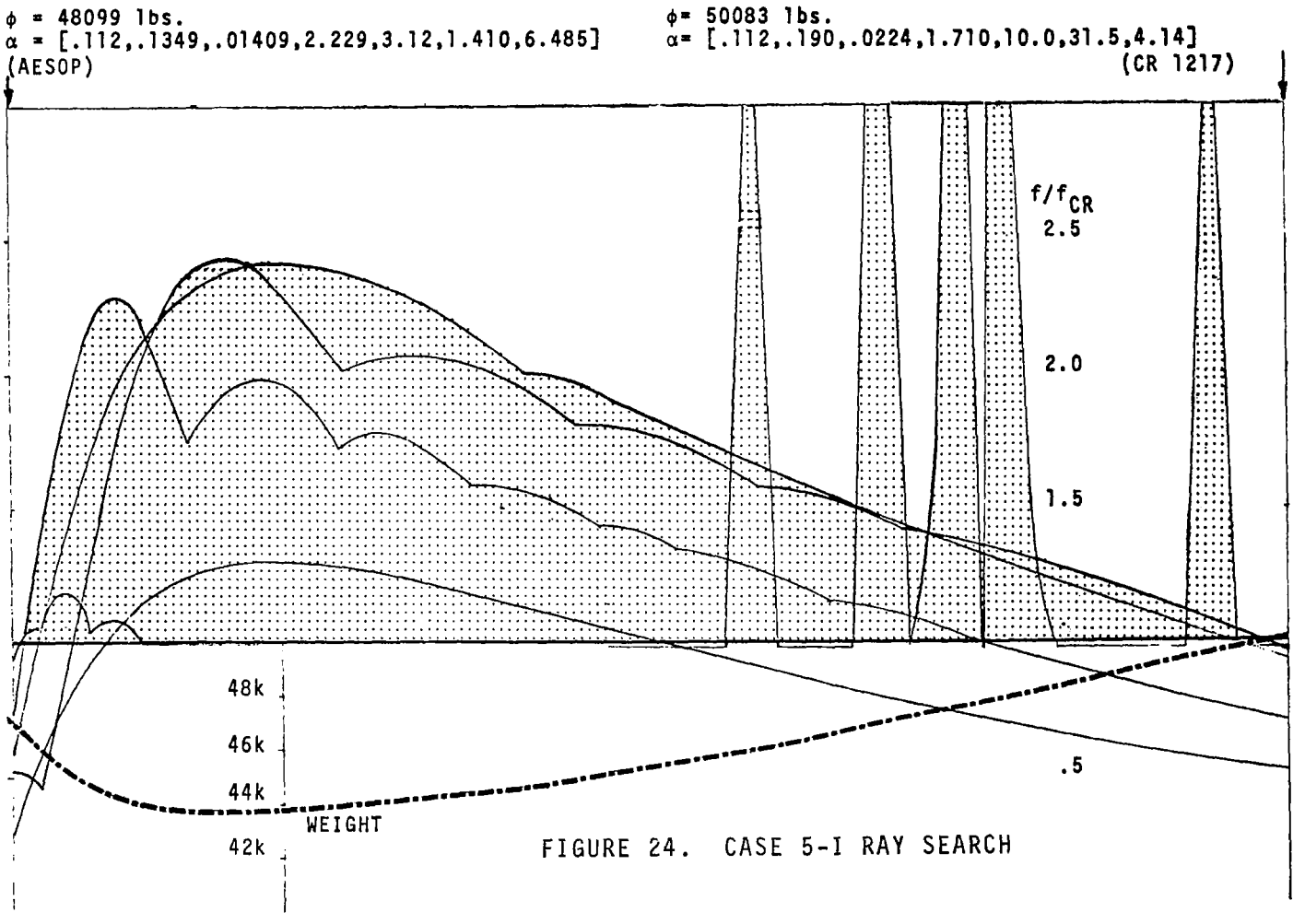

FIGURE 24. CASE 5-I RAY SEARCH

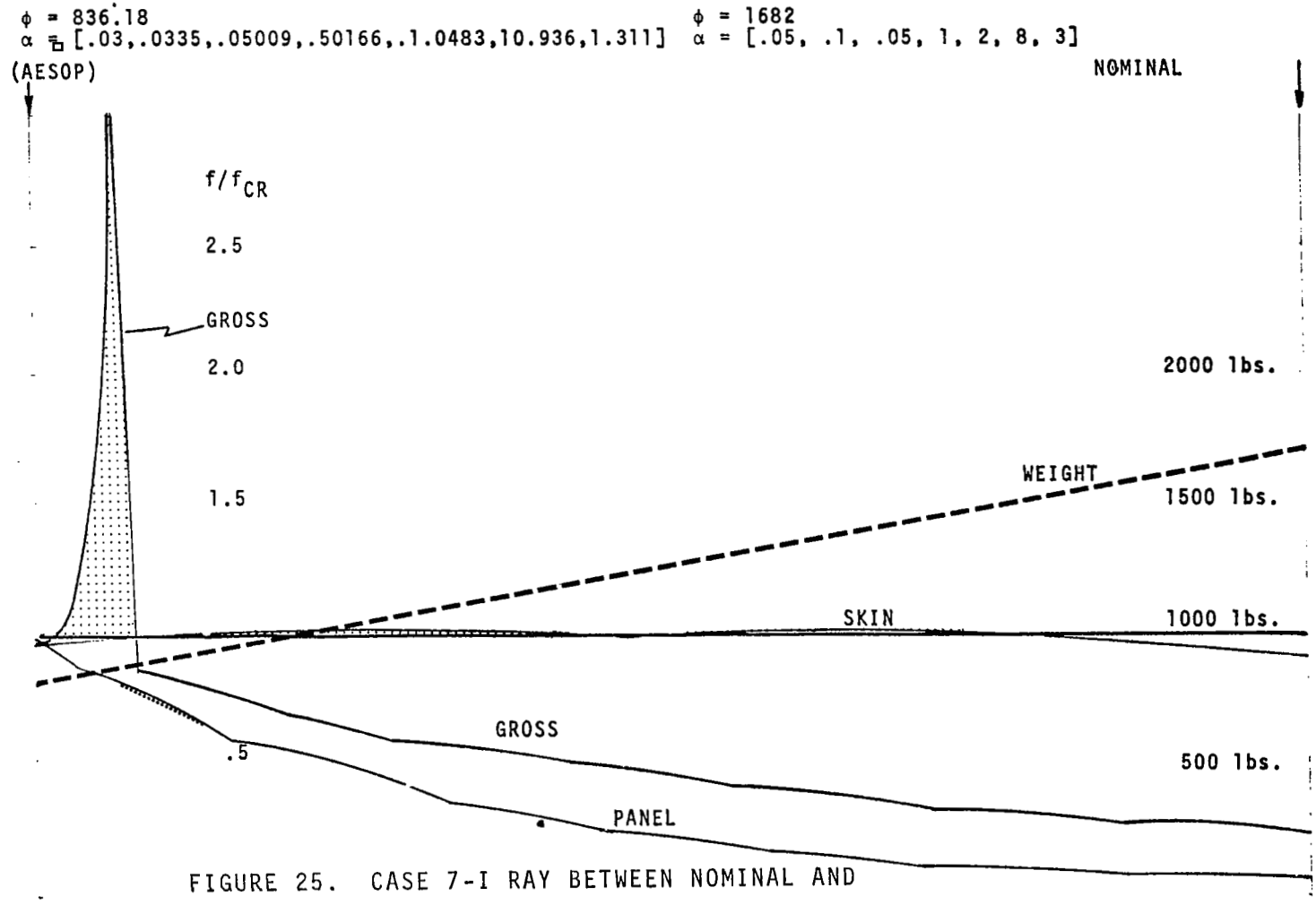

FIGURE 25. CASE 7-I RAY BETWEEN NOMINAL AND AESOP SOLUTION

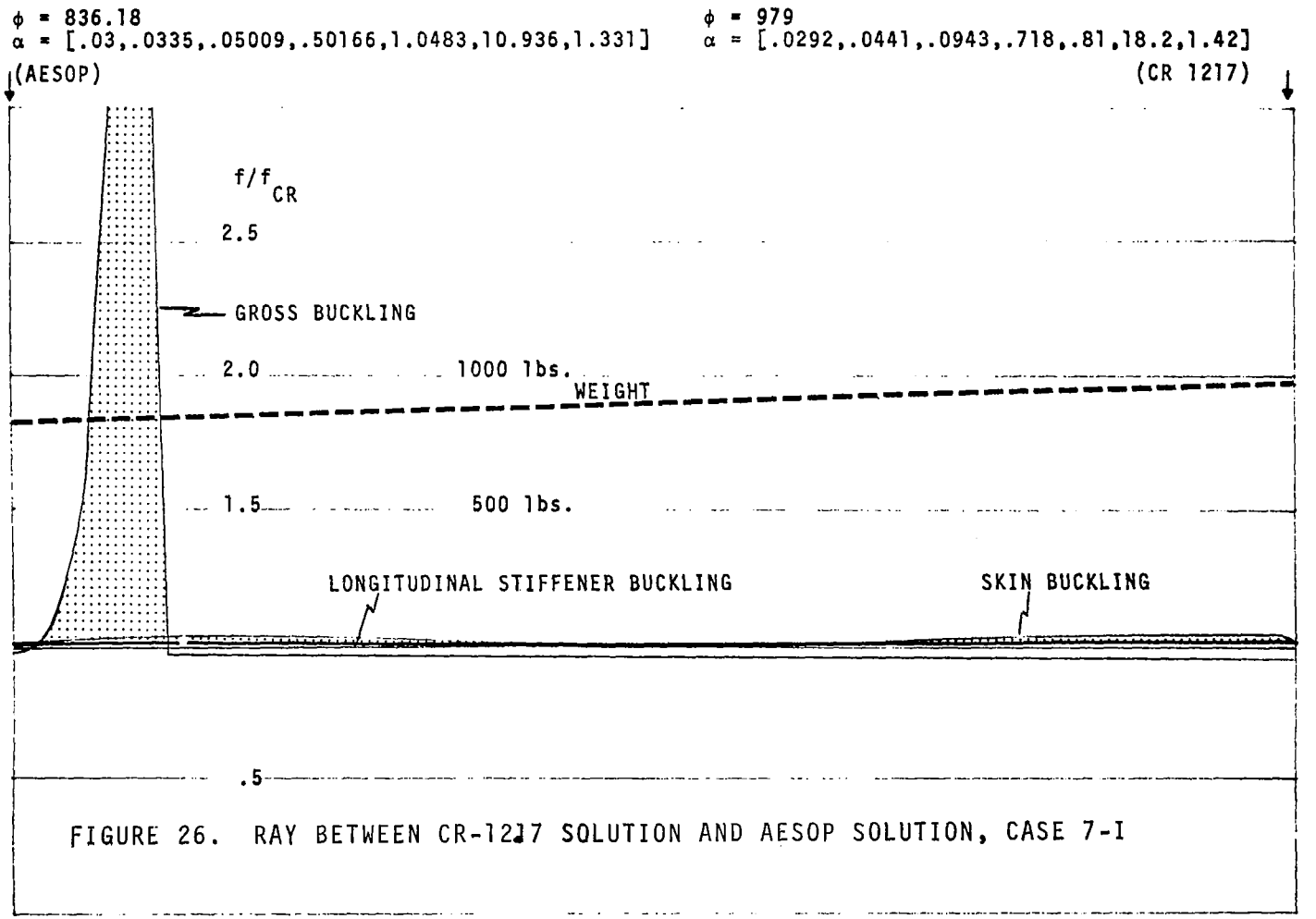

FIGURE 26. RAY BETWEEN CR-1217 SOLUTION AND AESOP SOLUTION, CASE 7-I

present 48097 pound solution to Case 5-I and the 50083 pound solution reported in reference 9. It can be seen that a set of multiple-arced constraint violations lie between the two solutions and that an interior penalty function procedure would be unable to proceed along this multidimensional ray as a result of these violations. Proceeding the 50083 pound design leftwards to the 48089 pound design constraint violations are encountered for

(a) Rib buckling in load case 2

(b) Skin buckling in load case 3

(c) Skin buckling in load case 2

(d) Rib buckling in load case 2

(e) Gross buckling in load case 2

Minimum weight is attained to the right of the 48089 pound cylinder but is accompanied by four constraint violations.

A similar result is shown in figures 25 and 26 for Case 7-I. Figure 25 illustrates function behavior on the ray between the nominal design and the present 836 pound design. Figure 26 presents behavior on the ray between the reference 9 best 979 pound solution to this problem and the present 836 pound design. It can be seen from figure 26 that the solution shown by reference 9 is locally constrained by skin buckling.

MULTIPLE EXTREMAL SEARCH PROCEDURE

The multiple extremal search procedure proposed in reference 1 has a straightforward basis. A multivariable extremal problem is solved by any of the recognized procedures, steepest-descent, second-order, random, or elemental perturbation techniques. With the position of an extremal known, a non-linear coordinate transformation which modifies the response surface but not the response surface topology is introduced. The transformation contracts an elemental "hyper volume" of the feasible region in the vicinity of the known extremal point and expands such an elemental volume at points far removed from the known extremal point. The feasible region boundaries are unchanged by the transformation. It follows directly that the "region of influence" of the known extremal is reduced in size and that the region of influence of a second extremal, if it exists, is increased in size. The degree of the expansion can readily be controlled.

If the degree of the warping transformation is sufficiently high, the probability of a second multivariable search in the transformed coordinate space, locating the first extremal becomes small provided a second extremal point reasonably well separated from the first point exists.

The multiple extremal feature of program AESOP was demonstrated on Case 7-I with limits on d/t (see Page 57). In order to use the multiple extremal feature of AESOP, it is first necessary to establish a warping origin in the parameter space. The warping origin is taken as the optimum design vector established in a previous run; this extremal is then effectively "swept out" of the response surface by the transformation. The exponent of the warping transformation in this study was taken as 2.0. The final control vector of the run presented in Table D8 was used as the warping origin. Results obtained using the warping transformation are presented in Table D14. (Note that this design was obtained with d/t limits imposed). It can be seen that the final weight obtained by the multiple extremal search, 838 pounds, is practically the same as that obtained prior to introduction of the warping transformation,837 pounds.

In an additional effort to locate a relative minima, Case 7-I was rerun using a 246 pound cylinder as the nominal. This run was made without the warping transformation. The results of this run are presented in Table D15. The constraint on panel buckling is still too large by about three per cent; additional running would eliminate this violation with no significant change in the cylinder weight. A final weight of 835 pounds was achieved. The 246 pound nominal was then rerun using the warping transformation centered at the final control vector of Table D15. The results obtained are presented in Table D16.

The weight of the lightest design obtained using the warping transformation is within four and one-half per cent of the weight of the lightest design obtained without application of the warping transformation. An additional run should significantly reduce the difference between the two solutions. This probably indicates the existence of a single minimal point in the *unconstrained* response surface.

One objective of the present study was a demonstration of the multiple extremal search on a problem having more than one extremal. Since this technique appears to be unnecessary in the case of stiffened cylinder design, a demonstration of the technique on a straightforward two-dimensional problem was undertaken. The problem considered is that of finding the eigenvalues of a complex matrix. The method could readily be extended to the general N × N complex eigenvalue problem, a problem of some interest in the area of structural dynamics and other engineering fields.

The 2 x 2 complex characteristic equation is

$$\begin{vmatrix} (a_{11} + jb_{11}) - \lambda & a_{12} + jb_{12} \\ a_{21} + jb_{21} & (a_{22} + jb_{22}) - \lambda \end{vmatrix} = 0 \qquad (45)$$

Here $j=\sqrt{-1}$ and λ is an eigenvalue of the matrix

$$[A] = [a_{mn} + jb_{mn}] \tag{46}$$

Expanding the determinental equation (36)

$$\lambda^2 + C\lambda + D = 0 \tag{47}$$

where

$$C = A_{11} + A_{22} \tag{48}$$

$$D = \begin{vmatrix} A_{11} & A_{12} \\ A_{21} & A_{22} \end{vmatrix} \tag{49}$$

and

$$A_{mn} = a_{mn} + jb_{mn} \tag{50}$$

It follows that

$$\lambda = \frac{-C \pm \sqrt{C^2 - 4D}}{2} \tag{51}$$

This problem can readily be solved by multivariable search. Suppose

$$\lambda = a_1 + ja_2 \tag{52}$$

The eigenvalues λ are given by the points (a_1, a_2) which satisfy

$$\text{Min } (|A(\lambda)|^2) = \text{Min } (|A(a_1, a_2)|^2) = 0 \tag{53}$$

This problem is solved below using the matrix

$$[A] = \begin{vmatrix} (1 - j) & (1 + j0) \\ (0 + j) & (0 + j0) \end{vmatrix} \tag{54}$$

The eigenvalues of the characteristic equation of this matrix are

$$\lambda_1 = 1 - j0 \quad \text{and} \quad \lambda_2 = 0 - j \tag{55}$$

Solutions to the eigenvalue problem above were obtained by program AESOP using the adaptive search, an elemental perturbation technique, in conjunction with the "pattern" acceleration procedure. The feasibly region employed was defined by

$$\alpha_{L_1} < \alpha_1 < \alpha_{H_1} \qquad \text{where} \quad \alpha_{L_1} = \alpha_{L_2} = -2$$

$$\alpha_{L_2} < \alpha_2 < \alpha_{H_2} \qquad \alpha_{H_1} = \alpha_{H_2} = 2 \tag{56}$$

The eigenvalue problem was solved from five starting points both with and without warping. From each point the problem was first solved without warping. The resulting extremal point was then used as the origin of a second order warping transformation (N = 2), and the problem was solved again from the same initial starting point. The second search should then have increased the probability of locating the second extremal. In all five cases the second search successfully found the second extremal. Figure 27 presents the results and the starting points. Figures 28a and 28b display convergence from a typical starting point.

The example presented appears to confirm the practicality of the warping technique at least on problems of moderate

RESULTS OF THE FIVE MULTIPLE EXTREMAL SEARCHES		
CASE	STARTING POINT	EXTREMAL POINT
1	(0, 0)	(1, 0)
1 (Warped)	(0, 0)	(0,-1)
2	(2, 2)	(1, 0)
2 (Warped)	(2, 2)	(0,-1)
3	(-2, 2)	(1, 0)
3 (Warped)	(-2, 2)	(0,-1)
4	(2,-2)	(0,-1)
4 (Warped)	(2,-2)	(1, 0)
5	(-2,-2)	(0,-1)
5 (Warped)	(-2,-2)	(1, 0)

FIGURE 27. MULTIPLE EXTREMAL PROBLEM

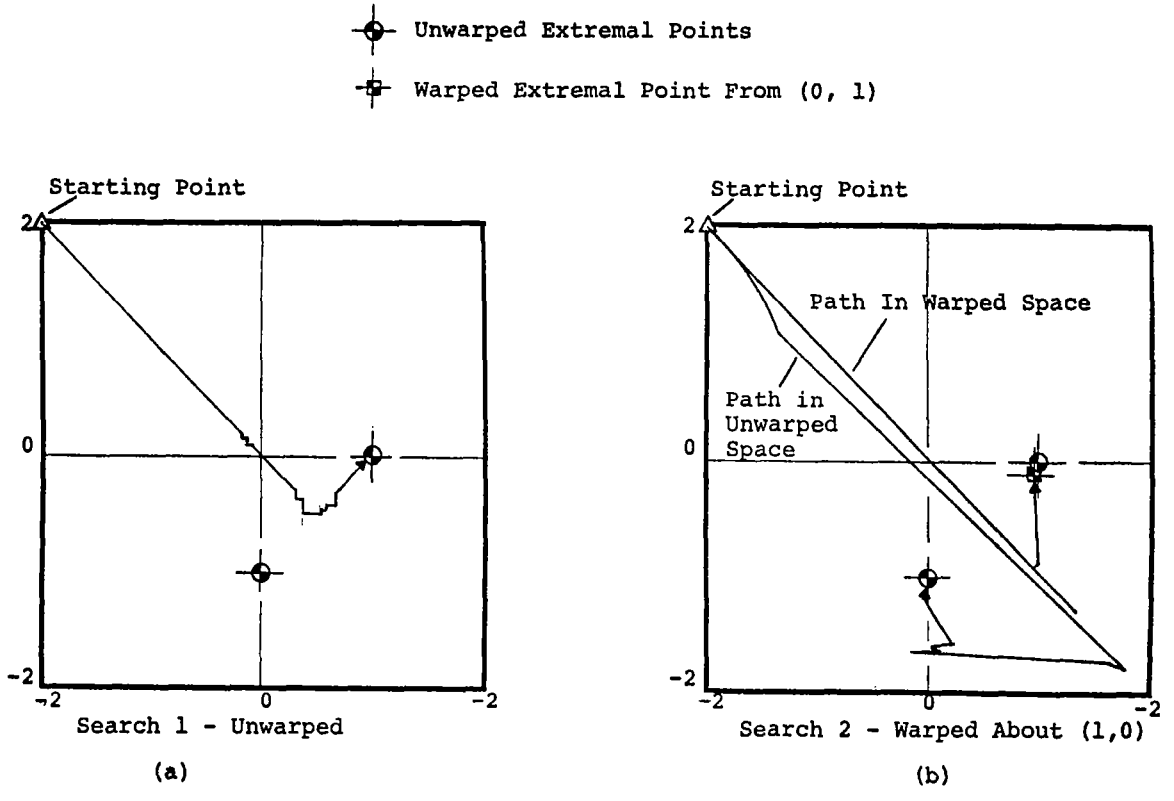

FIGURE 28. TYPICAL SEARCH PATHS

complexity (here, a fourth-order polynomial, eq. (44)). The regularity with which both extremals were found is surprising. The technique merely increases the probability of finding a second extremal; it does not guarantee that a second extremal will be found if one exists. Clearly, further tests of the technique are in order; equally clearly, the multiple extremal problem is not intractable when the elementary technique of reference 1 can be applied so successfully.

EMPIRICAL DESIGN OF RING STIFFENED CYLINDERS

This section contains a comparison between stiffened cylinder designs obtained from linear theory and *ring stiffened* cylinders obtained using empirical buckling data. The program used for the empirical design of ring stiffened shells is briefly described. In its present form this program does not consider longitudinally stiffened shells or positive internal pressure loads. The comparisons are shown in figure 29 and, therefore, omit load conditions with internal pressure. It can be seen from figure 29 that the cylinders designed on an empirical buckling basis are between 1.50 to 3.50 times heavier than those designed on the basis of linear theory. These ratios would probably increase if the second load case of problems 1-I to 5-I were considered.

The program uses an empirical method of analysis to design cylindrical or conical shell-type structures. Statistically determined buckling coefficients are used to compute the allowable loads. The program has been designed to allow buckling coefficient data to be described

CASE	EMPIRICAL DESIGN						LINEAR THEORY	WEIGHT/W*
	Load Condition	h	B	n	I_y	Weight	W*	
1-I	1	.1097	4.34	8	1.492E-3	703.2	226	3.10
1-I	3	.0734	4.34	7	5.868E-4	489.6		
2-I	1	.1389	4.34	7	4.906E-4	898.4	257	3.50
2-I	3	.0932	4.34	7	1.448E-3	629.8		
3-I	1	.1594	4.34	7	9.860E-4	1038.0	381	2.72
3-I	3	.1071	4.34	6	2.382E-3	729.7		
4-I	1	.3358	13.16	7	.2092	23087.3	14252	1.63
4-I	3	.4472	13.16	7	6.452E-2	29367.0		
5-I	1	.2925	10.53	3	.9472	93123.2		
5-I	3	.3885	10.53	4	6.655E-2	103609.9	48097	2.16
6-I	1	.0501	6.33	6	1.275E-5	11.6	3.58	3.24
7-I	1	.1061	3.83	8	4.301E-4	1948.3	683	2.85
8-I	1	.4848	9.5	10	1.476	58295.2	38824	1.50

FIGURE 29. COMPARISON OF CYLINDERS DESIGNED USING EMPIRICAL BUCKLING DATA WITH LINEAR THEORY

in several different ways. Most of the statistically determined buckling data appearing in the literature can be described by one of the forms available in the program. For example, figure 30 compares the buckling coefficient for axial compression versus R/t used by three major aerospace vehicle manufacturers. The input statements of the program to some degree permit the user to control the method used to compute the allowable loads and the factor of utilization.

Applied Loads

Any combination of axial compression, bending, shear, and uniform external lateral pressure may be applied to the shell. Any of the above loads may be zero.

The running load due to axial compression is computed by

$$W_{A_a} = P/[2\pi R_1 \cos(\xi)] \tag{57}$$

The maximum value of the running load due to bending is computed by

$$W_{B_a} = M/[\pi R_1^2 \cos(\xi)] \tag{58}$$

The maximum value of the running load due to shear is computed by

$$W_{S_a} = V/(\pi R_1) + T/(2\pi R_1^2) \tag{59}$$

The running load due to uniform external lateral pressure is computed by

$$W_{Q_a} = QR \tag{60}$$

R_1 is given by

$$R_1 = R - L \sin(\xi)/2 \cos(\xi) \tag{61}$$

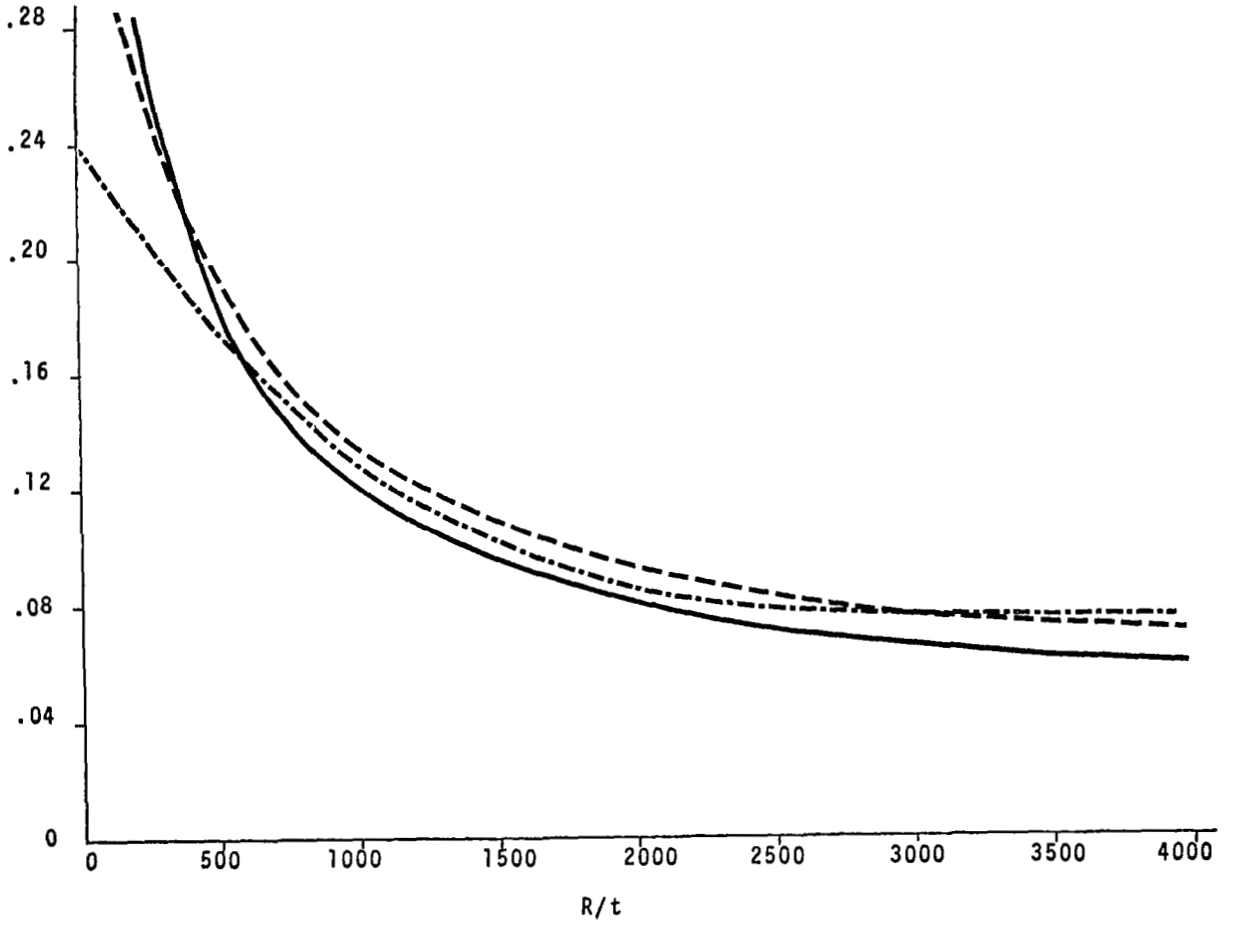

FIGURE 30. AXIAL BUCKLING COEFFICIENTS VERSUS R/t DATA FROM VARIOUS MANUFACTURERS

The Elastic Modulus at room temperature (E_{RT}) is input to the program. A table is also input giving per cent of E_{RT} as a function of temperature so that the elastic modulus at other than room temperature may be determined as a tabular function.

Elastic Buckling Stresses

The program has been designed to allow buckling coefficient data to be described in several different ways.

Axial Compression. The program standard option computes the buckling coefficient for axial compression as given by Seide, reference 11, as

$$C_A = 0.606 - 0.546(1-\beta_1) \qquad (62)$$

The elastic buckling stress for axial compression is then found to be

$$\sigma A/\eta = \frac{C_A E \cos(\xi)}{\beta} \qquad Z \geq \frac{\pi^2}{6C_A\sqrt{1-\mu^2}} \qquad (63)$$

for

$$Z < \frac{\pi^2}{6C_A\sqrt{1-\mu^2}}$$

and *simply supported edges*, (see references 12, 13, and 14)

the buckling coefficient for axial compression is

$$K_A = 1 + \frac{36(1-\mu^2)C_A^2 Z^2}{\pi^4} \qquad (64)$$

and the elastic buckling stress for axial compression is then computed from

$$\sigma_A/\eta = \frac{K_A \pi^2 E h^2 \cos^2(\xi)}{12B^2(1-\mu^2)} \qquad (65)$$

Alternatively, in a second option, the buckling coefficient for axial compression, C_A, is input to the program. The user has a choice of describing the axial buckling coefficient as a table function or as a polynomial. The polynomial form adopted is

$$C_A = \sum_{i=0}^{N_A} A_{ai}\, \beta^i; \qquad N_A \leq 7 \qquad (66)$$

and the elastic buckling stress for axial compression will be computed from

$$\sigma_A/\eta = \frac{C_A E \cos(\xi)}{\beta} \qquad (67)$$

In the third option the buckling coefficient for axial compression is computed from

$$K_A = \left(\frac{12\sqrt{1-\mu^2}}{\pi^2}\right) C_A Z \; ; \qquad Z \geq \frac{\pi^2}{6C_A\sqrt{1-\mu^2}} \qquad (68)$$

where C_A is determined as above, and the elastic buckling stress for axial compression is computed as

$$\sigma_A/\eta = \frac{K_A \pi^2 E h^2 \cos^2(\xi)}{12 B^2 (1-\mu^2)} \qquad (69)$$

In a final fourth program option, the buckling coefficient for axial compression is taken from reference 11 as

$$C_A = 0.606 - 0.546\ (1-\beta_1) + 0.16\ [\frac{h\ \cos(\xi)}{B}\ ]^{0.3} \qquad (70)$$

and the elastic buckling stress for axial compression is computed from

$$\sigma_A/\eta = \frac{C_A E\ \cos(\xi)}{\beta}\ ; \qquad Z \geq \frac{\pi^2}{6C_A\sqrt{1-\mu^2}} \qquad (71)$$

For

$$Z < \frac{\pi^2}{6C_A\sqrt{1-\mu^2}}$$

and simply supported edges, the buckling coefficient for axial compression is found from

$$K_A = 1 + \frac{36(1-\mu^2)\ C_A^2\ Z^2}{\pi^4} \qquad (72)$$

and the elastic buckling stress for axial compression is computed from

$$\sigma_A/\eta = \frac{K_A\ \pi^2\ E\ h^2\ \cos^2(\xi)}{12\ B^2\ (1-\mu^2)} \qquad (73)$$

Bending

The program standard option computes the buckling coefficient for bending from reference 11 as

$$C_B = 0.606 - 0.443\ (1-\beta_1) \qquad (74)$$

The elastic buckling stre- for bending is then found to be

$$\sigma_B/\eta = \frac{C_B\ E\ \cos(\xi)}{\beta} \qquad \begin{matrix}\beta \geq 100 \\ Z \geq 20\end{matrix} \qquad (75)$$

The value of σ_B/η is conservative for $Z < 20$.

In a second option, the buckling coefficient for bending is input to the program. The user has a choice of describing the bending buckling coefficient as a table function or as a polynomial. In the polynomial form

$$C_B = \sum_{i=0}^{N_B} A_{B_i}\ \beta^i \ ; \qquad N_B \leq 7 \qquad (76)$$

and the elastic buckling stress for bending is computed as

$$\sigma_B/\eta = \frac{C_B\ E\ \cos(\xi)}{\beta} \qquad (77)$$

The third option computes the buckling coefficient for bending as

$$K_B = Z\ C_B \qquad (78)$$

where C_B is determined as above, and the elastic buckling stress for bending is computed from

$$\sigma_B/\eta = \frac{K_B \pi^2 E h^2 \cos^2(\xi)}{12 B^2 (1-\mu^2)} \qquad (79)$$

Shear Loads

The standard program option computes the buckling coefficient for shear as given by Seide in reference 11 as

$$C_s = \frac{0.6375 \overset{*}{R}^2 \overset{*}{Z}^{3/4}}{R_1^2} \qquad (80)$$

and the elastic buckling stress for shear is computed as

$$\sigma_s/\eta = \frac{C_s \pi^2 E h^2}{12 B^2 (1-\mu^2)} \qquad (81)$$

The value of σ_s/η is conservative for $z < 40$.

In a second option, the buckling coefficient for shear is input to the program. The user has a choice of describing the shear buckling coefficient as a table function or as a polynomial. In the polynomial option

$$C_s = Z^{3/4} \sum_{i=0}^{N_s} A_{si} \beta^i \; ; \qquad N_s \leq 7 \qquad (82)$$

and the elastic buckling stress for shear is computed as

$$\sigma_s/\eta = \frac{C_s \pi^2 E h^2}{12 B^2 (1-\mu^2)} \qquad (83)$$

Uniform External Lateral Pressure

In the standard program option, the buckling coefficient for uniform external lateral pressure is taken from reference 11 and the elastic buckling stress for uniform external lateral pressure is computed as

$$\sigma_p/\eta = \frac{K_p \pi^2 E h^2}{12 B^2 (1-\mu^2)} \qquad (84)$$

In a second option the buckling coefficient for uniform external lateral pressure is input to the program. The user has a choice of describing the pressure buckling coefficient as a table function or as a polynomial. In the polynomial option

$$K_p = \sum_{i=0}^{N_p} A_{pi} Z^i \; ; \qquad N_p \leq 7 \qquad (85)$$

and the elastic buckling stress for uniform external lateral pressure is computed as

$$\sigma_p/\eta = \frac{K_p \pi^2 E h^2}{12 B^2 (1-\mu^2)} \qquad (86)$$

Plasticity Correction

In the standard program option, the elastic buckling stresses are not corrected for the effects of plasticity. The allowable buckling stresses are set equal to the elastic buckling stresses

$$\sigma = \sigma/\eta \tag{87}$$

In a second program option the elastic buckling stresses are corrected for the effects of plasticity. The following procedure is used to compute the allowable buckling stresses.

If $\sigma/\eta \geq \sigma_{uE}$ then $\sigma = \sigma_{uA}$ (88)

If $\sigma/\eta \leq \sigma_L$ then $\sigma = \sigma/\eta$ (89)

If $\sigma_L < \sigma/\eta < \sigma_{uE}$ then σ will be computed as

$$\sigma = \frac{\sigma_2-\sigma_1}{T_2-T_1}(T-T_1) + \sigma_1 \tag{90}$$

where

$$T_1 \leq T < T_2$$

and

$$\sigma_1 = \sum_{i=0}^{N} A1_i(\sigma/\eta)^i \qquad N \leq 4$$

$$\sigma_2 = \sum_{i=0}^{N} A2_i\,(\sigma/\eta)^i \qquad N \leq 4$$

Ratio of Applied to Allowable Loads

The allowable buckling stresses described above are used to compute the allowable loads and the ratio of applied to allowable load as follows:

The allowable axial compressive loads are given by

$$w_A = h\,\sigma_A \tag{91}$$

and

$$P_{CR} = 2\pi\, w_A\, R_1 \cos(\xi) \tag{92}$$

The ratio of applied axial load to allowable axial load is

$$R_A = \frac{P}{P_{CR}} \tag{93}$$

The allowable bending loads are given by

$$w_B = h\,\sigma_B \tag{94}$$

and

$$M_{CR} = \pi\, w_B\, R_1^2 \cos(\xi) \tag{95}$$

The ratio of applied bending load to allowable axial load is

$$R_B = \frac{M}{M_{CR}} \tag{96}$$

The allowable shear loads are given by

$$w_s = h\,\sigma_s \tag{97}$$

The ratio of applied shear load to the allowable shear load is

$$R_s = w_{sa}/w_s \tag{98}$$

The allowable uniform external lateral pressure load is given by

$$w_p = h\,\sigma_p \tag{99}$$

and

$$Q_{CR} = w_p/R \tag{100}$$

The ratio of applied pressure load to allowable pressure load is

$$R_p = Q/Q_{CR} \tag{101}$$

Interaction of Combined Loads

In the standard program option the exponents used in the interaction equation are given by

$$\bar{\gamma} = \left[1 + 0.7\left(\frac{B}{R}\right) - 0.04\left(\frac{B}{R}\right)^2\right]^{1/2} \qquad \frac{B}{R} < 10$$

$$\bar{\gamma} = 2.0 \qquad \frac{B}{R} \geq 10$$

$$\gamma_p = \bar{\gamma}$$

$$\gamma_A = \gamma_B = \gamma_s = 1.0 \tag{102}$$

Alternately, the exponents γ_A, γ_B, γ_s, $\bar{\gamma}$, and γ_p may be input as data.

The factor of utilization is computed from

$$1.0 = \left[\left(\frac{R_A}{U}\right)^{\gamma_A} + \left(\frac{R_B}{U}\right)^{\gamma_B} + \left(\frac{R_s}{U}\right)^{\gamma_s}\right]^{\bar{\gamma}} + \left(\frac{R_p}{U}\right)^{\gamma_p} \qquad (103)$$

or optionally as

$$1.0 = \left[\left(\frac{R_A}{U}\right)^{\gamma_A} + \left(\frac{R_B}{U}\right)^{\gamma_B}\right]^{\bar{\gamma}} + \left(\frac{R_s}{U}\right)^{\gamma_s} + \left(\frac{R_p}{U}\right)^{\gamma_p} \qquad (104)$$

The margin of safety is found from

$$M.S. = \{(1/U) - 1\} \qquad (105)$$

Frame Stiffness Requirements

The required frame stiffness, EI_y, is given by Timoshenko, reference 15, for cylinders subject to uniform external lateral pressure and axial compressive force as: (NOTE: The spacing of the frames is assumed to be small compared to the radius of the shell)

$$\alpha_1 = Iy \frac{(1-\mu^2)}{B\ h\ R^2} \qquad (106)$$

Where Iy is the effective Iy when the shell is subjected to the design loads

α_1 is obtained from

$$C_1 + C_2\alpha + C_3\alpha_1 = C_4\phi_1 + C_5\phi_2 \qquad (107)$$

where

$$C_1 = s\lambda^4$$

$$C_2 = \lambda^6(\lambda^2+2n^2) + s\lambda^2n^2[2(\lambda^2-1)^2+2(n^2-1)^2+ 5\lambda^2n^2 - 2]$$

$$C_3 = (n^2-1)^2\ [\lambda^4+s(2\lambda^2+n^2)n^2]$$

$$C_4 = \lambda^4n^2 + s(2\lambda^2 + n^2)n^4 - s(3\lambda^2 + n^2)n^2$$

$$C_5 = \lambda^6 + s\lambda^2n^2(2\lambda^2 + n^2 + 1) \qquad (108)$$

Set m = 1 and let n = 2, 3, 4, . . ., so that the maximum value of α_1 may be determined.

In the above equations the parameters α, λ, s hy, ϕ_1, ϕ_2, and $\overset{*}{P}$ were determined from

$$\alpha = \frac{h}{12R^2} \qquad \lambda = \frac{m\pi R}{L}$$

$$s = hy\ \frac{(1-\mu^2)}{h} \qquad hy = h + (Ay/B)$$

$$\phi_1 = \frac{QR(1-\mu^2)}{Eh} \quad \text{and} \quad \frac{\overset{*}{P}\ (1-\mu^2)}{2\pi\ R\ Eh} = -\phi_2$$

$$\overset{*}{P} = \frac{2M}{R} + P \qquad (109)$$

For the value of α_1 computed above to be the valid, the following must be true:

$$U \simeq 1.0 \qquad (110)$$

Hess, reference 16, gives a graphical method for solving the above equations for α_1. In the present study the equations are solved numerically.

Weights

Shell weight is given by

$$WT_s = 2\pi RLhp \tag{111}$$

For frame weight, assume "z" section frames and flange length to thickness ratio of 10 and a frame web flat height of 20t. The frame area is approximately

$$A_F = 40 \sqrt{\frac{I_F}{2474}} \tag{112}$$

Normally, the program uses the criteria that the two end frames must provide "fixed" edges assuming that an end ring stiffness to intermediate frame stiffness ratio of 20 will provide "fixed" ends. With this assumption, the total weight of the frames is approximately given by

$$WT_F = \left\{(20)\ (2)\ (40 \sqrt{\frac{I_F}{2474}}) + (NOF-2)\ 40 \sqrt{\frac{I_F}{2474}}\right\} 2\pi R_p \tag{113}$$

The end frame weights are omitted in the present study.

Total weight is given by

$$WT_{TOTAL} = WT_F + WT_s \tag{114}$$

CONCLUSION

It is apparent that modern multivariable optimization techniques are capable of solving the class of structural design problems considered in this report. Optimal designs are achieved routinely in a reasonably efficient manner; each solution obtained required the expenditure of approximately three minutes' time on a high speed large-scale digital computer (the CDC 6600) using a single load case.

The study results lend support to the view that topographically complex constrained optimization problems can be more reliably solved by sequential application of several search algorithms than by the repeated application of a single search algorithm. This premise underlies the optimizing program AESOP which was employed in the study. It is considered significant that the search combination utilized throughout the major portion of the study consisted of a random technique, an elementary perturbation technique, and two straightforward search acceleration techniques. Over the spectrum of problems considered in this study, no advantage was perceived in the use of more organized techniques such as gradient methods or second-order methods. In point of fact, experience in the solution of both the present problems and a variety of optimization problems in other fields tends to support the view that as response surface complexity increases, the selected search procedure should be weighted towards the use of techniques such as the random ray procedure.

It would appear that the exterior penalty function approach is well suited to solution of multivariable optimization problems which involve non-convex constraint boundaries. This characteristic of the exterior penalty function technique is dependent on an ability to penetrate constraint boundaries in pursuit of improved performance. With non-convex constraints the improved performance can often be retained provided the constraint boundary subsequently enters the region of improved performance. Successful exploitation of the exterior penalty function technique in the presence of non-convex constraint boundaries is somewhat dependent on the use of adaptively determined constraint weighting factors and a willingness to restart the solution using relaxed weights following convergence to an initial constrained optimum.

No evidence of multimodal behavior in the unconstrained response function (cylinder weight) surface itself was detected. When the unconstrained response surface itself possesses more than one extremal, the search techniques applied here can be combined with a true multiple extremal search procedure such as the topographically invariant warping of program AESOP.

It is well known that a linear buckling analysis will result in an unconservative design. This point is clearly demonstrated by the present study; for minimum weight designs are obtained by the application of both linear and empirical buckling criteria. Cylinder weights obtained by the two approaches differ by factors as high as 3.5 even though in some cases the critical load case was not considered in the empirically based design. Inclusion of this

load case can only lead to higher weight empirically designed cylinders. It is accordingly recommended that the input of practical buckling criteria be considered in future studies of the present type. It is also recommended that future studies incorporate realistic geometries on stiffener members.

The successful application of multivariable search techniques to the stiffened cylinder design problem encourages their further application to structural design. Ultimately, one seeks a method capable of practical application to large-scale general purpose structural analysis programs such as the National Aeronautics and Space Administration NASTRAN program. Further development of the multivariable search procedures may be required before such an approach becomes practical with today's computers. On the next generation of computers such as the CDC 7600 or possibly the STAR computers present techniques would appear capable of optimal structural definition through general purpose codes provided efficient multiple analysis techniques are employed.

REFERENCES

1. Hague, D.S. and Glatt, C.R., An Introduction to Multivariable Search Techniques for Parameter Optimization, NASA CR-73200, 1968.

2. Hague, D.S. and Glatt, C.R., A Guide to the Automated Engineering and Scientific Optimization Program, AESOP, NASA CR-73201, April 1968.

3. Hague, D.S. and Glatt, C.R., Application of Multivariable Search Techniques to the Optimal Design of a Hypersonic Cruise Vehicle, NASA CR-73202, 1968.

4. Bryson, A.E., and Denham, W.F., A Steepest-Ascent Method for Solving Optimum Programming Problems, Raytheon Report B31303.

5. Hague, D.S., Three-Degree-of-Freedom Problem Optimization Formulation, Part I, Volume 3, FDL-TDR-64-1, 1964.

6. Hague, D.S.,"The Optimization of Multiple-Arc Trajectories by the Steepest-Descent Method," *Recent Advances in Optimization Techniques*, Edited by Lavi and Vogl, (John Wiley: 1966),pages 489-517.

7. Hague, D.S., Atmospheric and Near Planet Trajectory Optimization by the Variational Steepest-Descent Method, NASA CR-73365, 1969.

8. Wilde, D.J., *Optimal Seeking Methods*, Prentice-Hall, 1964.

9. Morrow, William M. and Schmit, Lucien A., Structural Synthesis of a Stiffened Cylinder, NASA CR-1217, 1968.

10. Timoshenko, Stephen P., *Theory of Elastic Stability*, First Edition, McGraw-Hill, 1936.

11. Seide, P., Weingarten, V.I., and Margan, E.J., "Final Report on the Development of the Design Criteria and Elastic Stability of Thin Shell Structures, STL/TR-60-0000-19425, Space Technology Laboratories, In.,1960.

12. Batdorf, S.B., A Simplified Method of Elastic-Stability Analysis for Thin Cylindrical Shells. 1 - Donnell's Equation, NACA TN-1341, 1947.

13. Gerard, G. and Becker, H., Handbook of Structural Stability, Part III, Buckling of Curved Plates and Shells, NACA TN-3783, August 1957.

14. Harris, L.A., Suer, H.S., Skene, W.T., and Benjamin, R.J., "The Stability of Thin Walled Unstiffened Circular Cylinders under Axial Compression Including the Effects of Internal Pressure," *Journal of the Aeronautical Sciences*, August 1957.

15. Timoshenko, S.P. and Gere, J.M., *Theory of Elastic Stability*, Second Edition, McGraw-Hill (New York: 1961).

16. Hess, T.E. and Garber, A.M., Stability of Ring-Stiffened Conical Shells under Simultaneous Lateral Pressure and Axial Compression, Report R58SD226, General Electric, April 1958.

17. Hedgepeth, John M. and Hall, D.B., "Stability of Stiffened Cylinders," *American Institute of Aeronautics and Astronautics*, Paper No. 65-69, January 1965, pages 11-14.

18. Hutchinson, John W. and Amazigo, John C., "Imperfection Sensitivity of Eccentrically Stiffened Cylindrical Shells," *American Institute of Aeronautics and Astronautics Journal*, Volume 5, Number 3, March 1967.

19. Card, Michael F., Preliminary Results of Compression Tests on Cylinders with Eccentric Longitudinal Stiffeners, NASA TM-X1004.

20. Baruch, M. and Singer, J., "Effect of Eccentricity of Stiffeners on the General Instability of Stiffened Cylindrical Shells under Hydrostatic Pressure," *Journal of Mechanical Engineering Science*, Volume 5, Number 2., March 1963, pages 23-27.

21. Baruch, M., "Equilibrium and Stability Equations for Stiffened Shells," *The Sixth Annual Conference on Aviation and Astronautics*, Tel Aviv and Haifa, February 1964, pages 117-124.

22. Block, David L., Card, Michael F., and Mikulas, Martin, Buckling of Eccentrically Stiffened Orthotropic Cylinders, NASA TN D-2960, August 1965.

23. Van der Neut, A., "The General Instability of Stiffened Cylindrical Shells under Axial Compression," *National Aeronautical Research Institute*, Report S.314, Amsterdam 1947.

24. Flugge, Wilhelm, *Stresses in Shells*, Springer-Verlag, (New York: 1966), pages 304-307.

25. Timoshenko, S., and Goodier, J.N., *Theory of Elasticity*, McGraw-Hill (New York: 1951) page 305.

26. Novozhilov, V.V., *Foundations of the Nonlinear Theory of Elasticity*, Graylock Press (Rochester: 1953) page 189.

27. Crandall, Stephen H. and Dahl, Norman C.(Editors), *An Introduction to the Mechanics of Solids*, McGraw-Hill (New York: 1959), page 265.

28. Bleich, F., *Buckling Strength of Metal Structures*, McGraw-Hill, (New York: 1952), pages 327-329.

29. Chamis, C.C., Micro and Structural Mechanics and Structural Synthesis of Multilayered Filamentary Composite Panels, Case Western Reserve University, DSMSMD Report No. 9, pages 116-122, 1967.

30. Meissner, E., *Schweizerishe Bauzertung*, Volume 101, page 87, 1933 (in S. P. Timoshenko and Gere, *Theory of Elastic Stability*, McGraw-Hill (New York: 1961) pages 391-392).

31. Hague, D.S., Jones, R. T., and Glatt, C. R., Combat Optimization and Analysis Program--COAP, Volume I, AFFDL-TR-71-52, May 1971.

32. Hague, D.S. and Jones, R.T.,"Application of Multivariable Search Techniques to the Design of Low Sonic Boom Overpressure Body Shapes," *Third Conference on Sonic Boom Research*, NASA SP-255, October 1970, Pages 307-323.

33. Sandrin, W. A., Glatt, C. R., and Hague, D. S., Design of Arrays with Unequal Spacing and Partially Uniform Amplitude Taper, IEEE Transaction on Antennas and Propagation, September 1969.

34. Hague, D. S., Rozendall, H. L., and Woodward, F. A., "Application of Multivariable Search Techniques to Optimal Aerodynamic Shaping Problems," *Journal of the Astronautical Sciences*, November-December 1968.

35. Hague, D. S., Reichel, R. H., Jones, R. T., and Glatt, C. R., Optimizing a Liquid Propellant Rocket Engine with an Automated Combustor Design Code--AUTOCOM, NASA CR-120856, December 1971.

APPENDIX A

Development of the Analysis of the Stiffened Cylinder

A.1 Introduction

In this appendix all the equations needed to analyze the stiffened cylinder are presented. These include the overall buckling analysis of the cylinder as well as the buckling, stress and yield analyses of the skin and stiffeners.

It is well known that there is a large discrepancy between the buckling failure loads for monocoque cylinders which are predicted by classical buckling theory and the failure loads obtained in tests. However, it has been found recently that this is not necessarily the case for stiffened cylinders, reference 17. Linear theory is used here but it has been found that this may not apply in some cases, reference 18. The importance of including the effect of eccentricity of the stiffeners has been pointed out both experimentally, reference 19, and analytically, references 20, 21, and 22. Earlier investigators have also treated this effect analytically, references 23 and 24. In the analysis used here, eccentricity effects are included. This analysis follows closely that of Flügge in reference 24.

A.2 Stress-Strain Relations

The skin of the cylinder is assumed to be in a biaxial state of stress. The axes of elastic symmetry are in the longitudinal and circumferential directions. The x axis is in the longitudinal direction and the ϕ axis is in the circumferential direction. With these assumptions the stress-strain relations in the sheet are

$$\sigma_x = \frac{E_x}{1-\mu_x\mu_\phi}\left(\varepsilon_x + \mu_\phi\,\varepsilon_\phi\right)$$

$$\sigma_\phi = \frac{E_\phi}{1-\mu_x\mu_\phi}\left(\mu_x\,\varepsilon_x + \varepsilon_\phi\right)$$

$$\tau_{x\phi} = G\,\gamma_{x\phi} \qquad \text{(A1)}$$

The stiffeners are assumed to be in a uniaxial state of stress so that the stress-strain relations are

$$\sigma_{xs} = E_{xs}\,\varepsilon_x \qquad (A2)$$

$$\sigma_{\phi s} = E_{\phi s}\,\varepsilon_\phi$$

in the longitudinal and circumferential stiffeners respectively.

A.3 Strain-Displacement Relations

The reference surface of the shell is taken as the midsurface of the skin. With the z axis taken positive inward from the reference surface and u, v, and w being the displacements of the reference surface respectively in the positive x, ϕ, and z coordinate directions, the strain displacement relations are taken to be

$$\varepsilon_x = \frac{\partial u}{\partial x} - z\frac{\partial^2 w}{\partial x^2}$$

$$\varepsilon_\phi = \frac{1}{R}\frac{\partial v}{\partial \phi} - \frac{w}{R-z} - \frac{z}{R(R-z)}\frac{\partial^2 w}{\partial \phi^2} \qquad (A3)$$

$$\gamma_{x\phi} = \frac{1}{R-z}\frac{\partial u}{\partial \phi} + \left(\frac{R-z}{R}\right)\frac{\partial v}{\partial x} - \frac{\partial^2 w}{\partial x \partial \phi}\left(\frac{z}{R} + \frac{z}{R-z}\right)$$

where ε_x, ε_ϕ, and $\gamma_{x\phi}$ are the strains at a point in the shell ε_x and ε_ϕ are assumed to be continuous in the skin and x and ϕ stiffeners, respectively. These relations may be derived in a geometric manner as done by Flügge, pg. 212 of reference 24, or by reducing the linear three-dimensional strain displacement relations in cylindrical coordinates, reference 25. The latter is done by assuming the displacements vary linearly with the depth of the shell, reference 26, and by setting the transverse shear strains and the extensional strain in the z direction to zero.

The displacements of a point in the cylinder corresponding to these strain midsurface displacements are

$$\tilde{u} = u - z\frac{\partial w}{\partial x}$$

$$\tilde{v} = \frac{R-z}{R}v - \frac{z}{R}\frac{\partial w}{\partial \phi} \qquad \text{(A4)}$$

$$\tilde{w} = w$$

(see Figure A1).

The rotations of the normal used in the above displacements are

$$\omega_x = \frac{v}{R} + \frac{1}{R}\frac{\partial w}{\partial \phi}$$

$$\omega_\phi = \frac{\partial w}{\partial x}$$

The relative rotations per unit length are then

$$\theta_x = \frac{\partial \omega_x}{\partial x} = \frac{1}{R}\left(\frac{\partial v}{\partial x} + \frac{\partial^2 w}{\partial x \partial \phi}\right) \qquad \text{(A5)}$$

$$\theta_\phi = \frac{1}{R}\frac{\partial \omega_\phi}{\partial \phi} = \frac{1}{R}\frac{\partial^2 w}{\partial x \partial \phi}$$

A.4 Force Resultants

The force and moment resultants per unit length are obtained by performing the appropriate integrations of the stresses over the thickness of the skin and then adding to these the corresponding force and moment resultants per unit length in the stiffeners. The force and moment resultants per unit length in the stiffeners are obtained by dividing the resultant forces and moments by the stiffener spacings.

The extensional forces and bending moments in the stiffeners are obtained by performing the appropriate integrations of the extensional stresses in the stiffeners over the areas of the stiffeners. The stiffeners are assumed to carry no shear load; so they have no contribution to the shear

force resultants, but they are assumed to have a twisting moment resultant. The angle of twist is assumed to be the same as that of the normal to the skin. The torsional stiffnesses of the stiffeners are obtained from an approximate curve for data given by Crandal and Dahl, reference 27, for torsion of bars of rectangular cross section. Thus, the force resultants are obtained by substituting the strain displacement relations (A3) into the stress strain relations (A1) and (A2), then substituting the resulting stress displacement relations into the following formulas and performing the integrations:

$$N_x = \int_{-t_s/2}^{+t_s/2} \left(\frac{R-z}{R}\right) \sigma_x \, dz + \frac{t_x}{\ell_\phi} \int_{t_s/2}^{d_x+t_s/2} \sigma_{xs} \, dz$$

$$N_\phi = \int_{-t_s/2}^{+t_s/2} \sigma_\phi \, dz + \frac{t_\phi}{\ell_x} \int_{t_s/2}^{d_\phi+t_s/2} \sigma_{\phi s} \, dz$$

$$N_{x\phi} = \int_{-t_s/2}^{+t_s/2} \tau_{x\phi} \left(\frac{R-z}{R}\right) dz \qquad \text{(A6)}$$

$$N_{\phi x} = \int_{-t_s/2}^{+t_s/2} \tau_{x\phi} \, dz$$

$$M_x = \int_{-t_s/2}^{+t_s/2} \sigma_x \left(\frac{R-z}{R}\right) z \, dz + \frac{t_x}{\ell_\phi} \int_{t_s/2}^{d_x+t_s/2} \sigma_{xs} \, z \, dz$$

$$M_\phi = \int_{-t_s/2}^{+t_s/2} \sigma_\phi \, z \, dz + \frac{t_\phi}{\ell_x} \int_{t_s/2}^{d_\phi+t_s/2} \sigma_{\phi s} \, z \, dz$$

$$M_{x\phi} = \int_{-t_s/2}^{+t_s/2} \tau_{x\phi} \left(\frac{R-z}{R}\right) z \, dz - \frac{G_x J_x}{\ell_\phi} \theta_x$$

$$M_{\phi x} = \int_{-t_s/2}^{+t_s/2} \tau_{x\phi} \, z \, dz - \frac{G_\phi J_\phi}{\ell_x} \theta_\phi$$

The above expressions apply for stiffeners on the inside of the cylinder. For stiffeners on the outside of the cylinder the limits of integration on the stiffener integrals, the second terms, must be changed to go from $-(d_x + t_s/2)$ to $-t_s/2$ and $-(d_\phi + t_s/2)$ to $-t_s/2$ (see Figures 17 and A2) θ_x and θ_ϕ are the angles of twist of the normal to the skin, given in section A.3. J_x and J_ϕ are the section constants for a rectangular cross-section in torsion. These correspond to a polar moment of inertia and are approximate by the expression,

$$J = c \, ab^3 \qquad b \leq a$$

where c is given by

$$c = -0.285 \, e^{-0.49(a/b)} + 0.316$$

and a and b are the cross sectional dimensions of the stiffener, t_x and d_x, and t_ϕ and d_ϕ; b is taken as the dimension of smaller magnitude. After making the substitutions described above, performing the integrations, and neglecting terms of the order of the thickness of the skin divided by the radius and square of the depth of the stiffeners divided by the square of the radius with respect to 1, the force and moment resultants can be written:

$$N_x = (H_{s1} + H_x)\frac{\partial u}{\partial x} + H_\nu \frac{1}{R}\frac{\partial v}{\partial \phi} - H_\nu \frac{w}{R} - (H_x e_x - \frac{D_1}{R})\frac{\partial^2 w}{\partial x^2}$$

$$N_\phi = H_\nu \frac{\partial u}{\partial x} + (H_{s2} + H_\phi)\frac{1}{R}\frac{\partial v}{\partial \phi} - (H_{s2} + H_\phi (1 + \frac{e_\phi}{R}))\frac{w}{R}$$

$$- (\frac{D_2}{R} + H_\phi (e_\phi + \frac{\rho_\phi^2}{R}))\frac{1}{R^2}\frac{\partial^2 w}{\partial \phi^2}$$

$$N_{x\phi} = \frac{S}{R}\frac{\partial u}{\partial \phi} + S\frac{\partial v}{\partial x} + \frac{K}{R^2}\frac{\partial^2 w}{\partial x \partial \phi} \qquad (A7)$$

$$N_{\phi x} = \frac{S}{R}\frac{\partial u}{\partial \phi} + S\frac{\partial v}{\partial x} - \frac{K}{R^2}\frac{\partial^2 w}{\partial x \partial \phi}$$

$$M_x = (H_x e_x - \frac{D_1}{R})\frac{\partial u}{\partial x} - \frac{D_\nu}{R^2}\frac{\partial v}{\partial \phi}$$

$$- (D_1 + H_x \rho_x^2)\frac{\partial^2 w}{\partial x^2} - \frac{D_\nu}{R^2}\frac{\partial^2 w}{\partial \phi^2}$$

$$M_\phi = H_\phi \frac{e_\phi}{R}\frac{\partial v}{\partial \phi} - (\frac{D_2}{R} + H_\phi (e_\phi + \frac{\rho_\phi^2}{R}))\frac{w}{R}$$

$$- D_\nu \frac{\partial^2 w}{\partial x^2} - (D_2 + H_\phi (\rho_\phi^2 + \frac{\alpha_\phi^3}{R}))\frac{1}{R^2}\frac{\partial^2 w}{\partial \phi^2} .$$

$$M_{x\phi} = -\left(\frac{2K}{R} + \frac{T_x}{R}\right)\left(\frac{\partial v}{\partial x} + \frac{\partial^2 w}{\partial x \partial \phi}\right)$$

$$M_{\phi x} = \frac{K}{R^2}\frac{\partial u}{\partial \phi} - \frac{K}{R}\frac{\partial v}{\partial x} - \left(\frac{2K}{R} + \frac{T_\phi}{R}\right)\frac{\partial^2 w}{\partial x \partial \phi}$$

where the constants in the above expressions are given in terms of the material properties and the dimensions of the stiffened cylinder by

$$H_{s1} = \frac{E_x t_s}{1-\mu_x\mu_\phi} \qquad H_{s2} = \frac{E_\phi t_s}{1-\mu_x\mu_\phi}$$

$$H_x = \frac{E_{xs} t_x |d_x|}{\ell_\phi} \qquad H_\phi = \frac{E_{\phi s} t_\phi |d_\phi|}{\ell_x}$$

$$D_1 = \frac{E_x t_s^3}{12(1-\mu_x\mu_\phi)} \qquad D_2 = \frac{E_\phi t_s^3}{12(1-\mu_x\mu_\phi)}$$

$$D_\nu = \frac{E_x \mu_\phi t_s^3}{12(1-\mu_x\mu_\phi)} = \frac{E_\phi \mu_x t_s^3}{12(1-\mu_x\mu_\phi)}$$

$$H_\nu = \frac{E_x \mu_\phi t_s}{1-\mu_x\mu_\phi} = \frac{E_\phi \mu_x t_s}{1-\mu_x\mu_\phi}$$

$$S = Gt_s \qquad K = \frac{Gt_s^3}{12}$$

$$T_x = \frac{G_x J_x}{\ell_\phi} \qquad T_\phi = \frac{G_\phi J_\phi}{\ell_x} \qquad \text{(A8)}$$

$$\rho_x^2 = \frac{4d_x^2 + 6|d_x| t_s + 3t_s^2}{12}$$

$$\rho_\phi^2 = \frac{4d_\phi^2 + 6|d_\phi| t_s + 3t_s^2}{12}$$

$$e_x = \pm \frac{|d_x| + t_s}{2} \qquad \begin{matrix} + \text{ inside} \\ - \text{ outside} \end{matrix}$$

$$e_\phi = \pm \frac{|d_\phi| + t_s}{2}$$

$$\alpha_\phi^3 = \pm \frac{2|d_\phi|^3 + 4t_s d_\phi^2 + 3t_s^2 |d_\phi| + t_s^3}{8}$$

The effects of the eccentricity of the stiffeners are seen in the terms e_x, e_ϕ, and α_ϕ^3, which have a positive sign when the stiffeners are on the inside and a negative sign when the stiffeners are on the outside.

A.5 Prebuckle Forces and Stresses

It is assumed that when the cylinder is loaded there is a uniform change in length and a uniform change in radius. This implies that u, v, and w are independent of ϕ; w and v are independent of x; and that u is a linear function of x. Applying these assumptions to the force displacement relations (A.7), the forces in the cylinder are

$$N_x = (H_{s1} + H_x) \frac{\partial u}{\partial x} - H_\nu \frac{w}{R}$$

$$N_\phi = H_\nu \frac{\partial u}{\partial x} - (H_{s2} + H_\phi (1 + \frac{e_\phi}{R})) \frac{w}{R} \qquad \text{(A9)}$$

$$M_x = (H_x e_x - \frac{D_1}{R}) \frac{\partial u}{\partial x}$$

$$M_\phi = -(\frac{D_2}{R} + H_\phi (e_\phi + \frac{\rho_\phi^2}{R})) \frac{w}{R}$$

$$N_{x\phi} = N_{\phi x} = M_{x\phi} = M_{\phi x} = 0$$

By substituting these into the equilibrium equations, reference 24, page 209, the internal forces may be obtained in terms of the applied loads. The result is

$$N_x = - N$$
$$N_\phi = - pR \tag{A10}$$

where N is the applied axial compression load per unit length of circumference, and p is the applied external pressure per unit surface area.

With the assumptions about the prebuckled deformation, the midsurface prebuckle strains are obtained from the strain displacement relations as

$$\epsilon_{xp} = \frac{\partial u}{\partial x}, \qquad \epsilon_{\phi p} = - \frac{w}{R} \tag{A11}$$

By equating the expressions for the force resultants in terms of the displacements with the values of the force resultants in terms of the external forces and identifying the strains, the following expressions for the midsurface strains are obtained, after neglecting terms of the order of the depth of the stiffener divided by the radius with respect to one:

$$\epsilon_{xp} = \frac{H_\nu\, pR - (H_{s2} + H_\phi)\, N}{(H_{s1} + H_x)(H_{s2} + H_\phi) - H_\nu^2} \tag{A12}$$

$$\epsilon_{\phi p} = \frac{H_\nu\, N - (H_{s1} + H_x)\, pR}{(H_{s1} + H_x)(H_{s2} + H_\phi) - H_\nu^2}$$

Substituting these into the stress-strain relations (A.1) for the skin, the expressions for the stresses in the skin are obtained:

$$\sigma_{xp} = - \frac{1}{t_s} \frac{\left[\left(1 + \frac{H_\phi}{H_{s2}}\right) - \mu_x \mu_\phi\right] N + \mu_x \frac{H_x}{H_{s1}}\, pR}{\left(1 + \frac{H_x}{H_{s1}}\right)\left(1 + \frac{H_\phi}{H_{s2}}\right) - \mu_x \mu_\phi} \tag{A13}$$

$$\sigma_{\phi p} = -\frac{1}{t_s} \frac{\mu_\phi \frac{H_\phi}{H_{s2}} N - [\mu_x \mu_\phi - (1 + \frac{H_x}{H_{s1}})] pR}{(1 + \frac{\mu_x}{H_{s1}})(1 + \frac{H_\phi}{H_{s2}}) - \mu_x \mu_\phi}$$

The expressions for the stresses in the ribs neglecting terms involving the depth of the stiffener divided by the radius with respect to one are obtained by multiplying the stiffener modulus by the corresponding value of the midsurface prebuckle strain. These are

$$\sigma_{xsp} = E_{xs} \epsilon_{xp}$$

$$\sigma_{\phi sp} = E_{\phi s} \epsilon_{\phi p} \qquad \text{(A14)}$$

A.6 Buckling of the Cylinder and Skin

An expression for the critical buckling load of the cylinder is obtained in terms of two integer parameters representing the buckling mode shape. The lowest buckling load is then obtained by searching the buckling loads obtained from a large number of possible mode shapes.

The expression for the buckling load is obtained from the determinant of a set of homogeneous equations. These are obtained by substituting into the buckling equilibrium equations, in terms of displacements, an assumed solution which satisfies these equations and simple support boundary conditions. The displacement functions contain the two integer parameters representing the mode shape and arbitrary constants.

The buckling equilibrium equations are obtained in terms of displacements, by substituting the force resultants, in terms of the displacements, into the buckling equilibrium equations in terms of forces. The buckling equilibrium equations used are those given by Flugge, reference 24, page 422, but contain only the buckling force terms recommended by Hedgepeth and Hall, reference 17, page 9. With the changes required because of the different coordinate system used here these equations are

$$\frac{\partial N_x}{\partial x} + \frac{1}{R}\frac{\partial N_{\phi x}}{\partial \phi} = 0$$

$$\frac{1}{R}\frac{\partial N_\phi}{\partial \phi} + \frac{\partial N_{x\phi}}{\partial x} - \frac{1}{R^2}\frac{\partial M_\phi}{\partial \phi} - \frac{1}{R}\frac{\partial M_{x\phi}}{\partial x} - N\frac{\partial^2 v}{\partial x^2} = 0 \qquad \text{(A15)}$$

$$\frac{\partial^2 M_\phi}{\partial \phi^2} + R\frac{\partial^2 M_{x\phi}}{\partial x \partial \phi} + R\frac{\partial^2 M_{\phi x}}{\partial x\,\partial \phi} + R^2\frac{\partial^2 M_x}{\partial x^2} + R N_\phi$$

$$- NR^2\frac{\partial^2 w}{\partial x^2} - pR\left(\frac{\partial^2 w}{\partial \phi^2} + w\right) = 0$$

where N is the applied axial compressive force per unit length and p is the applied external radial pressure per unit area.

After substituting the force displacement relations (A7) into these equations, the buckling equilibrium equations in terms of displacement are obtained. These can be written in the form:

$$R\left(\frac{H_{s1}}{H_{s2}} + \frac{H_x}{H_{s2}}\right)\frac{\partial^2 u}{\partial x^2} + \frac{S}{H_{s2}}\frac{1}{R}\frac{\partial^2 u}{\partial \phi^2} + \left(\frac{H_\nu}{H_{s2}} + \frac{S}{H_{s2}}\right)\frac{\partial^2 v}{\partial x \partial \phi}$$

$$- \frac{H_\nu}{H_{s2}}\frac{\partial w}{\partial x} - R\left(\frac{H_x}{H_{s2}}e_x - \frac{D_1}{H_{s2}R}\right)\frac{\partial^3 w}{\partial x^3} - \frac{K}{H_{s2}}\frac{1}{R^2}\frac{\partial^3 w}{\partial x \partial \phi^2} = 0$$

$$\left(\frac{H_\nu}{H_{s2}} + \frac{S}{H_{s2}}\right)\frac{\partial^2 u}{\partial x \partial \phi} + \left(1 + \frac{H_\phi}{H_{s2}}\left(1 - \frac{e_\phi}{R}\right)\right)\frac{1}{R}\frac{\partial^2 v}{\partial \phi^2} \qquad \text{(A16)}$$

$$+ \left(\frac{SR}{H_{s2}} + \frac{T_x}{H_{s2}R}\right)\frac{\partial^2 v}{\partial x^2} - \frac{NR}{H_{s2}}\frac{\partial^2 v}{\partial x^2} - \left(1 + \frac{H_\phi}{H_{s2}}\right)\frac{1}{R}\frac{\partial w}{\partial \phi}$$

$$- \left(\frac{H_\phi e_\phi}{H_{s2}}\right)\frac{1}{R^2}\frac{\partial^3 w}{\partial \phi^3} + \left(\frac{3K}{H_{s2}} + \frac{D_\nu}{H_{s2}} + \frac{T_x}{H_{s2}}\right)\frac{1}{R}\frac{\partial^3 w}{\partial x^2 \partial \phi} = 0$$

$$\frac{H_\nu}{H_{s2}} \frac{\partial u}{\partial x} + \left(\frac{H_x e_x}{H_{s2}} - \frac{D_2}{H_{s2}R}\right) R \frac{\partial^3 u}{\partial x^3} + \frac{K}{H_{s2}R^2} \frac{\partial^3 u}{\partial x \partial \phi^2}$$

$$\left(1 + \frac{H_\phi}{H_{s2}}\right) \frac{1}{R} \frac{\partial v}{\partial \phi} - \left(\frac{3K}{H} + \frac{D_\nu}{H_{s2}} + \frac{T_x}{H_{s2}}\right) \frac{1}{R} \frac{\partial^3 v}{\partial x^2 \partial \phi} + \frac{H_\phi e_\phi}{H_{s2}} \frac{1}{R^2} \frac{\partial^3 v}{\partial \phi^3}$$

$$- 2 \left(\frac{D_2}{H_{s2}R} + \frac{H_\phi}{H_{s2}} \left(e_\phi + \frac{\rho_\phi^2}{R}\right)\right) \frac{1}{R^3} \frac{\partial^2 w}{\partial \phi^2}$$

$$- \left(\frac{2D_\nu}{H_{s2}} + \frac{4K}{H_{s2}} + \frac{T_x}{H_{s2}} + \frac{T_\phi}{H_{s2}}\right) \frac{1}{R} \frac{\partial^4 w}{\partial x^2 \partial \phi^2}$$

$$- \left(\frac{D_2}{H_{s2}} + \frac{H_\phi}{H_{s2}} \left(\rho_\phi^2 + \frac{\alpha_\phi^3}{R}\right)\right) \frac{1}{R^2} \frac{\partial^4 w}{\partial \phi^4} - \left(\frac{D_1}{H_{s2}} + \frac{H_x \rho_x^2}{H_{s2}}\right) R \frac{\partial^4 w}{\partial x^4}$$

$$- \left(1 + \frac{H_\phi}{H_{s2}} \left(1 + \frac{e_\phi}{R}\right)\right) \frac{w}{R} - \frac{NR}{H_{s2}} \frac{\partial^2 w}{\partial x^2} - \frac{p}{H_{s2}} \left(\frac{\partial^2 w}{\partial \phi^2} + w\right) = 0$$

The assumed displacements which satisfy the above equations and the simple support boundary conditions are

$$u = A \sin n\phi \cos \lambda x$$

$$v = B \cos n\phi \sin \lambda x$$

$$w = C \sin n\phi \sin \lambda x$$

where for the complete cylinder

$$\lambda = \frac{m\pi}{L}, \qquad m = 1, 2, \ldots$$

$$n = n \qquad n = 0, 1, 2, \ldots$$

and L is the length of the cylinder.

For a cylindrical plate (the skin between stiffeners)

$$\lambda = \frac{m\pi}{\ell_x} \qquad m = 1, 2, \ldots$$

$$n = \frac{n\pi R}{\ell_\phi} \qquad n = 1, 2, \ldots$$

After the displacements are substituted into the displacement buckling equilibrium equations, these equations can be written in the form:

$$\begin{bmatrix} C_{11} & C_{12} & C_{13} \\ C_{12} & C_{22} + \frac{NR\lambda^2}{H_{s2}} & C_{23} \\ C_{31} & C_{23} & C_{33} + \frac{NR\lambda^2}{H_{s2}} + \frac{p}{H_{s2}}(n^2-1) \end{bmatrix} \begin{Bmatrix} A \\ B \\ C \end{Bmatrix} = \begin{Bmatrix} 0 \\ 0 \\ 0 \end{Bmatrix} \qquad \text{(A18)}$$

where the C's are given by

$$C_{11} = -R\left(\frac{H_{s1}}{H_{s2}} + \frac{H_x}{H_{s2}}\right)\lambda^2 - \frac{S}{H_{s2}}\frac{n^2}{R}$$

$$C_{12} = -\left(\frac{H_\nu}{H_{s2}} + \frac{S}{H_{s2}}\right) n\lambda$$

$$C_{13} = -\frac{H_\nu}{H_{s2}}\lambda + R\left(\frac{H_x e_x}{H_{s2}} - \frac{D_1}{H_{s2}R}\right)\lambda^3 + \frac{K}{H_{s2}}\frac{\lambda n^2}{R^2}$$

$$C_{31} = -\frac{H_\nu}{H_{s2}}\lambda + R\left(\frac{H_x e_x}{H_{s2}} - \frac{D_2}{H_{s2}R}\right)\lambda^3 + \frac{K}{H_{s2}}\frac{\lambda n^2}{R^2} \qquad \text{(A19)}$$

$$C_{22} = -\left(1 + \frac{H_\phi}{H_{s2}}\left(1 - \frac{e_\phi}{R}\right)\right) n^2 - \left(\frac{SR}{H_{s2}} + \frac{T_x}{H_{s2}R}\right)\lambda^2$$

$$C_{23} = -\left(1 + \frac{H_\phi}{H_{s2}}\right)\frac{n}{R} + \left(\frac{H_\phi e_\phi}{H_{s2}}\right)\frac{n^3}{R^2} - \left(\frac{3K}{H_{s2}} + \frac{D_\nu}{H_{s2}} + \frac{T_x}{H_{s2}}\right)\frac{\lambda^2 n}{R}$$

$$C_{33} = 2\left(\frac{D_2}{H_{s2}R} + \frac{H_\phi}{H_{s2}}\left(e_\phi + \frac{\rho_\phi^2}{R}\right)\right)\frac{n^2}{R^2}$$

$$-\left(2\frac{D_\nu}{H_{s2}} + \frac{4K}{H_{s2}} + \frac{T_x}{H_{s2}} + \frac{T_\phi}{H_{s2}}\right)\lambda^2\frac{n^2}{R}$$

$$-\left(\frac{D_2}{H_{s2}} + \frac{H_\phi}{H_{s2}}\left(\rho_\phi^2 + \frac{\alpha_\phi^3}{R}\right)\right)\frac{n^4}{R^3} - \left(\frac{D_1}{H_{s2}} + \frac{H_x \rho_x^2}{H_{s2}}\right) R\lambda^4$$

$$-\frac{1}{R}\left(1 + \frac{H_\phi}{H_{s2}}\left(1 + \frac{e_\phi}{R}\right)\right)$$

Since the values of the applied loads are known, a ratio between the axial load and pressure can be calculated. Letting

$$p = \alpha N$$

and setting to zero the determinant of the coefficients of A, B, and C in the last set of equations the expression for the critical axial load is obtained. This is

$$\left(\frac{N}{H_{s2}}\right)_{cr} = -\frac{\overline{B} \pm \sqrt{\overline{B}^2 - 4\,\overline{A}\,\overline{C}}}{2\overline{A}} \qquad \text{(A20)}$$

where

$$\overline{A} = C_{11}\left(R\lambda^4 + \lambda^2(n^2 - 1)\alpha\right)R$$

$$\overline{B} = \left[(C_{11}C_{22} - C_{12}^2) + (C_{11}C_{33} - C_{13}C_{31})\right]R\lambda^2$$

$$+ (C_{11}C_{22} - C_{12}^2)\alpha(n^2 - 1) \qquad \text{(A21)}$$

$$\overline{C} = C_{11} C_{22} C_{33} + C_{12} C_{23} C_{31} + C_{13} C_{12} C_{23}$$
$$- C_{12}^2 C_{33} - C_{13} C_{31} C_{22} - C_{23}^2 C_{11}$$

For each combination of the parameters m and n there are two possible values of $(N/H_{s2})_{cr}$. The one which has to be used as critical is the one with smallest magnitude and having the same sign as the applied load N. The critical buckling load is obtained by finding $(N/H_{s2})_{cr}$ for a large number of values of both m and n and then selecting the lowest magnitude value out of all of these.

For the special case when N = 0 the critical pressure must be found. This is given by

$$\left(\frac{p}{H_{s2}}\right)_{cr} = \frac{-\overline{C}}{(C_{11} C_{22} - C_{12}^2)(n^2 - 1)} \qquad \text{(A22)}$$

The above analysis is used for gross buckling, panel buckling, and sheet buckling. For gross buckling all the constants are calculate as given in the C's and the full length of the cylinder is used. For panel buckling, the terms which contain the properties of the circumferential stiffeners are set to zero and the length of the cylinder is taken as the circumferential ring spacing. For skin buckling, all terms containing stiffener properties are set to zero, n is changed to apply to a cylindrical plate with a width of the longitudinal stiffener spacing and the length of the cylinder is again taken as the length between circumferential stiffeners.

A.7 Longitudinal Stiffener Buckling

The critical buckling stress for the longitudinal stiffeners is obtained by applying a solution for the critical buckling stress of a flat rectangular plate to several different possible assumed modes of buckling of the stiffener. In all the possible assumed modes the longitudinal stiffener is assumed to be simply supported on three edges and free on the fourth. The critical buckling stress for such a flat plate is given by Bleich, reference 28, as

$$\sigma_c = \frac{\pi^2 E_{xs}}{12(1-\nu^2)} \left(\frac{t}{d}\right)^2 \left[\left(\frac{d}{\ell}\right)^2 + 0.425\right] \qquad \text{(A23)}$$

The notation has been changed here; t is the thickness of tne plate (i.e. the width of the stiffener), d the width of the plate (i.e. the depth of portion of the stiffener under consideration), and ℓ the length of stiffener under consideration.

The first failure mode to which this expression is applied is in the situation where the circumferential stiffeners are either on the opposite side of the cylinder from the longitudinal ones or where they are non-existent. In this case d is taken as d_x, the full depth of the stiffener, and ℓ is taken as L, the full length of the cylinder.

The second mode is where the circumferential stiffeners are on the same side of the cylinder as the longitudinal ones and are the deepest. In this case the critical buckling stress of the longitudinals is taken as that of a plate with depth d_x, the full depth of the longitudinal stiffeners, and a length ℓ_x, the length between circumferential stiffeners.

The third mode is where the circumferential stiffeners are on the same side as the longitudinal ones but are not as deep. In this case one would expect the stiffener to buckle in a manner coupling the material between the circumferential stiffeners with the material above the circumferential stiffeners. To obtain an estimation of the critical buckling stress two cases are considered. One assumes that the portion of the material between the circumferential stiffeners does not buckle but the outstanding portion does. In this case the formula is applied to a plate of the dimensions of the depth of the outstanding portion and the length of the entire cylinder ($d_x - d_\phi$ by L). The other case assumes that the material between the circumferential stiffeners does buckle with the outstanding portion of the longitudinal stiffener but that the circumferential stiffeners force nodes in the buckling of the longitudinal and these notes occur at the location of the circumferential stiffeners. The buckling stress in this case is taken as that for a plate and d equal to the full depth, d_x, of the stiffener and ℓ equal to ℓ_x, the circumferential

stiffener spacing. This is the same as the case where the circumferential stiffeners are deeper than the longitudinals.

A.8 Circumferential Stiffener Buckling

Similar situations are encountered with the buckling of the circumferential stiffeners as with the buckling of the longitudinal stiffeners. Here, however, an additional mode of buckling is encountered (see TablesA1 and A2). The external stiffeners not only can buckle when they are compressed, but due to their curvature can also buckle when they are expanded. An expression for the critical circumferential strain in the skin of the cylinder, or at the edge of the stiffener, is obtained (in Section A.9) by doing an assumed mode solution of the buckling problem. This expression is

$$\varepsilon_{\phi cr} = -\left(\frac{t_\phi}{d}\right)^2 \left(\frac{1}{12(1-\nu^2)}\right) \left(\frac{2 + 2(1-\nu)\left(\zeta + \zeta^2/2\right)}{1 + 2\zeta + \zeta^2}\right) \times \left[\frac{(1 + 2n^2(1-\nu))\,\zeta + (2n^2(2-\nu)-1)\,\frac{\zeta^2}{2} + (n^2-1)^2\,\zeta^3/3 + \ldots}{1 + \left(\frac{2n^2-1}{3}\right)\zeta + \left(\frac{3-4n^2}{12}\right)\zeta^2 + \ldots}\right] \tag{A24}$$

where d is the depth of the stiffener portion in question; and ζ is the ratio of the stiffener depth, d, to the radius of the unsupported edge of the stiffener; ζ is a positive number if the stiffener is inside and negative if the stiffener is outside; and n is the number of full waves in the circumferential direction.

With the circumferential stiffeners on the inside of the cylinder, ζ positive, the value of $\varepsilon_{\phi cr}$ is negative for all values of n and increases in magnitude as n increases. This means that inside circumferential stiffeners can buckle only when the cylinder contracts under load.

With the circumferential stiffeners inside the cylinder and the longitudinals outside or non-existent the critical buckling value for $\varepsilon_{\phi cr}$ is obtained with n = 0.

With both the circumferential and the longitudinal stiffeners inside the cylinder and with the longitudinal stiffeners deeper than the circumferential ones, the circumferential stiffeners are physically restrained from buckling into a smaller number of half waves than the number of spaces between longitudinal stiffeners. Since $\varepsilon_{\phi cr}$ increases in magnitude as n increases, the critical buckling value for this situation is obtained by using for n the number of spaces in half the circumference of the cylinder.

In the situation with the circumferential stiffeners deeper than the longitudinal ones two values of $\varepsilon_{\phi cr}$ are obtained. One is for the unsupported portion of the circumferential with $d = d_\phi - d_x$ and $n = 0$. The other is obtained as above, for the supported stiffeners, for the full depth of the stiffener assuming that nodes are forced at the locations of the longitudinal stiffeners. This is similar to the case of the longitudinal stiffeners.

With the circumferential stiffeners outside, ζ negative, $\varepsilon_{\phi cr}$ is positive for small values of n and increases in magnitude as n increases. When n becomes large enough $\varepsilon_{\phi cr}$ becomes negative and then as n increases the magnitude of $\varepsilon_{\phi cr}$ decreases while the value remains negative. The magnitude of $\varepsilon_{\phi cr}$ decreases until for some value of n a minimum is obtained. Thus the circumferential stiffener can buckle for small values of n when the cylinder expands, $\varepsilon_{\phi cr}$ positive, or can buckle for large values of n when the cylinder contracts, $\varepsilon_{\phi cr}$ negative.

For the case of external circumferential stiffeners with the longitudinal stiffeners inside or non-existent, the critical positive value of $\varepsilon_{\phi cr}$ is obtained with $n = 0$, and the critical negative value is found by searching for the lowest magnitude negative value of $\varepsilon_{\phi cr}$.

With the longitudinal stiffeners also on the outside and deeper than the circumferential the circumferential stiffeners are again physically restrained from buckling into a smaller number of half waves than the number of spaces between the longitudinal stiffeners. A value of $\varepsilon_{\phi cr}$ is calculated for n equal to the number of spaces in half the circumference $n = \pi R/\ell_\phi$. If this value is positive then this is the critical value for an expansion of the cylinder. If it is negative there is no critical value for an expansion of the cylinder. Several possibilities exist for the

negative buckling value. If the above value of $\varepsilon_{\phi cr}$ is positive then the negative value is the one given by the minimum magnitude value found for the unsupported stiffener, since this value has a larger number of circumferential waves than spaces between stiffeners. If the value for $n = \pi R/\ell_\phi$ is negative then there is a choice between this value and the value minimum $|\varepsilon_{\phi cr}|$. The one which has the larger value of n is used. The reasons for this are as follows: if $n = \pi R/\ell_\phi$ is the largest then a smaller n is physically impossible; if the n for minimum $|\varepsilon_{\phi cr}|$ is larger then this gives smallest $|\varepsilon_{\phi cr}|$ for $\varepsilon_{\phi cr}$ negative and is physically possible. For the case of all external stiffeners with the circumferential ones having the greater depth the problem is again split into two parts, one an unsupported circumferential stiffener with depth $d_\phi - d_x$ and the other a stiffener with the full depth d_ϕ, assuming nodes at the location of the longitudinal stiffeners. Values are then obtained for each case in a manner similar to that described above for external stiffeners. Two results are then obtained and compared to find the critical value.

In this treatment n is considered as a continuous variable instead of integer as it actually is and no arguments about the compatibility of the mode shapes are made. Introducing these restrictions would increase the buckling values so that the treatment used is conservative.

This buckling solution does not apply where the circumferential stiffener is thick compared with its depth. This is because the assumed simply supported boundary condition does not apply. In situations where the outstanding portion of the stiffener has a depth to thickness ratio of less than ten the yield limit is substituted for the buckling limit.

A.9 Solution of the Circumferential Stiffener Critical Buckling Strain

An approximate solution is obtained for the buckling of a circular plate with a large hole in it. The plate is assumed to be simply supported at one edge and free at the other (see Figure A3). The simply supported edge is the edge which attaches to the cylinder and thus must have the same displacements as the cylinder. The critical buckling parameter is taken as the tangential strain on the simply supported edge. The solution is obtained using an assumed mode variational method.

The variational formulation of the problem of elastic stability is given by Novozhilov, reference 26, page 173, as

$$\delta[\, A^{(2)} \,] \;=\; \delta\, R_2^{(2)}$$

In the cases in which the initial stress state can be determined using classical theory, this is such a case, $A^{(2)}$ is given in cylindrical coordinates as

$$A^{(2)} = \frac{E}{2(1+\nu)} \iiint \left\{ \frac{1}{1-\nu} \left(b_2'\right)^2 - 2b_1' \right\} r\, dr\, d\theta\, dz$$

$$+ \frac{1}{2} \iiint \left\{ \sigma_r^\circ \left(\omega_\theta'^2 + \omega_z'^2\right) + \sigma_\theta^\circ \left(\omega_r'^2 + \omega_z'^2\right) + \sigma_z^\circ \left(\omega_r'^2 + \omega_\theta'^2\right) \right.$$

$$\left. - 2\left[\tau_{r\theta}^\circ\, \omega_r'\omega_\theta' + \tau_{rz}^\circ\, \omega_r'\omega_z' + \tau_{\theta z}^\circ\, \omega_\theta'\omega_z'\right] \right\} r\, dr\, d\theta\, dz$$

where

$$b_2' = \varepsilon_r' + \varepsilon_\theta' + \varepsilon_z'$$

$$b_1' = \varepsilon_r'\varepsilon_\theta' + \varepsilon_r'\varepsilon_z' + \varepsilon_\theta'\varepsilon_z' - \frac{1}{4}\left(\varepsilon_{r\theta}'^2 + \varepsilon_{rz}'^2 + \varepsilon_{\theta z}'^2\right)$$

and

$$\varepsilon_r' = \frac{\partial \tilde{u}'}{\partial r}, \qquad \varepsilon_\theta' = \frac{1}{r}\frac{\partial \tilde{v}'}{\partial \theta} + \frac{\tilde{u}'}{r}, \qquad \varepsilon_z = \frac{\partial \tilde{w}'}{\partial z}$$

$$\varepsilon_{r\theta}' = \frac{\partial \tilde{v}'}{\partial r} - \frac{\tilde{v}'}{r} + \frac{1}{r}\frac{\partial \tilde{u}'}{\partial \theta}, \qquad \varepsilon_{rz}' = \frac{\partial \tilde{u}'}{\partial z} + \frac{\partial \tilde{w}'}{\partial r}, \qquad \varepsilon_{\theta z}' = \frac{1}{r}\frac{\partial \tilde{w}'}{\partial \theta} + \frac{\partial \tilde{v}'}{\partial z}$$

$$2\omega_r' = \frac{1}{r}\frac{\partial \tilde{w}'}{\partial \theta} - \frac{\partial v'}{\partial z}, \qquad 2\omega_\theta' = \frac{\partial \tilde{u}'}{\partial z} - \frac{\partial \tilde{w}'}{\partial r}, \qquad 2\omega_z' = \frac{\partial \tilde{v}'}{\partial r} + \frac{\tilde{v}'}{r} - \frac{1}{r}\frac{\partial \tilde{u}'}{\partial \theta}$$

The primes denote the buckle state and zero the initial state. By the same type of procedure as used for the derivation of the strain displacement relations in the cylinder the above strain displacement relations can be reduced to strain midsurface displacement relations. Thus, by assuming the displacements vary linearly with depth, the transverse shear strains are zero, and the normal strain is zero, the strain displacement relations reduce to

$$\varepsilon_r' = \frac{\partial u'}{\partial r} - z\frac{\partial^2 w'}{\partial r^2}$$

$$\varepsilon_\theta' = \frac{1}{r}\frac{\partial v'}{\partial \theta} + \frac{u'}{r} - \frac{z}{r}\left(\frac{1}{r}\frac{\partial^2 w'}{\partial \theta^2} + \frac{\partial w'}{\partial r}\right)$$

$$\varepsilon_{r\theta}' = \frac{\partial v'}{\partial r} - \frac{v'}{r} + \frac{1}{r}\frac{\partial u'}{\partial \theta} - \frac{2z}{r}\left(\frac{\partial^2 w'}{\partial r\,\partial \theta} - \frac{1}{r}\frac{\partial w'}{\partial \theta}\right)$$

$$\omega_r' = \frac{1}{r}\frac{\partial w'}{\partial \theta}, \quad \omega_\theta' = -\frac{\partial w'}{\partial r}, \quad \omega_z' = \frac{\partial v'}{\partial r} + \frac{v'}{r} - \frac{1}{r}\frac{\partial u'}{\partial \theta}$$

Note that the displacements in these expressions are the midsurface displacements and not the displacements of a point as in the previous expressions, also u', v', and w' are the displacements in the r, θ, and z directions and are not the same as the u, v, and w for the cylinder.

The stresses in the plate prior to buckling are given by Timoshenko, reference 25, page 59, in terms of a radially inward pressure at the outer edge as

$$\sigma_r^\circ = -p\frac{b^2}{r^2}\frac{(r^2 - a^2)}{(b^2 - a^2)}$$

$$\sigma_\theta^\circ = -p\frac{b^2}{r^2}\frac{(r^2 + a^2)}{(b^2 - a^2)}$$

$$\tau_{r\theta}^\circ = \tau_{rz} = \tau_{\theta z} = \sigma_z = 0$$

P is the radial pressure. These may be transformed to be in terms of the tangential strain at the edge $r = b$, $\bar{\varepsilon}_\theta$, by using the stress strain relations to solve for P in terms of $\bar{\varepsilon}_\theta$ and substituting the result into the above expressions for the stresses

$$\sigma_r^\circ = \frac{b^2 \bar{\varepsilon}_\theta \left(1 - \frac{a^2}{r^2}\right) E_{\phi s}}{a^2 + b^2 + \nu(a^2 - b^2)} \qquad (A25)$$

$$\sigma_\theta^\circ = \frac{b^2 \bar{\varepsilon}_\theta \left(1 + \frac{a^2}{r^2}\right) E_{\phi s}}{a^2 + b^2 + \nu(a^2 - b^2)}$$

The following set of buckling displacements satisfy the displacement boundary conditions:

$$u' = v' = 0$$

$$w' = A\,(b-r) \sin n\theta$$

These displacements are then substituted into the strain-displacement relations and the resulting expressions along with the prebuckle stresses are then substituted into the expression for $A^{(2)}$. When the integration is carried out and $\delta[A^{(2)}]$ is set to zero ($\delta R_2^{(2)}$ is zero for the problem since the forces are constant on one edge and the displacements are constant on the other), reference 26, pg. 172, the following expression is obtained for the critical $\bar{\varepsilon}_\theta$:

$$\bar{\varepsilon}_\theta = -\frac{t^2}{12(1-\nu^2)} \left[\frac{a^2 + b^2 + \nu(a^2 - b^2)}{b^2}\right]$$

$$\left[\frac{(n^2-1)^2 \ln\frac{b}{a} + 2n^2(1-n^2)\frac{b-a}{a} + n^2\frac{(n^2 + 2(1-\nu))}{2}\left(\frac{b^2 - a^2}{a^2}\right)}{\frac{1-2n^2}{2}(b^2 - a^2) + (b^2n^2 + a^2(n^2-1)) \ln\frac{b}{a}}\right] \qquad (A26)$$

Now $(\frac{b-a}{a})$ is set equal to ζ and the expression is expanded in terms of this quantity. The result of doing this and setting the critical $\bar{\varepsilon}_\theta$ equal to the critical strain in the cylinder is the expression:

$$\varepsilon_{\phi cr} = -\left(\frac{t}{d}\right)^2 \left(\frac{1}{12(1-\nu^2)}\right) \frac{(2 + 2(1-\nu)(\zeta + \frac{\zeta^2}{2}))}{(1 + 2\zeta + \zeta^2)}$$

$$\left[\frac{(1+2n^2(1-\nu))\zeta + (2n^2(2-\nu) - 1)\frac{\zeta^2}{2} + (n^2-1)^2(\frac{\zeta^3}{3} - \frac{\zeta^4}{4}) + \ldots}{1 + (\frac{2n^2-1}{3})\zeta + \frac{3-4n^2}{12}\zeta^2 + \ldots}\right]$$

Specialization of this solution in two limiting cases, for which solutions are available in the literature, is given in Appendix B.

A.10 Yield Failure

The principal stresses in the skin are given by σ_{xp} and $\sigma_{\phi p}$ (A13). It is assumed that the yield criterion for the cylindrical shell skin material is of the following form, reference 29.

$$f_D^2 = \left(\frac{\sigma_{xp}}{\sigma_{x0\alpha}}\right)^2 - \kappa_{\alpha\beta} \frac{\sigma_{xp}}{|\sigma_{x0\alpha}|} \frac{\sigma_{\phi p}}{|\sigma_{\phi 0\beta}|} + \left(\frac{\sigma_\phi}{\sigma_{\phi 0\beta}}\right)^2 \leq 1 \qquad \text{(A27)}$$

where

$\sigma_{x0\alpha} = \sigma_{x0T}$ the longitudinal tension yield stress in the skin if $\sigma_{xp} > 0$

$\sigma_{x0\alpha} = \sigma_{x0C}$ the longitudinal compression yield stress in the skin if $\sigma_{xp} < 0$

$\sigma_{\phi 0\beta} = \sigma_{\phi 0T}$ the circumferential tension yield stress in the skin if $\sigma_{\phi p} > 0$

$\sigma_{\phi 0\beta} = \sigma_{\phi 0C}$ the circumferential compression yield stress in the skin if $\sigma_{\phi p} < 0$

$\kappa_{\alpha\beta} = \kappa_{TT}$ constant defining yield envelope in first quadrant $\sigma_{xp} > 0$ and $\alpha_{\phi p} > 0$

$\kappa_{\alpha\beta} = \kappa_{CT}$ constant defining yield envelope in second quadrant $\sigma_{xp} < 0$ and $\sigma_{\phi p} > 0$

$\kappa_{\alpha\beta} = \kappa_{CC}$ constant defining yield envelope in third quadrant $\sigma_{xp} < 0$ and $\sigma_{\phi p} < 0$

$\kappa_{\alpha\beta} = \kappa_{TC}$ constant defining yield envelope in fourth quadrant $\sigma_{xp} > 0$ and $\sigma_{\phi p} < 0$

For the case of an isotropic material that behaves identically in tension and compression with yield stress σ_{0D} Eqs. A27 when specialized by the following substitutions:

$$\sigma_{x0T} = \sigma_{x0C} = \sigma_{\phi 0T} = \sigma_{\phi 0C} = \sigma_{0D}$$

$$\kappa_{\alpha\beta} = 1$$

reduce to the distortion energy yield criterion

$$\sigma_{xp}^2 - \sigma_{xp}\sigma_{\phi p} + \sigma_{\phi p}^2 \leq \sigma_{0D}^2 \tag{A28}$$

The stiffeners are in a uniaxial state of stress so the stresses (A14) must satisfy the yield conditions:

$$\begin{aligned} \sigma_{xSOC} \leq \sigma_{xsp} \leq \sigma_{xSOT} \\ \sigma_{\phi SOC} \leq \sigma_{\phi sp} \leq \sigma_{\phi SOT} \end{aligned} \tag{A29}$$

where the subscript x refers to the longitudinal stiffener; ϕ refers to the circumferential stiffener; 0 refers to yield; C refers to compression; and T refers to tension.

TABLE A1. SELECTION OF CIRCUMFERENTIAL STIFFENER BUCKLING MODE $(\varepsilon_\phi)_{cr}$ - CONTRACTION

d_ϕ	Opposite Sides	$\lvert d_\phi \rvert \leq \lvert d_x \rvert$	d	n	$(\varepsilon_\phi)_{cr}$
Inside + Outside - Inside +	Yes Yes No	N/A N/A Yes	d_ϕ d_ϕ d_ϕ	$n = 0$ $n = n^*$ $n = \frac{\pi R}{\ell_\phi}$	$(\varepsilon_\phi)_{cr} = (\varepsilon_\phi)_{cr}\lvert_{n=0}$ $(\varepsilon_\phi)_{cr} = (\varepsilon_\phi)_{cr}\lvert_{n=n^*}$ $(\varepsilon_\phi)_{cr} = (\varepsilon_\phi)_{cr}\lvert_{n=\pi R/\ell_\phi}$
Outside -	No	Yes	d_ϕ d_ϕ	$n = \frac{\pi R}{\ell_\phi}$ $n = n^*$	if $(\varepsilon_\phi)_{cr}\lvert_{n=\pi R/\ell_\phi} \geq 0$ then use $(\varepsilon_\phi)_{cr}\lvert_{n=n^*}$ otherwise use $(\varepsilon_\phi)_{cr}\lvert_{n=\max(n,n^*)}$
Inside +	No	No	$d_\phi - d_x$ d_ϕ	$n = 0$ $n = \frac{\pi R}{\ell_\phi}$	$(\varepsilon_\phi)_{cr}^{(1)}$, $(\varepsilon_\phi)_{cr}^{(2)}$: if $\lvert(\varepsilon_\phi)_{cr}^{(1)}\rvert \geq \lvert(\varepsilon_\phi)_{cr}^{(2)}\rvert$ then $(\varepsilon_\phi)_{cr} = (\varepsilon_\phi)_{cr}^{(2)}$ otherwise $(\varepsilon_\phi)_{cr} = (\varepsilon_\phi)_{cr}^{(1)}$
Outside -	No	No	$\lvert d_\phi \rvert - \lvert d_x \rvert$	$n = n^*$	$(\varepsilon_\phi)_{cr}^{(1)}$
			d_ϕ d_ϕ	$n = \frac{\pi R}{\ell_\phi}$ $n = n^*$	if $(\varepsilon_\phi)_{cr\ n=\pi R/\ell_\phi} \geq 0$ then $(\varepsilon_\phi)_{cr}^{(2)}\lvert_{n=n^*}$ otherwise $(\varepsilon_\phi)_{cr}\lvert_{n=\max(n,n^*)}$
				$(\varepsilon_\phi)_{cr}^{(1)}$, $(\varepsilon_\phi)_{cr}^{(2)}$	if $\lvert(\varepsilon_\phi)_{cr}^{(1)}\rvert \geq \lvert(\varepsilon_\phi)_{cr}^{(2)}\rvert$ then $(\varepsilon_\phi)_{cr} = (\varepsilon_\phi)_{cr}^{(2)}$ otherwise $(\varepsilon_\phi)_{cr} = (\varepsilon_\phi)_{cr}^{(1)}$

$$\zeta = \frac{d_\phi}{R - d_\phi - \frac{t_s}{2}} \quad ; \qquad d_\phi > 0 \text{ inside}$$

$$\zeta = \frac{d_\phi}{R + \lvert d_\phi \rvert + \frac{t_s}{2}} \quad ; \qquad d_\phi < 0 \text{ outside}$$

n^* positive integer such that $(\varepsilon_\phi)_{cr} < 0$ and $\lvert(\varepsilon_\phi)_{cr}\rvert\rvert_{n=n^*}$ is a minimum.

TABLE A2. SELECTION OF CIRCUMFERENTIAL STIFFENER BUCKLING MODE $(\varepsilon_\phi)_{cr}$ - EXPANSION

d_ϕ	Opposite Side	$\lvert d_\phi \rvert \leq \lvert d_x \rvert$	d	n	$(\varepsilon_\phi)_{cr}$
Outside -	Yes	N/A	d_ϕ	0	$(\varepsilon_\phi)_{cr} = (\varepsilon_\phi)_{cr}\big\rvert_{n=0}$
Outside -	No	Yes	d_ϕ	$\frac{\pi R}{\ell_\phi}$	$(\varepsilon_\phi)_{cr} = (\varepsilon_\phi)_{cr}\big\rvert_{n=\frac{\pi R}{\ell_\phi}}$ $(\varepsilon_\phi)_{cr}\big\rvert_{n=\frac{\pi R}{\ell_\phi}} > 0$ otherwise no buckling in this case
Outside -	No	No	$\lvert d_\phi \rvert - \lvert d_x \rvert$	0	$(\varepsilon_\phi)_{cr}^{(1)}$ if $(\varepsilon_\phi)_{cr}^{(2)} \leq 0$ then $(\varepsilon_\phi)_{cr} = (\varepsilon_\phi)_{cr}^{(1)}$
			d_ϕ	$\frac{\pi R}{\ell_\phi}$	$(\varepsilon_\phi)_{cr}^{(2)}$ if $(\varepsilon_\phi)_{cr}^{(2)} > 0$ then $(\varepsilon_\phi)_{cr} = \min((\varepsilon_\phi)_{cr}^{(1)}, (\varepsilon_\phi)_{cr}^{(2)})$

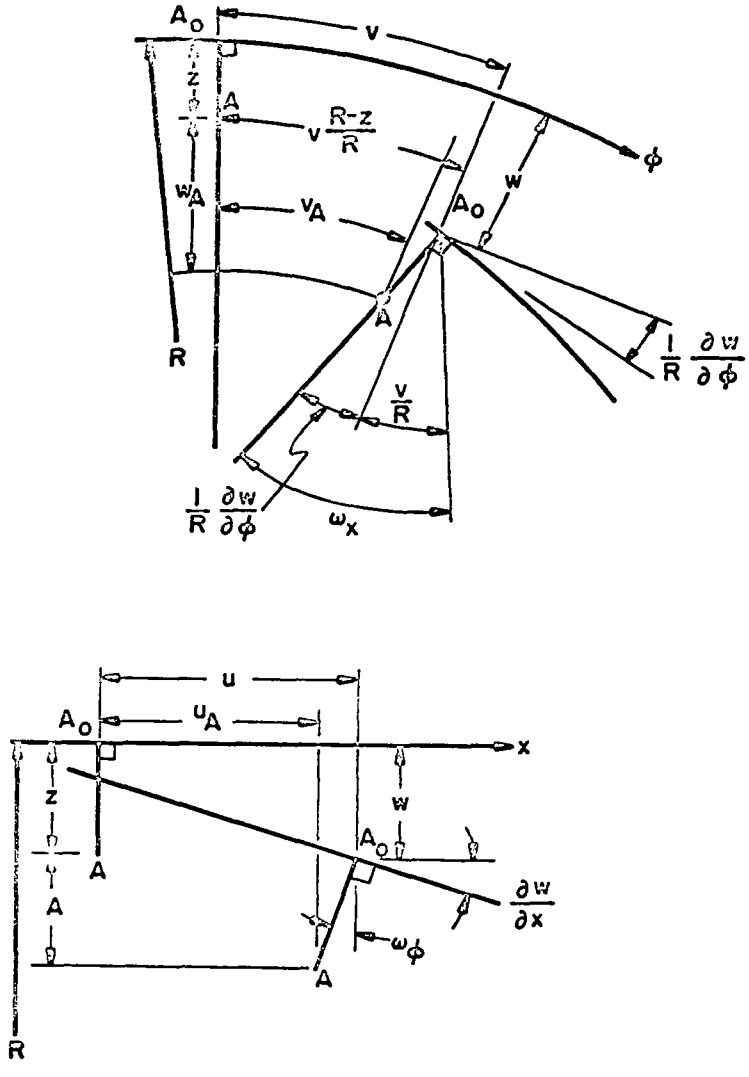

FIGURE A1. DISPLACEMENTS AND ROTATIONS OF A SHELL ELEMENT

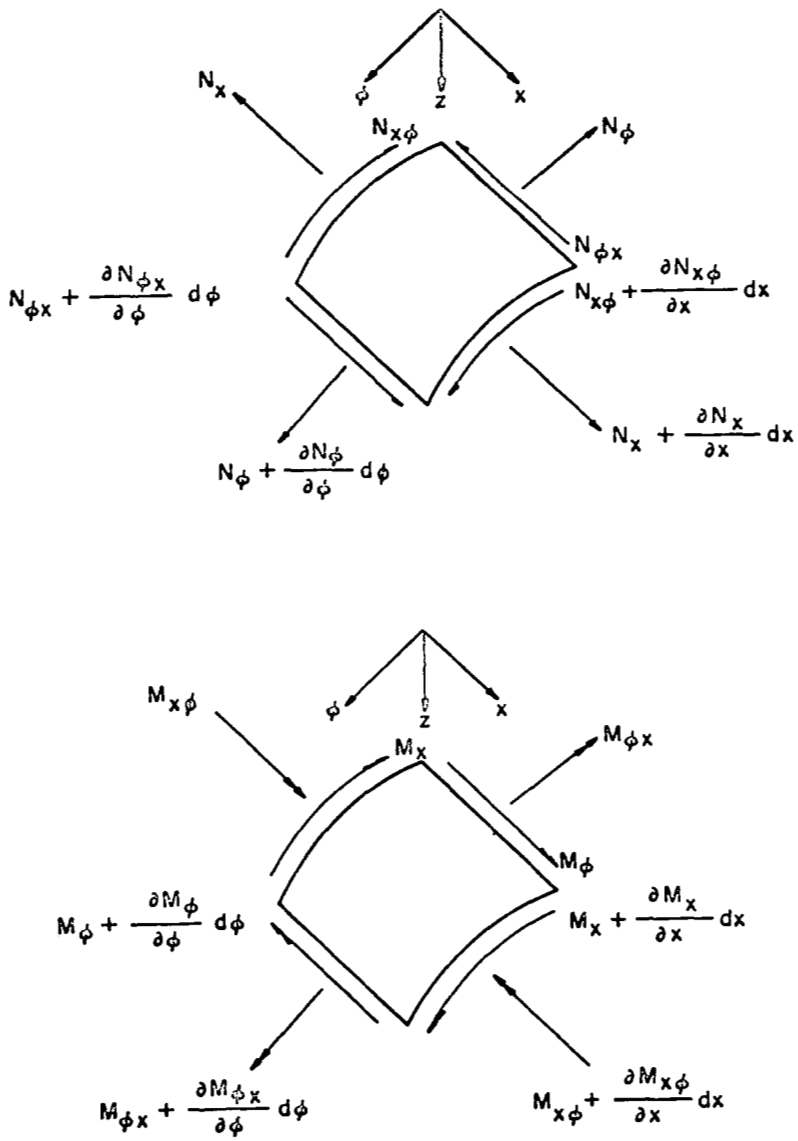

FIGURE A2. FORCE RESULTANTS

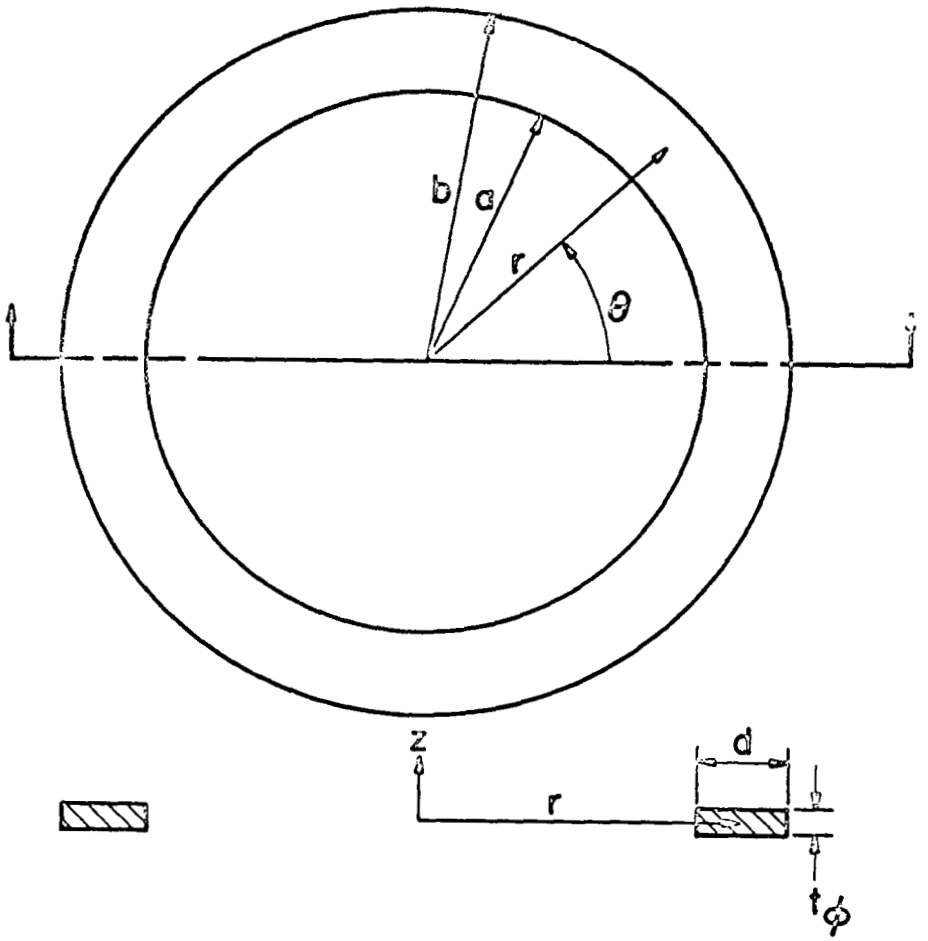

FIGURE A3. CIRCUMFERENTIAL STIFFENER

APPENDIX B

Verification of the Circumferential Stiffener Buckling Solution

Two limiting cases for $\varepsilon_{\phi cr}$ are obtained. One is for the washer mode of buckling with no circumferential waves. The other case is for a large number of waves. These cases are checked with existing solutions.

With n = 0 and neglecting terms involving the depth of the stiffener divided by the radius, ζ, with respect to one, the expression for the washer mode is

$$\varepsilon_{\phi cr} = -\left(\frac{t}{d}\right)^2 \frac{1}{12(1-\nu^2)} (2)\zeta \qquad \text{(B1)}$$

With n large and again neglecting ζ with respect to one the expression for $\varepsilon_{\phi cr}$ is

$$\varepsilon_{\phi cr} = -\left(\frac{t}{d}\right)^2 \frac{2}{12(1-\nu^2)} \left(\frac{n^2\zeta^2}{2} + 3(1-\nu)\right) \qquad \text{(B2)}$$

Substituting the expression for the critical strain in the washer mode (B1) into the expression for the stress in the radial direction (A25) and obtaining the value at the supported boundary, r = b, the following expression is obtained:

$$\sigma_{rcr} = \frac{-E_{\phi s}}{12(1-\nu^2)} \left(\frac{t}{d}\right)^2 \zeta\,(2\zeta)$$

Writing ζ as d/R and making the definition $D = E_{\phi s}t^2/12(1-\nu^2)$ this expression is

$$\sigma_r = -\frac{2D}{R^2}$$

The negative sign signifies that the stress is compressive. The above value agrees closely with the exact solution for the axisymmetric case done by

Meissner, reference 30, who obtain a value for the coefficient 1.86 instead of 2.

By substituting the value of $\varepsilon_{\theta cr}$ for n large (B2) into the expression for the tangential stress, σ_θ, (A25) at the supported edge, r = b, the following expression is obtained:

$$\sigma_\theta = \frac{-E_{\phi s}}{12(1-\nu^2)} \left(\frac{t}{d}\right)^2 \left(3(1-\nu) + \frac{n^2\zeta^2}{2}\right) \quad (2)$$

n is expressed in terms of the half wavelength, ℓ, as $\pi R/\ell$. Substituting for ζ and n the following expression is obtained:

$$\sigma_{\theta cr} = \frac{-E_{\phi s}\,\pi^2}{12\,(1-\nu^2)} \left(\frac{t}{d}\right)^2 \left(\left(\frac{d}{\ell}\right)^2 + \frac{6(1-\nu)}{\pi^2}\right)$$

If the value $\nu = .3$ is used this becomes

$$\sigma_{\theta cr} = \frac{-E_{\phi}\,\pi^2}{12(1-\nu^2)} \left(\frac{t}{d}\right)^2 \left(\left(\frac{d}{\ell}\right)^2 + 0.425\right)$$

which is the same as the expression for the critical buckling stress for a rectangular plate (see Section A.7).

APPENDIX C - DETAILED SOLUTIONS FROM EXTERIOR PENALTY FUNCTION METHOD

Case 1-I

	t_s	t_x	t_ϕ	d_x	d_ϕ	ℓ_x	ℓ_ϕ	W
Final	.02179	.03047	.00629	.3608	2.0	7.2379	.8768	225.93
Initial	.099	.06	.06	.5	.5	6.0	3.0	714.92
U. B.	.5	.5	.5	2.0	2.0	10.0	10.0	
L. B.	.0001	.0001	.0001	.0001	.0001	.0001	.0001	

f/f_{cr}

L.C.	1	2	3
G.B.	.7893	1.0044	.2450
P.B.	.8545	.9918	.3782
S.B.	.9153	1.0026	.3380
LRB.	.7195	1.0046	.2102
CRBU	0	0	0
CRBL	-8427.	-17874.	-1240.
S.Y.	.4041	.5863	.1164
LRYU	-.4057	-.5664	-.1185
LRYL	.4057	.5664	.1185
CRYU	.1261	.2676	.1857
CRYL	-.1261	-.2676	-.1857

LOADS

LC	N	P
1	700.	0.
2	940.	-2.
3	212.	.4

L = 165. R = 60.

Aluminum γ = .101

E = 10×10^6 ν = .333 σ_y = 50,000.

Wave Numbers

LC		Gross	Panel	Skin
1	M	14	1	8
	N	9	31	1
2	M	14	1	10
	N	9	24	1
3	M	13	1	7
	N	9	97	1

TABLE C1

Case 1 - I (B)

	t_s	t_x	t_ϕ	d_x	d_ϕ	ℓ_x	ℓ_ϕ	W
Final	.019892	.03097	.00851	.36516	1.91928	7.1545	.7971	227.72
Initial	.02000	.03120	.00907	.36500	1.92000	7.1500	.7920	230.39
U. B.	.5	.5	.5	2.0	2.0	10.0	10.0	
L. B.	.000001	.000001	.000001	.000001	.000001	.000001	.000001	

f/f_{cr}

L.C.	1	2	3
G.B.	.7768	.9999	.2449
P.B.	.7724	.9084	.3665
S.B.	.9247	.9999	.3481
LRB.	.7170	.9999	.2097
CRBU	0	0	0
CRBL	-4189.	-9150.	-563.8
S.Y.	.4058	.5891	.1172
LRYU	-.4080	-.5690	-.1194
LRYL	.4080	.5690	.1194
CRYU	.1232	.2691	.1658
CRYL	-.1232	-.2691	-.1658

LOADS

LC	N	P
1	700.	0
2	940.	-2.
3	212	.4

L = 165. R = 60.

Aluminum γ = .101

E = 10×10^6 ν = .333 σ_y = 50,000.

Wave Numbers

LC		Gross	Panel	Skin
1	M	13	1	9
	N	9	30	1
2	M	14	1	10
	N	9	23	1
3	M	13	1	7
	N	9	115	1

TABLE C2

Case 1 - I (A)

(With $|CRBL| \leq 1.0$)

	t_s	t_x	t_ϕ	d_x	d_ϕ	ℓ_x	ℓ_ϕ	W
Final	.02345	.03198	.04912	.3936	.8847	8.305	.947	261.8
Initial	.099	.06	.06	.5	.5	6.0	3.0	714.92
U. B.	.5	.5	.5	2.0	2.0	10.0	10.0	
L. B.	.0001	.0001	.0001	.0001	.0001	.0001	.0001	

f/f_{cr}

L.C.	1	2	3
G.B.	.8022	1.0032	.2894
P.B.	.8868	1.0020	.3993
S.B.	.8979	1.0039	.3258
LRB.	.7206	1.0020	.2114
CRBU	0	0	0
CRBL	-.1428	-.3024	-.02114
S.Y.	.3727	.5338	.1083
LRYU	-.3761	-.5229	-.1103
LRYL	.3761	.5229	.1103
CRYU	.1045	.2212	.01546
CRYL	-.1045	-.2212	-.01546

LOADS

LC	N	P
1	700.	0.
2	940.	-2.
3	212.	.4

L = 165. R = 60.

γ = .101

Aluminum

E = 10×10^6 ν = .333 σ_y = 50,000.

Wave Numbers

LC		Gross	Panel	Skin
1	M	11	1	8
	N	10	29	1
2	M	12	1	10
	N	10	22	1
3	M	1	1	7
	N	5	84	1

TABLE C3

CASE I

Using Large Constraint Weights 4×10^6

	t_s	t_x	t_ϕ	d_x	d_ϕ	ℓ_x	ℓ_ϕ	W
Final	04649	.1052	.0870	.3341	.3225	5.86	2.48	410.15
Initial	05455	.1198	.1381	.3238	.3659	5.84	2.57	489.78
U. B.	5	.5	.5	2.0	2.0	10.0	10.0	
L. B.	019	.05	.05	0.0	0.0	.05	.05	

L.C.	1	2	3
G.B.	.8833	.9537	.8130
P.B.	.4155	.5065	.1423
S.B.	.8725	.9994	.3144
LRB.	.0291	.0407	.0085
CRBU	0.0	0.0	0.0
CRBL	-.0698	-.1395	-.0120
S.Y.	.2278	.3271	.0658
LRYU	-.2289	-.3193	-.0669
LRYL	.2289	.3193	.0120
CRYU	.0698	.1395	.0120
CRYL	-.0698	-.1395	-.0120

LOADS

LC	N	P
1	700	0
2	940	-2
3	212	0.4

$L = 165$ $R = 60$

$\gamma = .101$

$E = 10 \times 10^6$ $\nu = .333$ $\sigma_y = 50000$

Wave Numbers

LC		Gross	Panel	Skin
1	M	9	1	2
	N	15	31	1
2	M	12	1	3
	N	15	25	1
3	M	1	1	2
	N	7	40	1

TABLE C4

CASE 2-I'

	t_s	t_x	t_ϕ	d_x	d_ϕ	ℓ_x	ℓ_ϕ	W
Final	.03392	.05	.05	.52871	1.2609	10.00	1.2078	387.40
Initial	.037	.0513	.0525	.519	.129	9.68	1.16	417.57
U.B.	.5	.5	.5	2.0	2.0	10.0	10.0	
L.B.	.019	.05	.05	-2.0	-2.0	.05	.05	

L = 165. R = 60.

γ = .101

E = 10.0 x 10^6 μ = .333 σ_y = 50,000.

L.B.	1	2	3
G.B.	.80999	1.00311	.26824
P.B.	.88770	1.00281	.38644
S.B.	.90988	1.00228	.33503
LRB	.70131	.97611	.20553
CRBU	0.	0.	0.
CRBL	-66.296	-142.74	-9.3358
S.Y.	.49254	.70889	.14285
LRYU	-.49642	-.69094	-.14548
LRYL	.49642	.69094	.14548
CRYU	.14186	.30543	.01998
CRYL	-.14186	-.30543	-.01998

LOADS

L.C.	N	P
1	1400.	0.
2	1880.	-4.
3	424.	.8

WAVE NUMBERS

LC		GROSS	PANEL	SKIN
1	M	10	1	8
	N	9	24	1
2	M	10	1	9
	N	9	19	1
3	M	1	1	6
	N	4	68	1

TABLE C5

CASE 3-I

	t_s	t_x	t_ϕ	d_x	d_ϕ	ℓ_x	ℓ_ϕ	W
Final	.04119	.05892	.01885	.55986	3.0	8.6238	1.3289	436.72
Initial	.1	.1	.1	.5	.5	3.0	3.0	835.26
U.B.	.5	.5	.5	3.0	3.0	10.0	10.0	
L.B.	.0000001	.0000001	.0000001	-3.0	-3.0	.0000001	.0000001	

$L = 165.$ $R = 60.$

$\gamma = .101$

$E = 10.0 \times 10^6$ $\mu = .333$ $\sigma_y = 50{,}000.$

L.C.	1	2	3
G.B.	.77665	1.00271	.24373
P.B.	.75647	.89355	.30150
S.B.	.91861	1.00322	.34171
LRB	.71905	1.00352	.21018
CRBU	0.	0.	0.
CRBL	-6486.11	-13838.17	-938.718
S.Y.	.62969	.91323	.18154
LRYU	-.63249	-.88272	-.18488
LRYL	.63249	.88272	.18488
CRYU	.19471	.41541	.28179
CRYL	-.19471	-.41541	-.28179

LOADS

L.C.	N	P
1	2100.	0.
2	2820.	-6.
3	636	1.2

WAVE NUMBERS

LC		GROSS	PANEL	SKIN
1	M	11	1	6
	N	7	25	1
2	M	11	1	8
	N	7	19	1
3	M	10	1	5
	N	7	68	1

TABLE C6

Case 4 - 0 Starting Point 1

	t_s	t_x	t_ϕ	d_x	d_ϕ	ℓ_x	ℓ_ϕ	W
Final	.1438	.1820	.2158	-1.750	-2.3028	39.96	4.6015	14252.6
Initial	.15	.20	.489	-1.84	-1.89	35.0	4.58	16184.3
U. B.	1.	20.	40.	4.	4.	40.	20.	
L. B.	.00001	.00001	.00001	-4.	-4.	.00001	.00001	

L.C.	1	2	3
G.B.	.9904	.9720	.8009
P.B.	.5593	.9841	.8732
S.B.	.3265	.5621	.6643
LRB.	.2224	1.008	.5457
CRBU	.0358	.7257	.1443
CRBL	-.0335	-.6792	-.1350
S.Y.	.1869	1.036	.4645
LRYU	-.1901	-.8618	-.4665
LRYL	.1901	.8618	.4665
CRYU	.3584	.7257	.1443
CRYL	-.3584	-.7257	-.1443

LOADS

LC	N	P
1	2100.	1.
2	8000.	-20.0
3	5000.	0

L = 500 R = 200

Aluminum γ = .101

E = 10 x 10^6 ν = .333 σ_y = 50,000.

Wave Numbers

LC		Gross	Panel	Skin
1	M	1	1	7
	N	6	48	1
2	M	13	1	14
	N	24	6	1
3	M	3	1	8
	N	9	27	1

TABLE C7

Case 4-0 Starting Point B

	t_s	t_x	t_ϕ	d_x	d_ϕ	ℓ_x	ℓ_ϕ	W
Final	.1470	.1849	.1503	-1.8194	-2.6810	40.0	4.84	14332.41
Initial	.216	.315	1.98	-1.38	-0.865	23.7	8.57	21300.00
U. B.	1.0	20.0	40.0	4.0	4.0	40.0	20.0	
L. B.	.00001	.00001	.00001	-4.0	-4.0	.00001	.00001	

L.C.	1	2	3
G.B.	.9224	.9092	.7584
P.B.	.5209	.9353	.8145
S.B.	.3386	.5823	.6899
LRB.	.2294	1.042	.5631
CRBU	.0360	.7232	.1443
CRBL	-.0868	-.1745	-.3481
S.Y.	.1841	1.027	.4581
LRYU	-.1873	-.8508	-.4596
LRYL	.1873	.8508	.4596
CRYU	.0360	.7231	.1443
CRYL	-.0360	-.7231	-.1443

LOADS

LC	N	P
1	2100.	1.
2	8000.	-20.0
3	5000.	0

$L = 500$ $R = 200$

Aluminum $\gamma = .101$

$E = 10 \times 10^6$ $\nu = .333$ $\sigma_y = 50{,}000.$

Wave Numbers

LC		Gross	Panel	Skin
1	M	1	1	7
	N	6	48	1
2	M	14	1	13
	N	0	5	1
3	M	3	1	8
	N	9	26	1

TABLE C8

CASE 5-I

	t_s	t_x	t_ϕ	d_x	d_ϕ	ℓ_x	ℓ_ϕ	W
Final	.11224	.13488	.01409	2.2286	3.1201	1.4105	6.4853	48097
Initial	.25	.25	.3	2.0	10.	25.	4.	124500
U. B.	.5	20.	1.	5.	10.1	100.	10.	
L. B.	.1	.02	.01	0.0	0.0	1.	1.	

L.C.	1	2	3
G.B.	1.0028	1.0028	0.8713
P.B.	0.0050	0.0190	0.0119
S.B.	0.2018	0.6969	0.4732
LRB	0.1220	0.5407	0.2981
CRBU	0.0	0.0	0.0
CRBL	-95.738	-18282.9	-3743.0
S.Y.	0.1730	0.8872	0.4259
LRYU	-0.1762	-0.7805	-0.4304
LRYL	0.1762	0.7805	0.4304
CRYU	0.0294	0.5614	0.1149
CRYL	-0.0294	-0.5614	-0.1149

LOADS

LC	N	P
1	2100.	1.
2	8000.	-20.
3	5000.	0.

$L = 2000.$ $R = 200.$

$\sigma_Y = 72000.$ $\gamma = .101$

$E = 10.5 \times 10^6$ $\nu = .333$

Wave Numbers

LC		Gross	Panel	Skin
1	M	1	3	1
	N	3	0	1
2	M	41	3	1
	N	8	0	1
3	M	31	3	1
	N	9	0	1

TABLE C9

C10

CASE 6-I

	t_s	t_x	t_ϕ	d_x	d_ϕ	ℓ_x	ℓ_ϕ	W
Final	.013634	.015188	.000533	.29760	.24387	.19178	2.000	3.8135
Initial	.04	.04	.04	.25	.25	1.0	1.0	13.723
U.B.	1.0	1.0	1.0	2.0	2.0	5.0	2.0	
L.B.	.0000001	.0000001	.0000001	2.0	-2.0	.0000001	.0000001	

L = 38.0 R= 9.55

γ= .101

E = 10.5×10^7 μ= .333 σ_y = 50000.

L.C.	1
G.B.	1.00660
P.B.	.01564
S.B.	.99987
LRB	.69918
CRBU	0.
CRBL	-1012.93
S.Y.	.99959
LRYU	-1.00215
LRYL	1.00215
CRYU	.31958
CRYL	-.31958

WAVE NUMBERS

L.C.		GROSS	PANEL	SKIN
1	M	6	4	1
	N	8	0	1

LOADS

L.C.	N	P
1	800.	0.

TABLE C10

CASE 6-I'

	t_s	t_x	t_ϕ	d_x	d_ϕ	ℓ_x	ℓ_ϕ	W
Final	.00998	.01244	.00027	.11348	1.0085	1.6519	.23791	3.700
Initial	.028	.05	.05	.1	.1	1.5	.25	11.787
U.B.	1.0	1.0	1.0	2.0	2.0	5.0	2.0	
L.B.	.0000001	.0000001	.0000001	.05	.05	.0000001	.0000001	

$L = 38.0$ $R = 9.55$

$\gamma = .101$

$E = 10.5 \times 10^6$ $\mu = .333$ $\sigma_y = 50{,}000.$

L.C.	
G.B.	1.00418
P.B.	.99432
S.B.	.74864
LRB	1.00065
CRBU	0.
CRBL	-1021695.
S.Y.	1.00300
LRYU	-1.00390
LRYL	1.00390
CRYU	.32948
CRYL	-.32948

LOADS

L.C.	N	P
1	800.	0.

L.C.		GROSS	PANEL	SKIN
1	M	13	1	7
	N	7	21	1

TABLE C11

CASE 7-I

	t_s	t_x	t_ϕ	d_x	d_ϕ	ℓ_x	ℓ_ϕ	W
Final	.03044	.0276	.000022	.3879	20.0	3.229	1.3162	682.54
Initial	.05	.1	.05	1.0	2.0	8.0	3.0	1681.74
U. B.	10.0	10.0	10.0	20.0	20.0	50.0	20.0	
L. B.	.0000001	.0000001	.0000001	.00000001	.0000001	.0000001	.0000001	

L = 291 R = 95.5

γ = .101

E = 10×10^6 ν = .333 σ_y = 50000

L.C.	1	2	3
G.B.	1.0028	----	---
P.B.	.2173	----	---
S.B.	1.0051	----	---
LRB.	1.0071	----	---
CRBU	0.0	----	---
CRBL	-1.5×10^{10}	----	---
S.Y.	.4145	----	---
LRYU	-.4146	----	---
LRYL	.4146	----	---
CRYU	.1375	----	---
CRYL	0.1375	----	---

LOADS

LC	N	P
1	800	0.0
2	-----	---
3	---	---

Wave Numbers

LC		Gross	Panel	Skin
1	M	27	1	2
	N	6	62	1
2	M	--	--	--
	N	--	--	--
3	M	--	--	--
	N	--	--	--

TABLE C12

CASE 8-I,O

	t_s	t_x	t_ϕ	d_x	d_ϕ	ℓ_x	ℓ_ϕ	W
Final	.2155	.3238	.0789	- 3.6867	9.9965	48.7457	7.3671	38824
Initial	.231	.340	.268	- 3.92	3.86	17.7	7.17	46840
U. B.	1.0	10.0	10.0	- 0.5	10.0	80.0	20.0	
L. B.	.019	.05	.05	-10.0	.5	.05	.05	

L.C.	1	2	3
G.B.	1.0041	--	--
P.B.	.4992	--	--
S.B.	1.0028	--	--
LRB.	1.0057	--	--
CRBU	0.0	--	--
CRBL	-3.57×10^3	--	--
S.Y.	.6384	--	--
LRYU	-.6408	--	--
LRYL	.6408	--	--
CRYU	.2000	--	--
CRYL	-.2000	--	--

LOADS

LC	N	P
1	12150	0
2	---	---
3	---	---

$L = 361$ $R = 433$

$\gamma = .101$

$E = 10.5 \times 10^6$ $\nu = .333$ $\sigma_y = 50000$

Wave Numbers

LC		Gross	Panel	Skin
1	M	3	1	6
	N	10	7	1
2	M	--	--	--
	N	--	--	--
3	M	--	--	--
	N	--	--	--

TABLE C13

APPENDIX D

SOLUTION TO CASE 7-I USING SEARCH COMBINATION (9,2,9,2,5,2,3)

	t_s	t_x	t_ϕ	d_x	d_ϕ	ℓ_x	ℓ_ϕ	W
Final	.03044	.0276	.000022	.3879	20.0	3.229	1.3162	682.54
Initial	0.05	0.1	0.05	1.0	2.0	8.0	3.0	1681.7
U. B.	10.0	10.0	10.0	20.0	20.0	50.0	20.0	
L. B.	1.0E-7	1.0E-7	1.0E-7	1.0E-7	1.0E-7	1.0E-7	1.0E-7	

L.C.	1
G.B.	1.0028
P.B.	.2173
S.B.	1.0051
LRB	1.0071
CRBU	0
CRBL	−1.5E+10
S.Y.	.4145
LRYU	-.4146
LRYL	.4146
CRYU	.1375
CRYL	-.1375

NUMOPT = 7

METHOP = 9,2,9,2,5,2,3

L = 291.0 R = 95.5 $\frac{d\phi}{t\phi}$ = 910000.0

σ_y = 50000. γ = 0.101

E = 10.5E6 ν = .333 $\frac{dx}{tx}$ = 14.1

Wave Numbers

LC		Gross	Panel	Skin
1	M	27	1	2
	N	6	62	1

SEARCH TECHNIQUES USED:

Random Ray (Method 9)
Pattern (Method 2)
Creeping (Method 5)
Magnification (Method 3)

LOADS

LC	N	P
1	800	0

TABLE D1.

SOLUTION TO CASE 7-I USING SEARCH COMBINATION (5,2,5,2)

	t_s	t_x	t_ϕ	d_x	d_ϕ	ℓ_x	ℓ_ϕ	W
Final	.10904	.00959	.00020	.000008	2.00737	2.46866	20.0	1925.84
Initial	0.05	0.1	0.05	1.0	2.0	8.0	3.0	1681.7
U. B.	10.0	10.0	10.0	20.0	20.0	50.0	20.0	
L. B.	1.0E-7	1.0E-7	1.0E-7	1.0E-7	1.0E-7	1.0E-7	1.0E-7	

L.C.	1
G.B.	1.00367
P.B.	.37317
S.B.	.36318
LRB	1.1E-9
CRBU	0
CRBL	6.1E+8
S.Y.	.1467
LRYU	-.1467
LRYL	.1467
CRYU	.04879
CRYL	-.04879

NUMOPT = 4
METHOP = 5,2,5.2

L = 291.0 R = 95.5 $\frac{d\phi}{t\phi}$ = 10000.0
σ_y = 50000. γ = 0.101
E = 10.5E6 ν = 0.333 $\frac{dx}{tx}$ = .00089

Wave Numbers

LC		Gross	Panel	Skin
1	M	48	1	1
	N	14	0	1

SEARCH TECHNIQUES USED:

Creeping (Method 5)
Pattern (Method 2)

LOADS

LC	N	P
1	800	0

TABLE D2

SOLUTION TO CASE 7-I USING SEARCH COMBINATION (6,2,6,2)

	t_s	t_x	t_ϕ	d_x	d_ϕ	ℓ_x	ℓ_ϕ	W
Final	.05785	1.OE-7	1.OE-7	1.OE-7	1.OE-7	1.OE-7	12.4752	1020.25
Initial	0.05	0.1	0.05	1.0	2.0	8.0	3.0	1681.7
U. B.	10.0	10.0	10.0	20.0	20.0	50.0	20.0	
L. B.	1.OE-7	1.OE-7	1.OE-7	1.OE-7	1.OE-7	1.OE-7	1.OE-7	

L.C.	1
G.B.	3.6162*
P.B.	.00369
S.B.	.00369
LRB	.00100
CRBU	0
CRBL	-.0921
S.Y.	.2765
LRYU	-.2765
LRYL	.0921
CRYU	-.0921
CRYL	

NUMOPT = 4

METHOP = 6,2,6,2

L = 291.0 R = 95.5 $\frac{d\phi}{t\phi}$ = 1

σ_Y = 50000. γ = 0.101

E = 10.5E6 ν = 0.333 $\frac{dx}{tx}$ = 1

Wave Numbers

LC		Gross	Panel	Skin
1	M	15	11	11
	N	30	Upper Limit 100	15

SEARCH TECHNIQUES USED:

Quadratic (Method 6)
Pattern (Method 2)

NOTE: The results presented are those obtained from the first run. The second run was aborted due to a singular matrix.

* Excessive constraint violation

LOADS

LC	N	P
1	800	0

TABLE D3

SOLUTION TO CASE 7-1 USING SEARCH COMBINATION (7,2,7,2)

	t_s	t_x	t_ϕ	d_x	d_ϕ	ℓ_x	ℓ_ϕ	W
Final	.02260	.03022	.00794	.41874	2.54229	7.45131	.93042	684.44
Initial	0.05	0.1	0.05	1.0	2.0	8.0	3.0	1681.7
U. B.	10.0	10.0	10.0	20.0	20.0	50.0	20.0	
L. B.	1.0E-7	1.0E-7	1.0E-7	1.0E-7	1.0E-7	1.0E-7	1.0E-7	

L.C.	1
G.B.	1.0405 *
P.B.	.6944
S.B.	1.0178
LRB	1.0123
CRBU	0
CRBL	-1.09E+6
S.Y.	.4362
LRYU	-.4386
LRYL	.4386
CRYU	.1320
CRYL	-.1329

NUMOPT = 4
METHOP = 7,2,7,2

$L = 291.0$ $R = 95.5$ $\frac{d\phi}{t\phi} = 321.0$
$\sigma_y = 50000.$ $\gamma = 0.101$
$E = 10.5E6$ $\nu = 0.333$ $\frac{dx}{tx} = 13.8$

Wave Numbers

LC		Gross	Panel	Skin
1	M	19	1	8
	N	10	40	1

SEARCH TECHNIQUES USED:
Davidon (Method 7)
Pattern (Method 2)

* Excessive constraint violation

LOADS

LC	N	P
1	800	0

TABLE D4

SOLUTION TO CASE 7-I USING SEARCH COMBINATION (4,2,4,2)

	t_s	t_x	t_ϕ	d_x	d_ϕ	ℓ_x	ℓ_ϕ	W
Final	.10321	1.0E-7	.00001	1.0E-7	7.32029	4.3547	2.89986	1820.4
Initial	0.05	0.1	0.05	1.0	2.0	8.0	3.0	1681.7
U. B.	10.0	10.0	10.0	20.0	20.0	50.0	20.0	
L. B.	1.0E-7	1.0E-7	1.0E-7	1.0E-7	1.0E-7	1.0E-7	1.0E-7	

L.C.	1
G.B.	1.1174*
P.B.	1.0110
S.B.	.1467
LRB	.0019
CRBU	0
CRBL	-8.9E+11
S.Y.	.1550
LRYU	-.1550
LRYL	.1550
CRYU	.0516
CRYL	-.0516

NUMOPT = 4
METHOP = 4,2,4,2

L = 291.0 R = 95.5 $\frac{d\phi}{t\phi}$ = 732029.0
σ_y = 50000 γ = 0.101
E = 10.5E6 ν = 0.333 $\frac{dx}{d\lambda}$ = 1

Wave Numbers

LC		Gross	Panel	Skin
1	M	Upper Limit 50	1	2
	N	12	0	1

SEARCH TECHNIQUES USED:
Steepest-Descent (Method 4)
Pattern (Method 2)

* Excessive Constraint Violation

LOADS

LC	N	P
1	800	0

TABLE D5.

SOLUTION TO CASE 7-I USING SEARCH COMBINATION (5,2,3)

	t_s	t_x	t_ϕ	d_x	d_ϕ	ℓ_x	ℓ_ϕ	W
Final	.07795	.13221	.03189	.01691	.67382	2.71116	.86511	1558.30
Initial	0.05	0.1	0.05	1.0	2.0	8.0	3.0	1681.7
U. B.	10.0	10.0	10.0	20.0	20.0	50.0	20.0	
L. B.	1.OE-7	1.OE-7	1.OE-7	1.OE-7	1.OE-7	1.OE-7	1.OE-7	

L.C.	1
G.B.	1.7832 *
P.B.	1.0227
S.B.	.03301
LRB	.00003
CRBU	0
CRBL	-94.37
S.Y.	.1957
LRYU	-.1967
LRYL	.1967
CRYU	.06007
CRYL	-.06007

NUMOPT = 2
METHOP = 5,2,3

L = 291.0 R = 95.5 $\frac{d\phi}{t\phi}$ = 21.1
σ_y = 50000. γ = 0.101
E = 10.5E6 ν = 0.333 $\frac{dx}{tx}$ = .0128

Wave Numbers

LC		Gross	Panel	Skin
1	M	Upper Limit 50	1	3
	N	15	0	1

SEARCH TECHNIQUES USED:
Creeping (Method 5)
Pattern (Method 2)

* Excessive constraint Violation

LOADS

LC	N	P
1	800	0

TABLE D6.

SOLUTION TO CASE 7-I USING SEARCH COMBINATION (1,2)

	t_s	t_x	t_ϕ	d_x	d_ϕ	ℓ_x	ℓ_ϕ	W
Final	.00941	.08609	1.0E-7	.96933	20.0	.03294	16.679	255.08
Initial	0.05	0.1	0.05	1.0	2.0	8.0	3.0	1681.7
U. B.	10.0	10.0	10.0	20.0	20.0	50.0	20.0	
L. B.	1.0E-7	1.0E-7	1.0E-7	1.0E-7	1.0E-7	1.0E-7	1.0E-7	

L.C.	1
G.B.	1.1308*
P.B.	.0227
S.B.	.01480
LRB	.00084
CRBU	0
CRBL	-1.8E+17
S.Y.	1.1095
LRYU	-1.110*
LRYL	1.110*
CRYU	.3675
CRYL	-.3675

*Excessive constraint violation

NUMOPT = 2

METHOP = 1,2

L = 291.0 R = 95.5 $\frac{d\phi}{t\phi}$ = 20.0E+7

σ_y = 50000. γ = 0.101

E = 10.5E6 ν = 0.933 $\frac{dx}{tx}$ = ±1.15

Wave Numbers

LC		Gross	Panel	Skin
1	M	13	6	14
	N	7	19	3

SEARCH TECHNIQUES USED:
Sectioning (Method 1)
Pattern (Method 2)

LOADS

LC	N	P
1	800	0

TABLE D7.

SOLUTION TO CASE 7-I USING SEARCH COMBINATION (9,2,9,2,5,2,3)

(Limits imposed on d/t)

	t_s	t_x	t_ϕ	d_x	d_ϕ	ℓ_x	ℓ_ϕ	W
Final	0.030	0.0335	0.05009	0.50166	1.0483	10.936	1.3110	831.21
Initial	0.05	0.1	0.05	1.0	2.0	8.0	3.0	1681.7
U. B.	10.0	10.0	10.0	20.0	20.0	50.0	20.0	
L. B.	1.0E-7	1.0E-7	1.0E-7	1.0E-7	1.0E-7	1.0E-7	1.0E-7	

L.C.	1
G.B.	1.0046
P.B.	1.0058
S.B.	1.0072
LRB	1.0028
CRBU	0
CRBL	-57.114
S.Y.	0.3695
LRYU	-0.3721
LRYL	0.3721
CRYU	0.1083
CRYL	-0.1083

NUMOPT = 7

METHOP = 9,2 9,2,5,2,3

$L = 291.0$ $R = 95.5$ $\frac{d\phi}{t\phi} = 21.0$

$\sigma_Y = 50000.$ $\gamma = 0.101$

$E = 10.5E6$ $\nu = 0.333$ $\frac{dx}{tx} = 15.0$

Wave Numbers

LC		Gross	Panel	Skin
1	M	15	1	8
	N	13	35	1

SEARCH TECHNIQUES USED:

Random Ray (Method 9)
Pattern (Method 2)
Creeping (Method 5)
Magnification (Method 3)

LOADS

LC	N	P
1	800	0

TABLE D8

SOLUTION TO CASE 7-I USING SEARCH COMBINATION (5,2,5,2)

(Limits imposed on d/t)

	t_s	t_x	t_ϕ	d_x	d_ϕ	ℓ_x	ℓ_ϕ	W
Final	.02446	.03211	.06172	.46184	1.2766	10.280	1.0132	819.04
Initial	0.05	0.1	0.05	1.0	2.0	8.0	3.0	1681.7
U. B.	10.0	10.0	10.0	20.0	20.0	50.0	20.0	
L. B.	1.0E-7	1.0E-7	1.0E-7	1.0E-7	1.0E-7	1.0E-7	1.0E-7	

L.C.	1
G.B.	1.0044
P.B.	1.0050
S.B.	1.0050
LRB	1.0033
CRBU	0
CRBL	-54.339
S.Y.	.3979
LRYU	-.4024
LRYL	.4024
CRYU	.1048
CRYL	-.1048

NUMOPT = 4

METHOP = 5,2,5,2

L = 291.0 R = 95.5 $\frac{d\phi}{t\phi}$ = 20.7

σ_Y = 50000. γ = 0.101

E = 10.5E6 ν = 0.333 $\frac{dx}{tx}$ = 14.4

Wave Numbers

LC		Gross	Panel	Skin
1	M	16	1	9
	N	11	35	1

SEARCH TECHNIQUES USED:

Creeping (Method 5)

Pattern (Method 2)

LOADS

LC	N	P
1	800	0

Table D9.

SOLUTION TO CASE 7-I USING SEARCH COMBINATION (6,2,6,2)

(Limits imposed on d/t)

	t_s	t_x	t_ϕ	d_x	d_ϕ	ℓ_x	ℓ_ϕ	W
Final	.02544	.02891	.05625	.44930	1.3713	9.5067	1.0375	806.85
Initial	0.05	0.1	0.05	1.0	2.0	8.0	3.0	1681.7
U. B.	10.0	10.0	10.0	20.0	20.0	50.0	20.0	
L. B.	1.0E-7	1.0E-7	1.0E-7	1.0E-7	1.0E-7	1.0E-7	1.0E-7	

L.C.	1
G.B.	1.0036
P.B.	1.0056
S.B.	1.0025
LRB	1.2045*
CRBU	0
CRBL	-75.909
S.Y.	.40922
LRYU	-.4139
LRYL	.4139
CRYU	.1074
CRYL	-.1074

NUMOPT = 4

METHOP = 6,2,6,2

L = 291.0 R = 95.5 $\frac{d\phi}{t\phi}$ = 24.4

σ_y = 50000. γ = 0.101

E = 10.5E6 ν = 0.333 $\frac{dx}{dy}$ = 15.6

Wave Numbers

LC		Gross	Panel	Skin
1	M	18	1	8
	N	10	37	1

SEARCH TECHNIQUES USED:
Quadratic (Method 6)
Pattern (Method 2)

* Excessive Constraint Violation

LOADS

LC	N	P
1	800	0

Table D10.

SOLUTION TO CASE 7-I USING SEARCH COMBINATION (7,2)

(Limits imposed on d/t)

	t_s	t_x	t_ϕ	d_x	d_ϕ	ℓ_x	ℓ_ϕ	W
Final	.03718	.03222	.03948	.50308	.90802	8.3231	1.7334	894.04
Initial	0.05	0.1	0.05	1.0	2.0	8.0	3.0	1681.7
U. B.	10.0	10.0	10.0	20.0	20.0	50.0	20.0	
L. B.	1.0E-7	1.0E-7	1.0E-7	1.0E-7	1.0E-7	1.0E-7	1.0E-7	

L.C.	1
G.B.	1.0072
P.B.	.6931
S.B.	1.0044
LRB	.9977
CRBU	0
CRBL	-64.618
S.Y.	.3389
LRYU	-.3407
LRYL	.3407
CRYU	.1029
CRYL	-.1029

NUMOPT = 2

METHOP = 7,2

L = 291.0 R = 95.5 $\frac{d\phi}{t\phi}$ = 20.8

σ_y = 50000. γ = 0.101

E = 10.5E6 ν = 0.333 $\frac{dx}{tx}$ = 14.1

Wave Numbers

LC		Gross	Panel	Skin
1	M	16	1	5
	N	14	40	1

SEARCH TECHNIQUES USED:

Davidon (Method 7)
Pattern (Method 2)

LOADS

LC	N	P
1	800	0

Table D11.

SOLUTION TO CASE 7-I USING SEARCH COMBINATION (4,2)

(Limits imposed on d/t)

	t_s	t_x	t_ϕ	d_x	d_ϕ	ℓ_x	ℓ_ϕ	W
Final	.02970	.03158	.04092	.46631	1.1744	8.3364	1.2821	824.52
Initial	0.05	0.1	0.05	1.0	2.0	8.0	3.0	1681.7
U. B.	10.0	10.0	10.0	20.0	20.0	50.0	20.0	
L. B.	1.0E-7	1.0E-7	1.0E-7	1.0E-7	1.0E-7	1.0E-7	1.0E-7	

L.C.	1
G.B.	.99903
P.B.	.73365
S.B.	1.0029
LRB	1.0053
CRBU	0
CRBL	-111.53
S.Y.	.3803
LRYU	-.3834
LRYL	.3834
CRYU	.1089
CRYL	-.1089

NUMOPT = 2

METHOP = 4,2

L = 291.0 R = 95.5 $\frac{d\phi}{t\phi}$ = 28.8

σ_Y = 50000. γ = 0.101

E = 10.5E6 ν = 0.333 $\frac{dx}{tx}$ = 14.75

Wave Numbers

LC		Gross	Panel	Skin
1	M	17	1	6
	N	12	39	1

SEARCH TECHNIQUES USED:

Steepest-Descent (Method 4)
Pattern (Method 2)

LOADS

LC	N	P
1	800	0

Table D12.

SOLUTION TO CASE 7-I USING SEARCH COMBINATION (1,2)

(Limits imposed on d/t)

	t_s	t_x	t_ϕ	d_x	d_ϕ	ℓ_x	ℓ_ϕ	W
Final	.02561	.03075	.05682	.43385	1.1801	9.3976	.97670	813.46
Initial	0.05	0.1	0.05	1.0	2.0	8.0	3.0	1681.7
U. B.	10.0	10.0	10.0	20.0	20.0	50.0	20.0	
L. B.	1.0E-7	1.0E-7	1.0E-7	1.0E-7	1.0E-7	1.0E-7	1.0E-7	

L.C.	1
G.B.	1.0690*
P.B.	.9811
S.B.	.8421
LRB	.9622
CRBU	0
CRBL	-59.967
S.Y.	.3969
LRYU	-.4010
LRYL	.4010
CRYU	.1070
CRYL	-.1070

*Excessive constraint violation

NUMOPT = 2

METHOP = 1,2

L = 291.0 R = 95.5 $\frac{d\phi}{t\phi}$ = 20.8

σ_y = 50,000. γ = 0.101

E = 10.5E6 ν = 0.333 $\frac{d_x}{t_x}$ = 14.4

Wave Numbers

LC		Gross	Panel	Skin
1	M	17	1	9
	N	11	37	1

SEARCH TECHNIQUES USED:

Sectioning (Method 1)
Pattern (Method 2)

LOADS

LC	N	P
1	800	0

Table D13.

SOLUTION TO CASE 7-I USING AESOP WARPING TRANSFORMATION

	t_s	t_x	t_ϕ	d_x	d_ϕ	ℓ_x	ℓ_ϕ	W
Final	.02899	.03203	.04921	.47911	.98	6.9709	1.1208	837.76
Initial	0.05	0.1	1.05	1.0	2.0	8.0	3.0	1681.7
U. B.	10.0	10.0	10.0	20.0	20.0	50.0	20.0	
L. B.	1.0E-7	1.0E-7	1.0E-7	1.0E-7	1.0E-7	1.0E-7	1.0E-7	
WARPAL	0.03	0.0335	0.05009	0.50166	1.0483	10.936	1.3110	

L.C.	1
G.B.	.9951
P.B.	.9644
S.B.	.9795
LRB	.9986
CRBU	0
CRBL	-56.66
S.Y.	.3669
LRYU	-.3695
LRYL	.3695
CRYU	.1075
CRYL	-.1075

NUMOPT = 7

METHOP = 9,2,9,2,5,2,3

L = 291.0 R = 95.5 $\frac{d\phi}{t\phi}$ = 19.8

σ_Y = 50000. γ = 0.101

E = 10.5E6 ν = 0.333 $\frac{dx}{tx}$ = 15.0

Wave Numbers

LC		Gross	Panel	Skin
1	M	15	1	8
	N	13	36	1

Search Techniques Used:

Pattern (Method 2)
Random Ray (Method 9)
Creeping (Method 5)
Magnification (Method 3)

LOADS

LC	N	P
1	800	0

TABLE D14.

SOLUTION TO CASE 7-I USING SEARCH COMBINATION (9,2,9,2,5,2,3)

	t_s	t_x	t_ϕ	d_x	d_ϕ	ℓ_x	ℓ_ϕ	W
Final	.02979	.03376	.05185	.50544	1.0381	11.239	1.3178	834.51
Initial	.01	.01	.01	.2	.2	1.0	1.0	246.74
U. B.	10.0	10.0	10.0	20.0	20.0	50.0	20.0	
L. B.	1.0E-7	1.0E-7	1.0E-7	1.0E-7	1.0E-7	1.0E-7	1.0E-7	

L.C.	1
G.B.	1.0018
P.B.	1.0329
S.B.	1.0061
LRB	1.0006
CRBU	0
CRBL	-51.736
S.Y.	.3677
LRYU	-.3703
LRYL	.3703
CRYU	.10789
CRYL	-.10789

NUMOPT = 7

METHOP = 9,2,9,2,5,2,3

L = 291.0 $\quad R$ = 95.5 $\quad \frac{d\phi}{t\phi}$ = 20.0

σ_y = 50000. $\quad \gamma$ = 0.101

E = 10.5E6 $\quad \nu$ = 0.333 $\quad \frac{dx}{tx}$ = 15.0

Wave Numbers

LC		Gross	Panel	Skin
1	M	15	1	8
	N	13	35	1

SEARCH TECHNIQUES USED:

Random Ray (Method 9)
Pattern (Method 2)
Creeping (Method 5)
Magnification (Method 3)

LOADS

LC	N	P
1	800	0

TABLE D15.

SOLUTION TO CASE 7-I USING AESOP WARPING TRANSFORMATION

	t_s	t_x	t_ϕ	d_x	d_ϕ	ℓ_x	ℓ_ϕ	W
Final	.02706	.10350	.02049	1.3206	.41088	.54820	20.0	867.48
Initial	.01	.01	.01	.2	.2	1.0	1.0	246.74
U. B.	10.0	10.0	10.0	20.0	20.0	50.0	20.0	
L. B.	1.OE-7	1.OE-7	1.OE-7	1.OE-7	1.OE-7	1.OE-7	1.OE-7	

L.C.	1
G.B.	1.0045
P.B.	.0079
S.B.	1.0029
LRB	.4275
CRBU	0.0
CRBL	-1.304
S.Y.	.4500
LRYU	-.4568
LRYL	.4568
CRYU	.1011
CRYL	-.1011

LOADS

LC	N	P
1	800	0

$L = 291.0$ $R = 95.5$

$\sigma_y = 50{,}000$ $\gamma = .101$

$E = 10.5E6$ $\nu = .333$

Wave Numbers

LC		Gross	Panel	Skin
1	M	6	2	1
	N	11	0	1

TABLE D16.

APPENDIX E

PROGRAM STRUCTURE AND DATA INPUT/OUTPUT DESCRIPTION

Figure E1 defines the overlay structure for the program. The central memory core storage requirement is 70000_8 locations. All data required by the program is input through two namelist data blocks. The first data block, "CR1217", is for the analysis data; the second data block, IAESOP, is for the optimization data.

For each complete analysis the following output is obtained:

CLT	These are the critical buckling load values divided by H_{s2} for the modes saved for the skin for the last load condition.
SMS	The values of m saved, starting with all the values for gross buckling for all load conditions,followed by panel buckling for all load conditions, followed by skin buckling for all load conditions.
SNS	Same as SMS but for the values of n which are saved.
CRITICAL LOADS	Each line contains the critical buckling load for gross, panel, and skin buckling for one load condition; successive load conditions are on successive lines.
MODE SHAPES	Same order as above giving the values of m and n.
LRS	Stress in the longitudinal rib for each load condition.
CRS	Stress in the circumferential rib for each load condition.
DES	Actual value of distortion energy stress squared for each load condition.

EBU	Critical strain value, circumferential rib, for an expansion of the cylinder, for each load condition.
EBL	Critical strain value, circumferential rib for a contraction of the cylinder.
LRCB	Critical buckling stress for the longitudinal rib, for each load condition.
BEU	Logical variables signifying the existence of a critical strain EBU, T for True, F for false.
BEL	Same as above for EBL.
BLR	Same as above for LRCB.
EPA	Actual value of circumferential strain for each load condition.
TS, TX, TY, DX, DY, LX, LY	These correspond to t_s, t_x, t_ϕ, d_x, d_ϕ, ℓ_x, ℓ_ϕ.
AX, AY	Areas of the longitudinal and circumferential stiffeners, respectively.

The following eleven lines of output are the ratios of actual values of the behavior variables to the critical values, in columns for each load condition.

G.B.	Gross buckling
P.B.	Panel buckling
S.B.	Skin buckling
LRB	Longitudinal stiffener buckling
CRBU	Circumferential stiffener buckling for an expansion of the cylinder.

CRBL	Circumferential stiffener buckling for a contraction of the cylinder.
S.Y.	Skin yield
LRYU	Longitudinal stiffener yield in tension
LRYL	Longitudinal stiffener yield in compression
CRYU	Circumferential stiffener yield in tension
CRYL	Circumferential stiffener yield in compression
WT	Weight of the cylinder in pounds.

The output obtained after each partial analysis is controlled by the user through the AESOP print control integers described later in this section. (See AESOP Namelist Input Description).

Namelist Data Block "CR1217"

This data block is read and defined in the analysis subprogram NL1217. All nominal data values are established by the analysis subprogram D1217. Data block CR1217 defines all the input variables required for the analysis subprograms. A complete list of the namelist data block CR1217 is presented in Table E1.

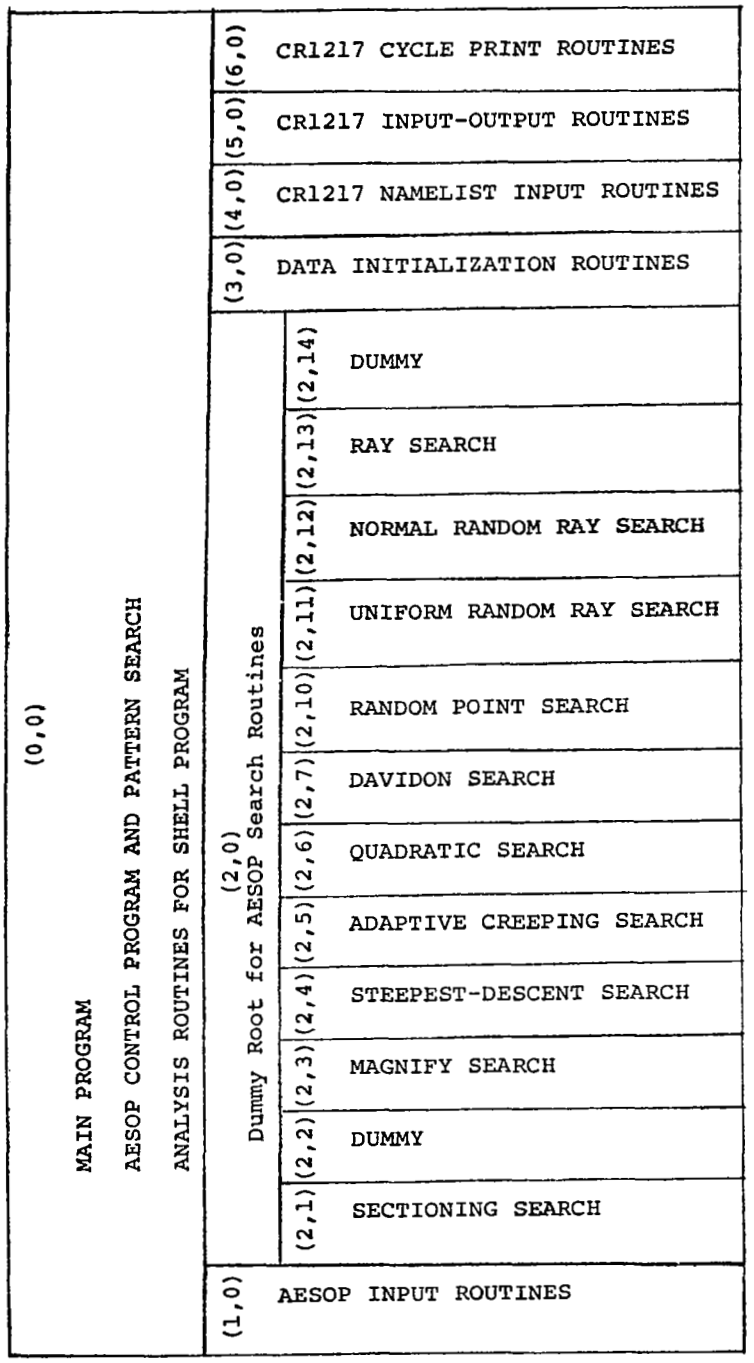

FIGURE E1. PROGRAM OVERLAY STRUCTURE

TABLE E1.

NAMELIST Data Block "CR1217"

NMENOMIC	NOMINAL VALUES	DESCRIPTION
BDV( )	First seven true, eighth false.	Logical variables determining active design variables. One for each design variable plus one to tell when the two depth variables are to be kept equal. The first seven quantities relate one-for-one the seven design variables in the following order: $t_s, t_x, t_\phi, d_x, d_\phi, \ell_x, \ell_\phi$. To make the two depth variables equal, the eighth value of the array BDV is made true, and the fifth value is made false. (The fifth value corresponds to d_ϕ). The program will then make d_ϕ d_x.
BOTULX	20.0	Upper limit for $(d/t)_x$
BOTULY	20.0	Upper limit for $(d/t)_\phi$
CRCL( )	-5.0E4	Compressive yield stress for circumferential stiffeners for each load condition, $\sigma_{\phi SOC}$ (lbs/in^2)
CRCU( )	5.0E4	Tensile yield stress for circumferential stiffeners for each load condition, $\sigma_{\phi SOT}$ (lbs/in^2)
DLT(2)	0.0	Indicator, zero when the longitudinal stiffeners are continuous; one otherwise, δ_{xw}.
DLT(3)	1.0	Indicator, zero when circumferential stiffeners are continuous,; one otherwise, $\delta_{\phi w}$.

MNEMONIC	NOMINAL VALUES	DESCRIPTION
EOF	False	Logical variable. If true, the program will terminate.
EX( )	1.0E7	Longitudinal stiffener modulus for each load condition, E_{xs}.
EY( )	1.0E7	Modulus of circumferential stiffener for each load condition, $E_{\phi s}$.
E1( )	1.0E7	Longitudinal modulus of skin for each load condition E_x (lbs/inch^2)
E2( )	1.0E7	Circumferential modulus of skin for each load condition, E_ϕ.
GAM( )	.101	Densities of the skin, circumferential stiffeners, and longitudinal stiffeners, respectively (lbs/inch^2)
GSM( )	3750937.7	Shear modulus of skin for each load condition, G.
I	1	Number of load conditions, eight maximum; integer.
ICACYC( )	1,2,3,4, 5,6,7,8, 9,10	An array of ten elements used to specify optimization cycles on which to perform a complete analysis.
IREAD	0	Integer variable. If 1217, the program will read data cards in the same format as specified by NASA CR-1217.

MNEMONIC	NOMINAL VALUES	DESCRIPTION
IWRITE	1217	Integer variable. If 1217, the program will print the input data in the same format as shown in NASA CR-1217.
KAPA(,)	1.0	Constants defining yield envelope, $K_{\alpha\beta}$. K_{TT} is read first for each load condition then K_{CT} for each load condition. Similarly, K_{CC} and K_{TC} are read.
L	10.0	Length of cylinder (inches).
LRCL( )	-5.0E4	Compressive yield stress for longitudinal stiffeners for each load condition, σ_{xSOC} (lbs/in^2)
LRCU( )	5.0E4	Tensile yield stress for the longitudinal stiffeners for each load condition, σ_{xSOT} (lbs/in^2)
ML(,)	20	Limit on the number of half wave numbers searched in the longitudinal direction for each load condition for each cylinder failure mode. The order is load condition then failure modes. Integer. (3 x I).
NL(,)	15	Limits on the number of full wave numbers searched.
NSM(,)	(Not set)	Number of modes saved for the approximate analysis. The values for the first load condition are read in the order gross, panel, skin, and then this is repeated for load condition two, etc. Integers (I x 3).

MNEMONIC	NOMINAL VALUES	DESCRIPTION
NUX( )	.333	Poisson's ratio of skin for each load condition, μ_x.
NUY( )	.333	Poisson's ratio of skin for each load condition, μ_ϕ.
NU1( )	.333	Poisson's ratio for the circumferential stiffeners for each load condition.
NU2( )	.333	Poisson's ratio for the longitudinal stiffeners for each load condition.
P1( )	0.0	Applied axial compressive loads for each load condition, N (lbs/inch).
P2( )	0.0	Applied external radial pressure for each load condition, p ($lbs/inch^2$)
R	10.0	Radius of cylinder (inches)
SO(,)	5.0E4	Skin yield stresses. First S_{xOT} is read for each load condition and then S_{xOC} is read for each load condition. Similarly $S_{\phi OT}$ and $S_{\phi OC}$ are read.

NOTE: Initial values of the design variables ($t_s, t_x, t_\phi, d_x, d_\phi, \ell_x, \ell_\phi$) are input to the program through the AESOP namelist "IAESOP" as the ALPHA vector.

NAMELIST Data Block "IAESOP"

This data block is read and defined in the optimization subprogram by subroutine BAESOP. All nominal data values are established by the optimization subroutine BDATA7. Data block IAESOP primarily defines which combination of the nine optimization search algorithms of the optimization subprogram are to be employed, how they are to be employed, and how many times the optimization cycle is to be repeated.

The nine search algorithms available are described in reference 1; these are listed below.

1. Sectioning
2. Pattern
3. Magnification
4. Steepest-Descent
5. Adaptive Creeping
6. Quadratic
7. Davidon
8. Random Point
9. Random Ray

A complete list of optimization data is presented in Tables E2. and E3. . Table E2 contains the basic optimization control data. Table E3 contains the specialized print control data. It should be emphasized that all items in Tables E2 and E3 are read by the single NAMELIST input block IAESOP.

AESOP Print Control

AESOP has a flexible print output capability. Varying levels of printout are available at user option as follows:

Summary of function and control parameter values at the beginning and end of the optimization process;

Summary of function and control parameters values at the end of each cycle;

Summary of function and control parameter values at the end of each evaluation;

Detailed printout of individual search parameters.

The convention adapted for print indicator is a six-letter mnemonic as described below.

NOTE: In all cases print is given when the indicator is non-zero and omitted when it is zero.

EXAMPLES: 1) IPACRP=1, Print control vector following creeping search

2) IPDPEN=1, Supply detailed print output from subroutine PENALTY

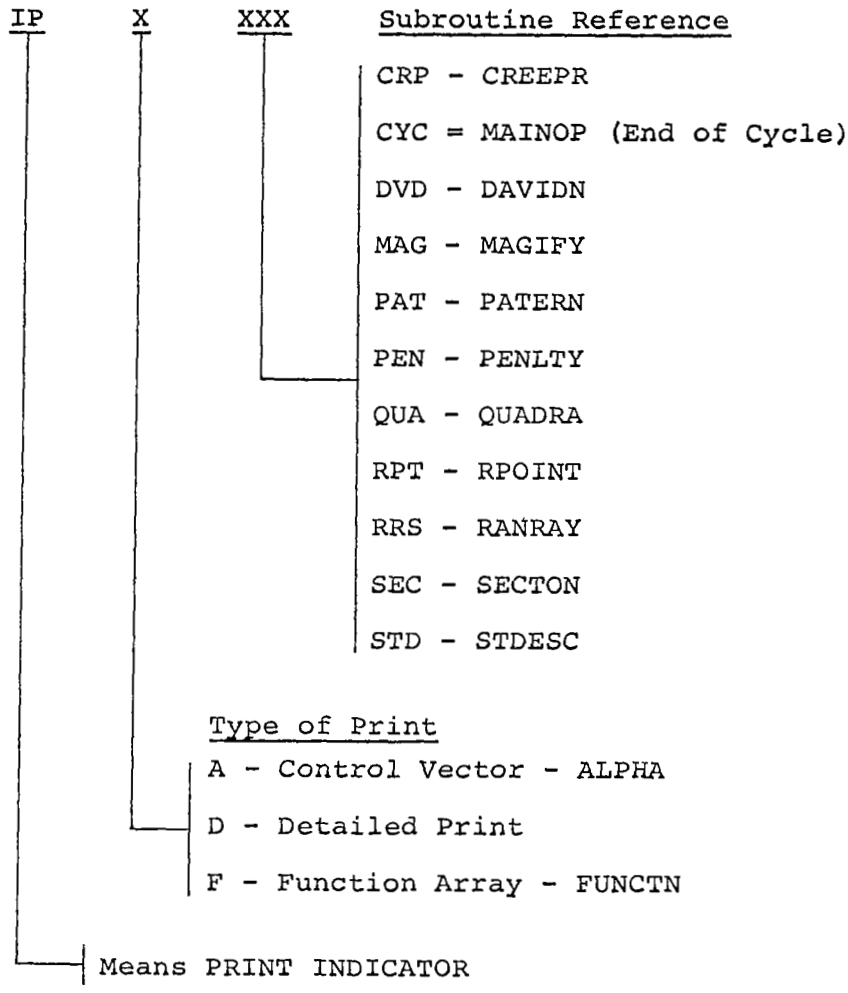

An alphabetical list of print control indicators follows in Table E3. relevant search is identified for each input in the same way described earlier for the optimization data.

TABLE E2..—BASIC OPTIMIZATION DATA

MNEMONIC	RELEVANT SEARCH 1 2 3	4 5 6	7 8 9	NOMINAL VALUES	DESCRIPTION
$ALFSIN_i$		X		100*1.	Determines first perturbation directions in creeping search.
$ALPHA_i$	X X X	X X X	X X X	100*1.	Nominal values of control parameters.
$ALPHI_i$	X X X	X X X	X X X	100*1.	Upper control parameter search limits.
$ALPLO_i$	X X X	X X X	X X X	100*1.	Lower control parameter search limits.
$CREPMN_i$		X		100* .0000001	Minimum perturbations to be employed in creeping search.
$DCREEP_i$		X		100*.001	Starting perturbations for creeping search.
FACTHI	X	X X	X	.001	Initial termination tolerance on Golden Section.
FACTLO	X	X X	X	.00001	Final termination tolerance on Golden Section
$FTOL_i$*	X X X	X X X	X X X	20*1.	Final desired constraint tolerances.
INDWMA		X		1	Steepest-descent weighting matrix indicator. 0 - Unit matrix 1 - Empirical matrix 2 - Alternates between unit and empirical matrix
IRANDM	X	X		0	Selects the order in which the control variables are perturbed and sectioning searches. 0 - Uniformly random 1 - Natural order 2 - Reverse natural order

* Used only in constraint logic

MNEMONIC	RELEVANT SEARCH 1 2 3	4 5 6	7 8 9	NOMINAL VALUES	DESCRIPTION
IREPET	X X X	X X X	X X X	10	Number of optimization cycles to be completed.
ISECOF				1000	Cycle number at which sectioning search is terminated.
ISIDE	X	X X	X	0	Selects extreme of the search interval to be used when performance is constant on search ray. 0 - Lower limit 1 - Upper limit
IWARP	X X X	X X X	X X X	0	Controls multiple extremal option. 0 - Performance response surface unaltered 1 - Performance response surface is warped
LIMIT	X			2	Number of sectioning searches.
MAXCRP		X		5	Number of complete creeping searches to be performed when search is called.
MAXDVD			X	10	The number of Davidon searches carried out when this method is selected.
MAXJJJ	X X X	X X X	X X X	200	The maximum number of performance evaluations.
MAXMAG	X			99	Maximum number of magnification searches in an optimization calculation.
MAXRPT			X	10	Number of random point evaluations.
MAXRRS			X	100	Number of random rays to be employed.

MNEMONIC	RELEVANT SEARCH 1 2 3	4 5 6	7 8 9	NOMINAL VALUES	DESCRIPTION
$METHOP_i$	X X X	X X X	X X X	1,2,3,4,5	The sequence of searches to be employed. 1 - Sectioning 2 - Pattern 3 - Magnify 4 - Steepest-Descent 5 - Creeping 6 - Quadratic 7 - Davidon 8 - Random Point 9 - Random Ray 11- Arbitrary Ray Search
NALPHA	X X X	X X X	X X X	3	Number of control parameters to be employed
NFUNC	X X X	X X X	X X X	1	Number of functions to be considered.
NMAXLO	X	X X	X	10	Initial maximum number of evaluations in Golden Section.
NMAXUP	X X	X X	X	20	Final maximum number of evaluations in Golden Section and to limit the number of evaluations in pattern.
NPHIAC	X X X	X X X	X X X	1	Function number of the performance criteria.
$NPSI_i$*	X X X	X X X	X X X	0	Constraint function numbers
NPTSRY†				10	Number of steps to take when the ray search is called
NUMOPT	X X X	X X X	X X X	5	Number of optimization searches to be employed
NUMPSI*	X X X	X X X	X X X	0	Number of constraints
NUMSTD		X		2	Number of steepest-descent searches
PHIEPS	X	X X	X	0.0	Performance values within PHIEPS of the minimum value yet attained are treated as being equal in Golden Section
$PSIWT_i$*	X X X	X X X	X X X	20*. .0001	Initial constraint error weights

* Used only in constraint logic
† Pertains to ray search

MNEMONIC	RELEVANT SEARCH 1 2 3	4 5 6	7 8 9	NOMINAL VALUES	DESCRIPTION
QFACTR		X		1.0	Quadratic perturbation factor
$QPERT_i$		X		20*.005	Initial control parameter perturbations for quadratic and Davidon searches
RALOHI†				True	Logical variable used to indicate direction to go along the multidimensional ray. I.e., if true, go from XTENLO to XTENHI; if false,go from XTENHI to XTENLO.
RANGEN			X X	1.0	Random number generator trigger (1.0 means uniform distribution),(-1.0 means normal distribution)
RAYDIV†				10.	Used to compute stepsize; i.e., if RAYDIV=10,the stepsize will be such as to require 10 steps to go from XTENLO to XTENHI.
RUFHI			X	.01	Maximum nondimensional random ray perturbation size on any component. Value of 1.0 gives maximum perturbation equal to search range.
RUFLO			X	.00001	Minimum nondimensional random ray perturbation size on any component
$SIBAR_i$*	X X X	X X X	X X X	20*0.0	Desired constraint values
$TOLFAC_i$*	X X X	X X X	X X X	20*0.5	Constraint tolerance reduction factor
$TTOL_i$*	X X X	X X X	X X X	20*100.	Initial constraint tolerances
$WITER_i$*	X X X	X X X	X X X	100*1.0	Starting values for iterative component of steepest-descent weighting matrix

* Used only in constraint logic
† Pertains to ray search

MNEMONIC	RELEVANT SEARCH 1 2 3	4 5 6	7 8 9	NOMINAL VALUES	DESCRIPTION
$WTDOWN_i$*	X	X X	X	20*0.5	Constraint weight decrease factor
$XTENHI_i$	X X X	X X X	X X X	100*0.0	Used to extend upper search limit
$XTENLO_i$	X	X X	X	100*0.0	Used to extend lower search limit in Golden Section if performance is constant in feasible region
$WARPAL_i$	X X X	X X X	X X X	100*0.0	The warping origin in the control parameter space for multiple extremal feature
WARPN	X X X	X X X	X X X	2.0	The exponent of the warping transformation

*Used only on constraint logic

TABLE E3 .—OPTIMIZATION PRINT CONTROL DATA

MNEMONIC	RELEVANT SEARCH 1 2 3	4 5 6	7 8 9	NOMINAL VALUES	DESCRIPTION
IPACRP		X		0	Creeping control parameter print indicator.
IPACYC	X X X	X X X	X X X	0	Cycle control parameter print indicator.
IPADVD			X	0	Davidon control parameter print indicator.
IPAMAG	X			0	Magnification control parameter print indicator.
IPAPAT	X			0	Pattern control parameter print indicator.
IPAPEN	X X X	X X X	X X X	0	Constraint penalty control parameter print indicator.
IPAQUA		X		0	Quadratic control parameter print indicator.
IPARPT			X	0	Random point control parameter print indicator.
IPARRS			X	0	Random ray control parameter print indicator.
IPASEC	X			0	Sectioning control parameter print indicator.
IPASTD	X			0	Steepest-descent control parameter print indicator.
IPDCRP		X		0	Detailed creeping print indicator.
IPDDVD		X		0	Detailed Davidon print indicator.

MNEMONIC	RELEVANT SEARCH 1	2	3	4	5	6	7	8	9	NOMINAL VALUES	DESCRIPTION
IPDMAG			X							0	Detailed magnification print indicator.
IPDPAT		X								0	Detailed pattern print indicator.
IPDQUA						X				0	Detailed quadratic print indicator.
IPDRIV				X		X				0	Detailed derivatives print indicator.
IPDRPT								X		0	Detailed random point print indicator.
IPDRRS									X	0	Detailed random ray print indicator.
IPDSEC	X									0	Detailed sectioning print indicator.
IPDSTD				X							Detailed steepest-descent print indicator.
IPFCRP					X					0	Creeping function print indicator.
IPFCYC	X	X	X	X	X	X	X	X	X	0	Optimal function print indicator at the end of each cycle.
IPFDVD							X			0	Davidon function print indicator.
IPFMAG			X							0	Magnification function print indicator.
IPFPAT		X								0	Pattern function print indicator.
IPFQUA						X				0	Quadratic function print indicator.
IPFRPT								X		0	Random point function print indicator.

MNEMONIC	RELEVANT SEARCH									NOMINAL VALUES	DESCRIPTION
	1	2	3	4	5	6	7	8	9		
IPFRRS									X	0	Random ray function print indicator.
IPFSEC	X									0	Sectioning function print indicator
IPFSTD				X						0	Steepest-descent function print indicator
IPGAIN	X	X	X	X	X	X	X	X	X	1	Print every iteration which will improve the performance.
IPNAML	X	X	X	X	X	X	X	X	X	1	Namelist output control = 0, omit print = 1, print namelist data

AESOP Data Listings

Program AESOP data can be conveniently grouped according to search and function. The user employing a particular search can independently specify the characteristics of that search and may not be concerned with input relevant to the other searches. Hence, a data grouping by search and by function is presented below for user convenience. It should be noted that certain inputs are common to more than one search; where this occurs, the input is repetitively defined in each search.

Search Selection and Control.—

NUMOPT - The number of optimization techniques to be employed. Each individual search request in a sequence of requests adds to this input (e.g., the search sequence 4,2,4,2 requires NUMOPT = 4). Maximum number of searches employed must satisfy NUMOPT $\leq$ 20.

$METHOP_i$ - The search sequence by numeric identification. For example, the input METHOP(1) = 1,2,3,4,5,6,7,8,9 signifies the following search sequence:

1 - Sectioning
2 - Pattern
3 - Magnification
4 - Steepest-Descent
5 - Adaptive Creeping
6 - Quadratic
7 - Davidon (Fletcher-Powell)
8 - Random Point (Monte-Carlo)
9 - Random Ray (random evolution)
11 - Arbitrary Ray

The complete search sequence will be referred to as an optimization cycle.

MAXJJJ - The maximum number of system evaluations. A direct iteration number limit.

IREPET - The maximum number of times the search sequence (optimization cycle) defined in $METHOP_i$ will be utilized

Parameter Selection.—

NALPHA - The number of parameters available for optimization. No more than one hundred parameters may be employed.

$ALPLO_i$ - Lower bounds on each parameter search range

$ALPHI_i$ - Upper bounds on each parameter search range

$ALPHA_i$ - The nominal parameter values. Note that $ALPLO_i \leq ALPHA_i \leq ALPHI_i$ must be satisfied. If a particular parameter, say $ALPHA_j$, is to be fixed in value in a particular computation, then set $ALPLO_j = ALPHA_j = ALPHI_j$. This effectively reduces the parameter space dimension by one for each such parameter.

Multiple Extremal Option.—

IWARP - Controls multiple extremal option
IWARP = 1, automatically warp the response surface
IWARP = 0, leaves the response surface unmodified

$WARPAL_i$ - The point at which the warping transformation is centered, i.e., the location of a known extremal point.

WARPN - The degree of the warping transformation. The greater WARPN, the greater the response surface distortion.

Optimization Function Selection.—

$FUNCTN_i$ - AN INTERNAL ARRAY CONTAINING ALL COMPUTED OPTIMIZATION FUNCTIONS

NFUNC - The total number of functions ($FUNCTN_i$) being computed in the system model
NOTE: NFUNC $\leq$ 100.

NPHIAC - The function to be minimized. AESOP always searches for a minimum; to maximize $FUNCTN_m$ define $FUNCTN_n = -FUNCTN_m$ and minimize $FUNCTN_n$.

NUMPSI - The total number of functions being constrained.
NOTE: NUMPSI $\leq$ 20.

$NPSI_i$ - The functions to be constrained, e.g., NPSI(1) = 3, 5, 1, 7 indicates that $FUNCTN_3$, $FUNCTN_5$, $FUNCTN_1$, and $FUNCTN_7$ are to be constrained.

$SIBAR_i$ - The desired values of the constraint functions defined by $NPSI_i$

$FTOL_i$ - The acceptable tolerances on the constraint function values, $SIBAR_i$

$TTOL_i$ - Initial acceptable tolerances on the constraint function values, (should be approximately 100 times greater than the corresponding $FTOL_i$).

$PSIWT_i$ - Initial constraint error weighting factors in the augmented performance function, ϕ^*, where

$$\phi^* = \phi + \sum_i W_i (\psi_i - \bar{\psi}_i)^2 \qquad (23)$$

Here

$$W_i \equiv PSIWT_i$$

$WTUP_i$ - Incremental multiplicative constants used to increase the W_i on constraints which prove difficult to satisfy. The nominal values of $WTUP_i$ = 2.0 should be acceptable; hence, this input can normally be omitted.

$WTDOWN_i$ - Decremental multiplicative constants used to decrease the W_i when a constraint is easily satisfied. The nominal values of $WTDOWN_i$ = 0.5 should be acceptable; hence, this input can normally be omitted.

Sectioning Search Data ($METHOP_i$ = 1).—

LIMIT - The number of times each parameter will be sectioned during a single sectioning search

NMAXLO Maximum number of point evaluations employed in a single parameter's sectioning at search commencement (first optimization cycle). In successive cycles, the maximum number of points employed is increased by one.

NMAXUP An upper bound on the maximum number of point evaluations employed in sectioning a particular parameter.

ISIDE - Indicator specifying selection of left or right boundary for a parameter that does not appear to affect the system performance

ISIDE = 0, Select lower limits
ISIDE = 1, Select upper limits

$XTENHI_i$ - Extension of higher search limits ($ALPHI_i$) for a parameter that does not appear to affect performance

$XTENLO_i$ - Extension of lower search limits for a parameter that does not appear to affect performance

IRANDM - Controls the order in which the parameters are sectioned

IRANDM = 0, Random order selected
IRANDM = 1, Natural order selected
IRANDM = 2, Reverse natural order selected

FACTHI - Section termination criteria. If three successive performance function values are within FACTHI of each other during sectioning of a given parameter on the first optimization cycle, the section search of that parameter will cease. The termination criteria is internally reduced with each optimization cycle.

FACTLO - The lower limit on the termination criteria in any optimization cycle.

ITRADE - Optimization/trade study indicator

ITRADE = 0, Carry out a normal optimization search
ITRADE = 1, Determine performance function sensitivity to each parameter by sectioning each parameter in turn about a given fixed point in parameter space.

IPASEC, IPDSEC, IPFSEC - Print indicators (See Table E3, page E17) for section search

Pattern Search Data ($METHOP_i = 2$).—

IPAPAT, IPDPAT, IPFPAT - Pattern Search print indicators

Magnification Search Data ($METHOP_i = 3$).—

MAXMAG - Maximum number of point evaluations performed during a single magnification search

DELMAG - The magnification perturbation size, nominally set to 1% of distance to origin. Not normally modified from nominal value

IPAMAG, IPDMAG, IPFMAG - Magnification search print indicators, (See Table E3, Pages E16 to E18).

Steepest-Descent Search Data ($METHOP_i = 4$).—

NUMSTD - Number of gradient evaluations and one-dimensional searches performed each time that a steepest-descent search is requested during the optimization cycle.

INDWMA - Steepest-descent weighting matrix indicator
INDWMA = 0., Unit matrix
INDWMA = 1., Empirical matrix
INDWMA = 2., Alternate on each cycle between unit and empirical matrices

$WITER_i$ - Learning factors for steepest-descent weighting matrix

NMAXLO - Maximum number of point evaluations employed in the steepest-descent one-dimensional ray search at search commencement (first optimization cycle). In successive cycles, the maximum number of point evaluations permitted is increased by one.

NMAXUP - Upper bound on the number of point evaluations along a steepest-descent one-dimensional ray in *any* optimization cycle.

FACTHI - One-dimensional steepest-descent ray search termination criteria during first cycle. The termination criteria is reduced in each successive optimization cycle.

FACTLO - Lower limit on one-dimensional steepest-descent ray search termination criteria, in *any* optimization cycle.

IPASTD, IPDSTD, IPFSTD - Steepest-descent search print control indicators,

Adaptive Creeping Search Data ($METHOP_i = 5$).—

MAXCRP - Number of creeping search perturbations introduced into each parameter by a single adaptive creeping search in the optimization cycle.

IRANDM - Controls the order in which parameters are perturbed
IRANDM = 0 , Random order
IRANDM = 1 , Natural order
IRANDM = 2 , Reverse natural order

$DCREEP_i$ - The initial perturbations to each parameter

$CREPMN_i$ - Minimum perturbations for each parameter

$CREPMX_i$ - Maximum perturbations for each parameter

$ALFSIN_i$ - Direction of perturbation for each parameter ($ALFSIN_j = \pm 1.0$)

IPACRP, IPDCRP, IPFCRP - Adaptive creeping search print indicators

Quadratic Search Data ($METHOP_i = 6$).—

$QPERT_i$ - Parameter perturbation magnitudes employed in computation of numerical partial derivative matrices $\frac{\partial^2 \phi}{\partial \alpha_i \partial \alpha_j}$ and $\frac{\partial \phi}{\partial \alpha_i}$

QFACTR - Scaling factor on the $QPERT_i$

NMAXLO - Maximum number of point evaluations employed in the quadratic one-dimensional ray search at search commencement (first optimization cycle). In successive optimization cycles, the number of point evaluations permitted increases by one.

NMAXUP - Upper bound on the number of point evaluations along a quadratic one-dimensional ray search, in *any* cycle.

FACTHI - One-dimensional quadratic ray search termination criteria during first cycle. The termination criteria is decreased in each successive optimization cycle.

FACTLO - Lower limit on one-dimensional quadratic ray search termination criteria, in *any* optimization cycle.

IPAQUA, IPDQUA, IPFQUA - Quadratic search print indicators

Davidon Search Data ($METHOP_i = 7$).—

MAXDVD - Number of Davidon (Fletcher-Powell) gradient evaluations and one-dimensional searches performed each time that a Davidon search is requested in the optimization cycle

$QPERT_i$ - Parameter perturbation magnitudes employed in computation of numerical partial derivatives,

$$\frac{\partial \phi}{\partial \alpha_j}$$

NMAXLO - Maximum number of point evaluations employed in the Davidon one-dimensional ray search at search commencement (first optimization cycle). In successive optimization cycles, the number of point evaluations permitted is increased by one.

NMAXUP - Upper bound on the number of point evaluations along a Davidon search one-dimensional ray in any cycle

FACTHI - One-dimensional Davidon ray search termination criteria during first optimization cycle. The termination criteria is decreased in each successive optimization cycle.

FACTLO - Lower limit on one-dimensional Davidon ray search termination criteria, in *any* optimization cycle

IPADVD, IPDDVD, IPFDVD - Davidon print control indicators.

Random Point Search ($METHOP_i = 8$).—

MAXRPT - The maximum number of random points to be employed in the first request for a random point search within the optimization cycle. In successive requests, MAXRPT is set to zero,and no evaluations result.

IPARPT, IPDRPT, IPFRPT - Random point search print control indicators

Random Ray Search (METHOP$_i$ = 9).

MAXRRS - The maximum number of random rays, one or two-sided, investigated each time the optimization cycle requests a random ray search.

RUFHI - The initial maximum non-dimension perturbation measure for each parameter. This is reduced each time random ray search consistently fails to improve performance.

RUFLO - Minimum-maximum dimensional perturbation measure for each parameter.

IPARRS, PIDRRS, IPFRRS - Random ray search print control indicators

Arbitrary Ray Search (METHOP$_i$ = 11).

The arbitrary ray search searches the ray passing through two specified points in the multidimensional control space. For printout it is suggested that the tabular summary feature of AESOP be used.

RALOHI — Defines which direction to search; i.e., if TRUE, search "LO" → "HI", if FALSE, search "HI" → "LO"

NPTSRY — Total number of evaluations to be used on ray search

RAYDIV — Defines stepsize for ray search; i.e., *control parameter step size* = (XTENHI$_i$ - XTENLO$_i$)/RAYDIV

XTENHI$_i$ — Defines the control parameter values at "HI"† end of the multidimensional ray to be searched.

XTENHI$_i$ need not be greater than XTENLO$_i$, and XTENLO$_j$ need not be less than XTENHI$_j$ *in this search*. These two arrays merely define the end points of a ray in the multidimensional control space.

006 001 C1 U 32 720428 S00903DS
DEPT OF THE AIR FORCE
AF WEAPONS LAB (AFSC)
TECH LIBRARY/WLOL/
ATTN: E LOU BOWMAN, CHIEF
KIRTLAND AFB NM 87117

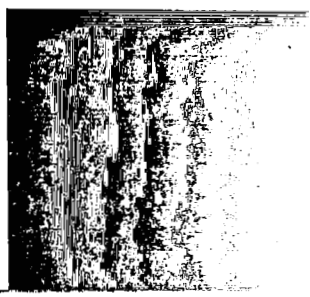

"The aeronautical and space activities of the United States shall be conducted so as to contribute . . . to the expansion of human knowledge of phenomena in the atmosphere and space. The Administration shall provide for the widest practicable and appropriate dissemination of information concerning its activities and the results thereof."

—NATIONAL AERONAUTICS AND SPACE ACT OF 1958

NASA SCIENTIFIC AND TECHNICAL PUBLICATIONS

TECHNICAL REPORTS: Scientific and technical information considered important, complete, and a lasting contribution to existing knowledge.

TECHNICAL NOTES: Information less broad in scope but nevertheless of importance as a contribution to existing knowledge.

TECHNICAL MEMORANDUMS: Information receiving limited distribution because of preliminary data, security classification, or other reasons.

CONTRACTOR REPORTS: Scientific and technical information generated under a NASA contract or grant and considered an important contribution to existing knowledge.

TECHNICAL TRANSLATIONS: Information published in a foreign language considered to merit NASA distribution in English.

SPECIAL PUBLICATIONS: Information derived from or of value to NASA activities. Publications include conference proceedings, monographs, data compilations, handbooks, sourcebooks, and special bibliographies.

TECHNOLOGY UTILIZATION PUBLICATIONS: Information on technology used by NASA that may be of particular interest in commercial and other non-aerospace applications. Publications include Tech Briefs, Technology Utilization Reports and Technology Surveys.

Details on the availability of these publications may be obtained from:

SCIENTIFIC AND TECHNICAL INFORMATION OFFICE

NATIONAL AERONAUTICS AND SPACE ADMINISTRATION

Washington, D.C. 20546